National Library of Canada
Acquisitions and Bibliographic Services Branch
395 Wellington Street
Ottawa, Ontario
K1A 0N4

Bibliothèque nationale du Canada
Direction des acquisitions et des services bibliographiques
395, rue Wellington
Ottawa (Ontario)
K1A 0N4

Your file Votre référence

Our file Notre référence

NOTICE

The quality of this microform is heavily dependent upon the quality of the original thesis submitted for microfilming. Every effort has been made to ensure the highest quality of reproduction possible.

If pages are missing, contact the university which granted the degree.

Some pages may have indistinct print especially if the original pages were typed with a poor typewriter ribbon or if the university sent us an inferior photocopy.

AVIS

La qualité de cette microforme dépend grandement de la qualité de la thèse soumise au microfilmage. Nous avons tout fait pour assurer une qualité supérieure de reproduction.

S'il manque des pages, veuillez communiquer avec l'université qui a conféré le grade.

La qualité d'impression de certaines pages peut laisser à désirer, surtout si les pages originales ont été dactylographiées à l'aide d'un ruban usé ou si l'université nous a fait parvenir une photocopie de qualité inférieure.

Canada

ISBN 0-612-00558-5

UNIVERSITÉ D'OTTAWA
UNIVERSITY OF OTTAWA

ACKNOWLEDGEMENTS

I must admit, I never thought that I would actually get to this stage! The acknowledgements are actually the first part of the thesis I planned in my head, but they are the last thing I am including in my thesis. I have always believed in saving the best for last. I have been here at the University of Ottawa for so long, I have a very long list of thanks, but without the help of all the people whom I will be thanking, I would not be writing this section at all!

First and foremost, I would like to thank my supervisor, Dr. Margaret H. Back. Dr. Back, you have been a source of inspiration and encouragement, always giving me that extra push when I needed it, and yet understanding instinctively when I needed more time. I can't thank you enough for supporting me in my research work as well as in my musical career. You always encouraged me to take the time for my music and I just wanted you to know that I really appreciated that. I have learned a lot from you, and it is not just science that I learned! Thank you for everything.

I would like to give an extra special thanks to my family. My father, who actually convinced me to transfer from the masters program to the doctoral program, and who took the time to proofread my thesis, gets a big thank you. So does my mom, who patiently put up with my easily aroused temper, who always provided big meals for my friends and I, and who supported me through these long years. Another big thank you to my brother, who finished just before me and who kept reminding me that I was almost done and not to give up. And of course, last but certainly not least, my sister Meena (how many do

I have?) who kept coming up with all the funny lines from our favourite movies, and who could at least tell everyone who asked, that I was doing my Ph.D. in Chemistry (that's PHYSICAL, not ANALYTICAL!!), even if she didn't exactly know what I was doing, gets a special vote of thanks. Thanks! to all of you for your support. I needed it.

Moving along to the Chemistry Department, the list of thanks gets quite large. Thanks are in order to all the technical and support staff, including Mme. Monique Levesque, M. Daniel Lafleur, M. Robert Nadon, Mrs. Guia Garces, Mme. Céline Clément, M. Martin Canuel, M. Martin Larabie, Mr. Raj Capoor, Mme. Lise Maisonneuve, M. Daniel Emard, M. Mario Savage, M. Fern Boucher, Mr. John Hopkins, Mr. Egon Kristof, Mr. Donald Hopkins, Mr. Lee Sorensen (to whom I owe a very special thanks for having repaired my pump two days before Christmas!), Mrs. Eva Szabo and M. François Allard. If I omitted anyone's name in this list, please accept my apologies, it is an oversight. Special thanks are in order to Mme. Corinne Bensimon, for her help in the interpretation and explanation of some XRD results, Mr. (soon to be Dr.!) Stephen J. Lang, for his help in the interpretation of the FTIR results and just for being such a great friend, Dr. Clem Kazakoff, for his mass spectrometric analysis of the carbon for fullerenes (and for all those racquetball tips, you get an extra thank you, Clem!), Dr. John Krause, for his patience in looking for small amounts of ^{13}C during the labelled methane experiments, and Dr. Alexander Mommers, for computer fixups, for keeping the MS-9 running when we needed it, and most of all, for introducing me to Souper Jazz, my musical family!

I would like to take this opportunity to say thank you to all the professors in the department. I can honestly say that I have learned something from all of them. I would

like to say a special thanks to Dr. Morrow, for making my "time" more interesting (I'm sure you'll pick up all the implications of that word, sir!), to Dr. Holmes, for allowing me to use their photocopier and laser printer in emergency situations, and for the interesting conversations we've had, and to Dr. Paul Wilde, for all his help in getting me onto Internet and for his support of the teaching labs and "kiddie khem". A special thanks to Dr. Fred Lossing, just for making the days brighter!

While there are so many others at the University to whom I owe a big thanks for making my stay here so enjoyable, I don't know if I can name them all. I would like to thank all my fellow graduate students (too numerous to mention by name, but all thought of with affection!) and the many post-docs with whom I have become good friends. In particular, I would like to thank Ms. Radojka Simpraga, for always perking me up! I will say thank you to everyone on the staff at the gym, to the maintenance people (they know who they are!), and to Doreen, for involving me in Pathmakers. I would like to give a special thanks to Mme. Colette Mangin, for all her support in getting me financial assistance. Thanks to you all, even if I can't name you all.

I would like to thank John P. McCaffrey, of NRC, for performing the SEM and TEM analyses of my carbon. I would like to thank Mr. John S. Loop for having performed the AES measurements. I would like to thank Dr. M. S. Seehra and V. Suresh Babu, of the West Virginia University, for having performed the FTIR and XRD analyses. I would also like to thank NSERC for the funding of this research project.

This now brings me to the even more pleasant task of thanking some special people, namely my co-workers. I would like to thank Dr. Alain Bossard for all his help

in my work, as well as for his extreme patience and humour in the job of translating all the "kiddie khem" material. I would like to thank Dr. Gérard Scacchi, who more or less decided the course of my work, for all his helpful suggestions and advice. I would like to thank my long-term colleague, Dr. Binjun Zhao, and his family, for having been so supportive and for being a great friend.

I owe a tremendous debt to a special friend whom I only got to know for a year, and yet I feel that I have known for years, and that is Dr. Phillip J. Gilbert. He was the first person with whom I could actually discuss my work and the insights which he provided are responsible for my being at this stage. I will never be able to thank you enough, Phil, and my only regret is that you could not actually be here when I submit this. To you and Jo, thanks a million!

THANK YOU, CATHERINE!! (I told you you'd get a big thanks in my thesis!) Thank you for the time you spent doing all those calculations I needed for my final version graphs, and thanks for staying WAY overtime to help me put them together. Thanks for introducing me to crossword puzzles, and just for being a great friend!

While being at the University taught me a lot, I must say that I learned most of my practical information from the Master himself, our master glassblower, Mr. Egon Kristof. How can I thank you, Egon, for the time you spent doing things for me, whether they were glass or other? I could ask you anything, and I could be assured that I would be given the right answer. You always managed to squeeze in the time to do emergency jobs for me, even though you were so busy. I'll never forget all the things that I have learned from you. Thank you for taking the time and having the patience to teach me.

Two other dear friends of mine who cannot go without mention are Céline Clément and Eva Szabo. Thanks to Céline for being a great friend and someone to whom I could always talk. As for dear Eva, you know these years would not have been the same without you. Thanks for all the beautiful figures in this thesis. This thesis would not be the same without them.

Thanks to Monique Levesque, for all the time she took to do little things (which were really not so little!). Thanks to Jeffrey, for being so fun to be with. Thanks to Ms. Wilma Nuyens, who was always so supportive and helpful.

And now, I get to say thank you to the two people who have had the greatest impact on me during my six years here.

Dr. John Krause has been my dear friend, my teacher, my role model, my guide, and my mentor. John, you showed me quite clearly what I want to do and you have helped me in all ways possible to achieve this goal. I don't know how to thank you enough for making me such an integral part of "kiddie khem" and all the other student activities you have been so instrumental in organizing. I have learned from you to understand the teacher's and the student's viewpoint. Moreover (that's my concession to you, instead of too!), I've learned a lot about administration from you. Thank you for being such a wonderful friend, and for doing crosswords with me, for the Saturday lunches, and for all the other things you know (and I know) that you've done for me.

M. Robert Nadon has been my dear friend almost since the day I joined here six years ago. Bobby, you thought your name would never be in a thesis. WELL, here it is! And if anyone deserves it, you do. You work so hard at helping people, and trying

to make them happy that I thought you deserved a little happiness too! Thank you for being such a super friend, for all the drives for different things I needed, for introducing me to the gym, and the wonderful world of "skipping" and racquetball, and most of all, for being the person to whom I could tell everything. Don't drop the Zen, OK?

There are so many people who have directly and indirectly helped me arrive at the completion of my thesis, and I wish I could thank each one by name. Since I can't, I will simply say thank you to everyone who has helped me. I truly appreciate it. Once again, if I have omitted anyone's name in this list, I sincerely apologize.

And so, I dedicate this thesis to John and Bob, the other two-thirds of the famous (or infamous!) trio, with love and respect.

TABLE OF CONTENTS

		Page
ACKNOWLEDGEMENTS		i
TABLE OF CONTENTS		vii
LIST OF TABLES		xiv
LIST OF FIGURES		xv
ABSTRACT		xviii
CHAPTER 1: INTRODUCTION		1
1.1	General	1
1.2	What is Carbon?	2
1.3	Carbon as an Inhibitor	6
1.4	Carbon as a Catalyst	8
1.5	Carbon as a Catalyst and an Inhibitor	13
1.6	Methane Conversion	16
1.6.1	Methane	16
1.6.2	Natural Gas	17
1.6.3	Methane Conversion	18
1.6.3.1	Thermal Reactions	19
1.6.3.2	Catalytic Reactions	21
1.7	Goals of this Study	26

CHAPTER 2: EXPERIMENTAL 27

2.1 Apparatus 27

2.2 Analytical System 29

2.3 Materials 30

2.4 Experimental Procedure 32

2.4.1 Deposition of the Carbon Film 32

2.4.2 Methane Reaction 32

2.4.3 Removal of the Carbon Film 34

2.4.4 Summary of Other Experimental Procedures 35

CHAPTER 3: RESULTS 36

3.1 Introduction 36

3.2 Yield as a Function of Time 36

3.2.1 Introduction 36

3.2.2 Experimental 37

3.2.2.1 In the Absence of Carbon 37

3.2.2.2 In the Presence of Carbon 38

3.2.3 Results 39

3.2.4 Discussion 39

3.2.4.1 Oxygen as a Contaminant 47

3.3 Consecutive Experiments 50

3.3.1 Introduction 50

3.3.2 Experimental 51

3.3.3 Results 52

3.3.4 Discussion 52

3.4 Rate as a Function of Amount of Carbon 59

3.4.1 Introduction 59

3.4.2 Experimental 60

3.4.3 Results 60

3.4.4 Discussion 63

3.5 Rate as a Function of Pressure 65

3.5.1 Introduction 65

3.5.2 Experimental 66

3.5.3 Results 66

3.5.4 Discussion 68

3.6 Rate as a Function of Temperature 69

3.6.1 Introduction 69

3.6.2 Experimental 69

3.6.3 Results 70

3.6.4 Discussion 70

3.6.4.1 Temperatures above 873 K 70

3.6.4.2 Temperatures below 873 K 74

3.7 Rate Measurements in a Packed Vessel 78

3.7.1 Introduction 78

3.7.2 Experimental 79

3.7.2.1 Packed Reaction Vessel 79

3.7.2.2 Experimental Procedure 79

3.7.3 Consecutive Experiments 80

3.7.3.1 Experimental 80

3.7.3.2 Results 80

3.7.3.3 Discussion 81

3.7.4 Rate as a Function of Amount of Carbon 87

3.7.4.1 Experimental 87

3.7.4.2 Results 88

3.7.4.3 Discussion 88

3.7.5 Rate as a Function of Pressure 91

3.7.5.1 Experimental 91

3.7.5.2 Results 91

3.7.5.3 Discussion 95

3.7.6 Rate as a Function of Temperature 96

3.7.6.1 Experimental 96

3.7.6.2 Results and Discussion 97

3.7.6.2.1 Temperatures above 873 K 97

3.7.6.2.2 Temperatures 873 K and below 99

CHAPTER 4: CARBON CHARACTERIZATION 102

4.1 Introduction 102

4.2 Hydrogen Content of the Carbon 103

	4.2.1	Introduction	103
	4.2.2	Experimental	104
	4.2.3	Results and Discussion	105
4.3	The Reactivity of Carbon as a Function of the Carbon Precursor		108
	4.3.1	Introduction	108
	4.3.2	Experimental	108
	4.3.3	Results and Discussion	108
4.4	Analysis of Carbon for Fullerenes		111
	4.4.1	Introduction	111
	4.4.2	Experimental	112
	4.4.3	Results and Discussion	112
4.5	Study of the Carbon Film by Electron Microscopy		114
	4.5.1	Introduction	114
	4.5.2	Experimental	115
	4.5.3	Results	116
	4.5.4	Discussion	116
4.6	X-Ray Diffraction Studies of the Carbon Film		118
	4.6.1	Introduction	118
	4.6.2	Experimental	120
	4.6.3	Results and Discussion	121
4.7	Analysis of Carbon Films by FTIR Spectroscopy		123
	4.7.1	Introduction	123

4.7.2 Experimental 123

4.7.3 Results and Discussion 124

4.8 Study of Carbon Reactivity using Labelled Methane 126

4.8.1 Introduction 126

4.8.2 Experimental 126

4.8.2.1 $^{13}CH_4$ as a Reactant 126

4.8.2.2 Experimental Procedure 127

4.8.3 Results 129

4.8.3.1 Interpretation of the Data 129

4.8.3.2 Observed Results 134

4.8.4 Discussion 135

CHAPTER 5: THE REACTIVITY OF CARBON-IRON FILMS 136

5.1 Introduction 136

5.1.1 Gasification Reactions 136

5.1.2 Catalysts for Steam Gasification 137

5.1.3 Methods of Catalyst Preparation 138

5.1.4 Novel Method of Iron Catalyst Preparation 140

5.1.5 Goal of This Study 141

5.2 Experimental 142

5.2.1 Deposition of a Pure Carbon Film 142

5.2.2 Calibration of the Quantity of Carbon in the Film 143

5.2.3 Deposition of a Carbon Film Containing Iron 143

5.2.4 Preparation of the Hydrogen/Water Mixture 144

5.2.5 Reaction Procedure 145

5.2.6 Analysis of the Reaction Vessel for Iron 146

5.3 Results and Discussion 146

5.4 Reactivity of Methane over the Iron Carbon Film 150

5.4.1 Introduction 150

5.4.2 Experimental 150

5.4.3 Results 151

5.4.4 Discussion 152

CHAPTER 6: SUMMARY 157

6.1 Discussion 157

6.2 Direction of Further Study 163

CLAIMS TO ORIGINAL RESEARCH 165

REFERENCES 166

LIST OF TABLES

TABLE NUMBER		PAGE
1.	Rate of Decomposition of Methane as a Function of Amount of Carbon in the Film	61
2.	Hydrogen to Carbon mole ratios and Initial Rates on C_p, C_b, and C_m at three different Temperatures	110
3.	Conditions of Preparation of Samples for Analysis by Electron Microscopy	115
4.	Conditions of Preparation of Samples for Analysis by X-Ray Diffraction and FTIR	120
5.	Expected Distribution of Peaks for $^{12}C^{13}CH_6$ and $^{13}C_2H_6$ based on Peak Distribution of $^{12}C_2H_6$	130
6.	Expected Distribution of Peaks for $^{12}C^{13}CH_4$ and $^{13}C_2H_4$ based on Peak Distribution of $^{12}C_2H_4$	131
7.	Sample Distribution obtained upon Mass Spectrometric Analysis of Gas Phase Reaction Products	133
8.	Iron Content of the Reaction Vessel after a Water Vapour Gasification Reaction	149
9.	Iron Content of the Reaction Vessel after a Methane Reaction	154

LIST OF FIGURES

FIGURE NUMBER		PAGE
1.	Different Forms of Carbon	3
2.	Buckminsterfullerene	5
3.	The Vacuum Apparatus	28
4.	Yield as a Function of Time with 20 Torr of Methane at 977 K on Quartz	40
5.	Yield as a Function of Time with 20 Torr of Methane at 977 K on C_p	41
6.	Yield as a Function of Time with 20 Torr of Methane at 977 K on C_m	42
7.	Mechanism of Formation of Ethane and Ethylene	46
8.	Rate of Loss of Methane Corrected for Deposited Carbon	48
9.	Rate of Ethane Formation in the Absence and Presence of Oxygen Impurity	49
10.	15 Minute Consecutive Experiments on C_p at 977 K with 20 Torr methane	53
11.	15 Minute Consecutive Experiments on C_m at 977 K with 20 Torr methane	54
12.	15 Minute Consecutive Experiments on heat treated C_p at 977 K with 20 Torr methane	58
13.	log R_o as a Function of [C]	62
14.	log R_o as a Functon of log $P_{methane}$	67
15.	ln R_o as a Function of 1/T for three Methane Pressures	71

16. Rate of Formation of Products as a Function of Temperature with 20 Torr methane on C_p 72

17. Rate of Formation of Products as a Function of Temperature with 200 Torr methane on C_p 73

18. Intermediates Ethylidene and Ethylidyne 78

19. 15 Minute Consecutive Experiments on C_{ppv} at 977 K with 641 Torr methane 83

20. 4 Minute Consecutive Experiments on C_{mpv} at 1026 K with 202 Torr methane 85

21. 15 Minute Consecutive Experiments on C_{ppv} at 977 K with 0.513 Torr methane 86

22. log R_o as a Function of [C] in packed and unpacked vessels 89

23. log R_o as a Function of log $P_{methane}$ in packed and unpacked vessels on Quartz 92

24. log R_o as a Function of log $P_{methane}$ in packed and unpacked vessels on C_p, C_b, and C_m 93

25. Comparison of Rates at 977 K with 200 Torr on four Different Surfaces in the Packed and Unpacked Vessels 94

26. ln R_o as a Function of 1/T on C_m and C_{mpv} above 873 K 98

27. Rate of Formation of Products as a Function of Temperature with 200 Torr methane on C_{ppv} 100

28. log [H] as a Function of log [C] 106

29. H/C as a Function of log [C] 107

30. ln R_o as a Function of 1/T with 20 Torr methane on C_p, C_m and C_b 109

31. Sample Mass Spectrum of Carbon analyzed for the Presence of Fullerenes 113

32. Transmission Electron Micrograph of Carbon Film 117

33.	Illustration of Bragg's Law	118
34.	Experimental Results of XRD Analysis of Carbon Film	122
35.	Curve-Fitted Results of XRD Analysis of Carbon Film	122
36.	Sample FTIR Spectrum of Vitrinite Concentrate (PSMC 52)	125
37.	FTIR Spectrum of Carbon	125
38.	Mass Spectrum of $^{12}C_2H_6$	130
39.	Mass Spectrum of $^{12}C_2H_4$	131
40.	Mass Spectrum of Products after Reaction with $^{13}CH_4$	133
41.	Rate of Carbon Removal in the Absence and Presence of Iron	147
42.	log R_o as a Function of [C] in the Absence and Presence of Iron	153
43.	15 Minute Consecutive Experiments on C-Fe Film at 977 K with 20 Torr Methane	155
44.	Reaction Mechanism	160

ABSTRACT

The goal of this project was to study the reactivity of thin pyrolitic carbon films on quartz, formed from propylene, methane and butadiene, using the methane conversion reaction as a test. The reactivity was compared to that of quartz.

The rate of dissociation of methane on the carbon surface was as much as forty times greater than on quartz. The actual rate increase depended on the precursor of the carbon film. When the reproducibility of the carbon films was tested, the rate was observed to decrease with consecutive experiments. Subsequent analysis showed that small amounts of carbon were deposited during the course of each reaction. Since small amounts of carbon caused inhibition, but carbon films caused catalysis, the rate of formation of ethane, a measure of the rate of dissociation of methane, was determined as a function of the amount of carbon.

The rate was also determined as a function of methane reactant pressure and temperature. All the results indicated that the methane was dissociated on the carbon surface to form methyl and hydrogen radicals. The increase in formation of these radicals led to the increased rate. The subsequent mechanism was similar to the homogeneous mechanism of methane decomposition. In order to confirm this result, the rate was determined in a reaction vessel with a different surface to volume ratio. The surface mechanism was confirmed.

The carbon film was characterized using different techniques. The hydrogen content of the films was determined and related to the reactivity of the carbon formed

from different precursors. The film was studied by electron microscopy, XRD, FTIR and mass spectrometry.

An overall mechanism was developed for the methane decomposition reaction in the presence of carbon which was extended over the different temperature and pressure conditions studied.

Finally, a new technique of synthesizing a catalyst containing carbon and iron, and results obtained in the study of water vapour gasification and methane conversion in the presence of this catalyst are discussed.

CHAPTER 1

INTRODUCTION

1.1 General

Carbon, in all forms, is of tremendous importance to society. Its versatility and strength are only two of the reasons behind the new and varied applications constantly being found for carbon. In the chemical industry alone, carbon is invaluable. In all fields of chemistry, carbon makes important contributions. From its property as an adsorbent to its activity as a catalyst, new applications are continually being developed.

In spite of its seemingly endless capacity to be useful, carbon is also capable of causing much misery, especially in industrial operations. All thermal reactions involving hydrocarbons or any carbon-containing material eventually cause the formation of considerable deposits of carbon. Removal of this carbon involves the expenditure of a considerable amount of time and money.

Thus, carbon exhibits two types of behaviour which may be referred to as positive, in the sense of providing useful applications, and negative in the sense of causing obstruction to industrial processing. While much attention has been devoted to both types of behaviour separately, little attention has been given to the relation, if any, between these opposite effects of carbon. The goal of this thesis is to explore the fundamental properties of carbon which control its reactivity and lead to its diverse uses, applications and constraints.

1.2 What is Carbon?

Carbon is known to form many compounds, in fact more than any other element except hydrogen[1]. When carbon is considered as an element, it is recognized in three main forms: diamond, graphite, and amorphous carbon. The latter is generally considered to encompass any form of carbon which is neither diamond nor graphite.

Diamond is a clear, crystalline form of carbon and is one of the hardest substances known[1]. In a three-dimensional diamond lattice, the carbon atoms are joined by covalent bonds in a tetrahedral geometry, as shown in Figure 1a.

Graphite, the second form of carbon, is well known for its layered structure. Within any layer, the carbon atoms are connected by means of covalent bonds in a fused ring system, such that any layer, if perfect, could be considered as a huge polynuclear aromatic molecule[2]. These layers are held together by means of weak Van der Waals forces. The strength of the bonds within the ring is much larger than that between the layers, and this gives graphite the properties of an excellent lubricant. As shown in Figure 1b, the interlayer distance in graphite is 0.335 nm and the stacking sequence is ABAB although some ABCABC stacking occurs[2]. At the edges of the graphite planes, free valences exist. These sites readily combine with foreign atoms and are generally thought to be responsible for the reactivity of graphite.

Amorphous carbon, otherwise known as microcrystalline carbon, consists of graphite-like layers stacked in packets of 3 - 30 layers which are approximately 1 - 10 nm thick[2]. The interlayer spacing is, however, greater than that found in graphite. The

FIGURE 1

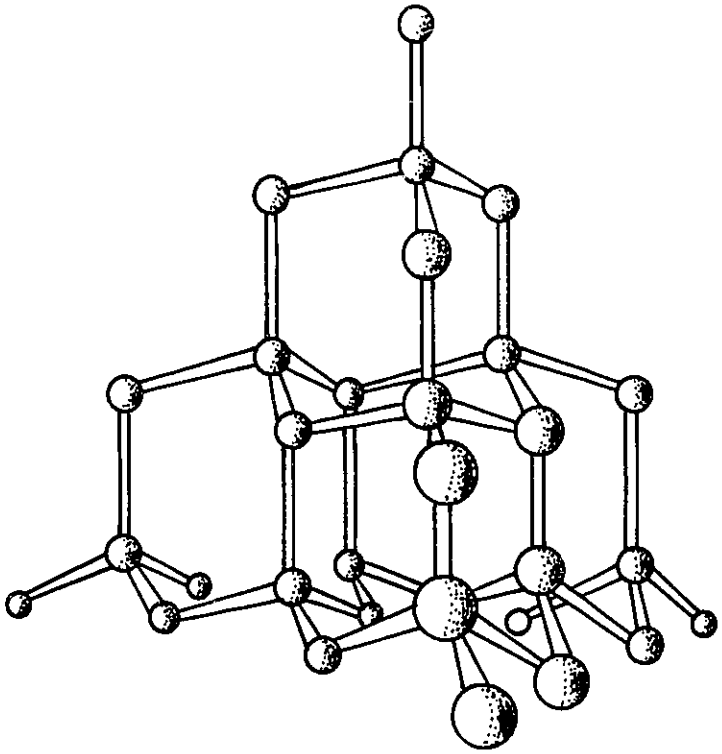

(a) Diamond

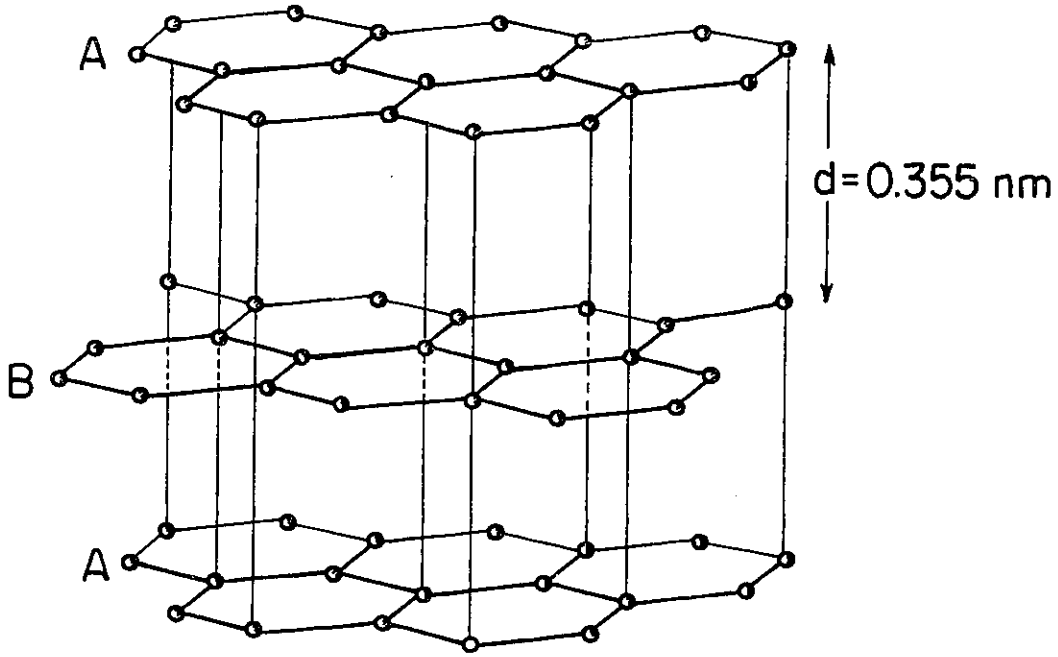

(b) Graphite

stacking sequence is also greatly perturbed, sometimes to the extent that layer planes may be tilted with respect to one another. Some of the layers may be crosslinked by means of disorganized tetrahedrally-bonded carbon. In addition, the layer planes may possess structural defects, such as holes or vacancies, claw and edge defects, and bond isomerism defects. As well, depending on the method of preparation or the source of the amorphous carbon, the layer planes may contain chemical impurities[2]. Amorphous carbon is thus characterized as having domains of minimal size, of the order of a few nanometres, with the perfect order of graphite separated by areas having some change or discontinuity in the arrangement of the constituent atoms[3].

Microcrystalline carbon is the most reactive of the three main forms of carbon. This reactivity is due to the fact that amorphous carbon has the most number of active sites, an active site being a point at which reaction is most likely to occur. Graphitic planes generally have two types of sites: basal plane sites and edge sites. The basal plane atoms adsorb only weakly using a graphitic π-electron system (except at lattice defects). Unsatisfied valences at the edges of the planes are more reactive and hence, edge sites are believed to be the most active sites. Since microcrystalline carbon is significantly more disordered than graphite, it has a greater number of edge sites relative to basal plane sites and this partially explains the greater reactivity of amorphous carbons. The presence of impurities, especially oxygen or halogens, is another factor which is responsible for the increased activity of amorphous carbons.

Soot, coke, and pyrolytic carbon, which may be formed by burning hydrocarbons or other carbon-containing materials, are some examples of well-known and widely

studied microcrystalline carbons. Some commonly used amorphous carbon precursors are Saran, wood, bones, and coconut shells. The carbons which are formed from these materials contain carbon, hydrogen and some impurities, which may be oxygen, sulfur, nitrogen, trace metals or some combination of these. The impurities which remain in the carbon depend on the temperature of formation and any pre- or post-treatment of the carbon. In certain cases, the carbon precursors are chosen because of the impurities they contain.

One other form of carbon which has recently been the focus of a considerable amount of study is Buckminsterfullerene, shown in Figure 2, which is a form of carbon consisting of molecules of C_{60}. It is a member of a class of a new form of carbon called fullerenes, which are even-numbered, spherical clusters of carbon atoms ranging from 44 to 84 (and possibly larger) in number[1]. C_{60} exists as a truncated icosahedron, containing twenty hexagonal and twelve pentagonal faces. While the full range of its chemical

FIGURE 2 Buckminsterfullerene

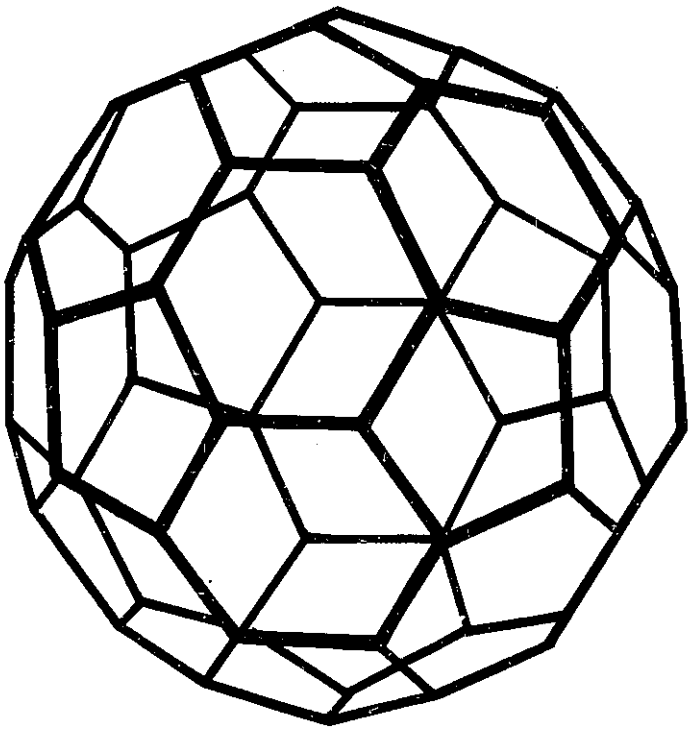

reactivity has not yet been explored, it is known that many different types of molecules can be chemically bonded to the carbon on the surface of the C_{60} cage. Metal ions may also be encapsulated within the cage[1]. Another interesting feature is that Buckminsterfullerene behaves as a superconductor at relatively high temperatures[1]. While Buckminsterfullerene is formed during laser or high-temperature arc vaporization of graphite, it is generally not formed during lower-temperature pyrolysis of hydrocarbons.

1.3 Carbon as an Inhibitor

In all thermal reactions involving carbon-containing materials, the formation of coke or pyrolytic carbon is inevitable[5,6]. Industrially, this is a very serious problem, especially on metal, metal oxide or catalyst surfaces. In some cases, carbon causes serious operational problems by forming a non-reactive film on the metal surface[7]. The carbon may also form whisker-like structures which cause fragmentation of the catalyst particles. In the presence of metal and metal oxide surfaces, carbon deposits arising from the thermal decomposition of carbon monoxide or hydrocarbons, accumulate on pipe or vessel walls, eventually restricting gas passage[8]. This decrease in reactor volume requires an increase in reactant flow rates and pressures in order to compensate for narrower reactor dimensions. Product selectivities and yields are often affected by such changes. Carbon deposits on the surface of heat exchangers adversely affect heat transfer properties. Coke deposits on the walls of heating coils hamper heat transfer from the furnace to the reacting gas. As compensation, external tube skin temperatures must be

raised without exceeding metallurgical limits[5]. Most serious of all, the deposited carbon acts as a poison for the surface, deactivating it over a period of time[6,8,9]. Different catalytic surfaces show varying sensitivity to the poisoning effect of the carbon. Some catalysts deactivate within seconds and some remain operational for months[10]. Thus, the coke deposits often regulate the length of operation cycles between regenerations, since deactivation by coking is more rapid than deactivation by other means such as sintering, poisoning and volatilization[9].

The catalyst surfaces may be regenerated by removal of the carbon deposits. In general, the deposited carbon is believed to exist in two or three different forms. Sárkány, Lieske, Szilágyi and Toth[11] have identified three different forms of carbonaceous deposits which they have labelled as DP-1, DP-2 and DP-3. DP-1 is believed to be a strongly bound, partly dehydrogenated hydrocarbon species. DP-2 and DP-3 are carbon types formed above 663 K and are considered as "coke" present on the metal and the support respectively. DP-2 may be formed either by the "carbon" or "polyene" route. The "carbon" route involves fragmentation of C-H and C-C bonds leading to the formation of surface carbon atoms, which may then migrate on the surface to form carbon islands. This process may be promoted on sites of low coordination such as edges and corners. These atoms may then migrate to the vicinity of the metal-support interface or they may accumulate on low index planes. The suggestion that a carbon deposit may be formed by the successive deposition of reactive carbon atoms has been made by other authors as well[10,12]. The "polyene" route involves formation of carbon by successive dehydrogenation of hydrocarbons to form higher molecular weight hydrocarbons. These

may increase in chain length until they condense in small droplets and deposit on the surface of the metal or support. DP-3 is considered to be a highly dehydrogenated form of carbon which is very difficult to remove and requires higher temperatures to oxidize. It is believed that the formation of coke is most often acid-catalyzed and therefore becomes a major concern when solid acid catalysts, such as zeolites, are used[5,6].

The formation of carbonaceous deposits is undoubtedly of concern to industry as regeneration of catalysts involves controlled combustion of the carbonaceous deposits. The removal of this carbon requires the interruption of production and this involves a tremendous loss of time and money. Thus a considerable amount of research has been directed towards the elimination or reduction of coking.

1.4 Carbon as a Catalyst

Carbon has been used extensively as an adsorbent and a catalyst support[4]. Commercially, active carbons such as carbon blacks effectively remove contaminants from solutions. These active carbons are generally in the form of amorphous carbon. Aika, Hari, and Ozaki[13] have shown that on an active carbon catalyst support in the presence of alkali metals , the activity of ruthenium for the synthesis of ammonia is increased. What is not so well known is that carbon itself exhibits catalytic activity under a wide range of conditions[2,14-18].

Graphitized carbons, or carbons that have been treated at very high temperatures, are known to catalyze hydrogen-deuterium exchange[3]. Hydrogen or deuterium adsorb

dissociatively and exchange occurs on the surface. The mechanism is believed to be the same as that for ortho-para conversion. Other reactions involving hydrogen which are catalyzed by carbon involve dehydrogenation of formic acid and coumarins, and dehydrocyclization of n-alkanes in the range 823 - 873 K. Some recent applications of carbon as a catalyst include dehydrogenation of cyclic sulfides and oxidative dehydrogenation of ethyl benzene and aliphatic paraffins[3].

Polymerization of olefins on carbon has been studied by Hill and Civen[14,15]. The polymerization of methyl olefins, which is accompanied by isomerization, is also known to be carbon catalyzed. Many halogenation reactions have been shown to be catalyzed by active carbons. The decomposition of 1,2 dichloroethane to vinyl chloride and hydrochloric acid and the decomposition of hydrogen peroxide are two examples of reactions which are known to be catalytic in the presence of carbon black or active carbon.

These results show that carbon is capable of acting as a catalyst for a number of diverse reactions. One explanation for this activity lies in the versatile nature of carbon. It is found, in general, that metal-like catalysts, which act as conductors, are suitable for dehydrogenation, hydrogenation and hydrogenolysis. Metal oxides and sulfides, which behave as semiconductors, serve as catalysts for oxidation, reduction, dehydrogenation, and cyclization. Salts and acid-site catalysts, which act as insulators, are important in reactions such as polymerization, cracking, and hydrogen transfer[2]. Carbon, depending on its method of preparation and the treatment to which it may be subjected, is capable of exhibiting all these different types of behaviour. Heat treatment or graphitization

favours metallic behaviour, oxidation favours semiconductivity, and any method which results in the formation of a highly disordered carbon could produce insulator-type behaviour. In addition, the broad spectrum of crystalline properties within a given carbon catalyst may be a partial explanation for the poor selectivity that is observed in certain reactions over carbon.

Several studies have been performed by Hoffman, Vastola, and Walker[16,17] on the pyrolysis of propylene on a carbon substrate. A commercial carbon, Graphon, was used in their study and their results always indicated that the rate of decomposition of propylene on the surface of Graphon was significantly higher than the rate obtained in a quartz vessel. The carbon surface was altered by means of oxidation, or burnoff, in order to increase the number of active sites available on the surface. This increased the rate of decomposition as well and indicated that active sites on the carbon surface were responsible for the decomposition of propylene. Makarov and Pechik[19] observed similar results for methane decomposition on graphitized and non-graphitized carbon blacks as well as channel blacks. The extent of decomposition was dependent on the temperatures studied and the nature of the carbon substrate. Szymański and Rychlicki[4] examined the decomposition of secondary C_3 -C_4 alcohols in the presence of carbon made by decomposition of poly(furfuryl alcohol). Their results indicated that the process of dehydration was controlled by surface processes.

The activity of carbon, derived from different sources and used under varying conditions of reaction, has thus been shown to be of interest with respect to industrially important processes. Evidence for the catalytic nature of carbon, however, can be seen

in other types of reactions. Even when the substrate is a metal, metal oxide or zeolite, carbon has been observed to possess an important role in the reaction pathway.

Much work has been performed by Somorjai and co-workers[20-24] on the importance of carbonaceous deposits formed on platinum surfaces during catalyzed hydrocarbon reactions. Somorjai et al[20] found that commercial catalysts, known to be active for thousands of hours before they need to be regenerated, accumulate steady state levels of carbonaceous deposits that appear to form instantaneously. They maintained that the presence of this deposit was essential to the catalytic chemical process. They believed that the deposited carbon existed on the metal surface in the form of small islands, some two-dimensional and others three-dimensional, and that these islands provided sites for hydrogen transfer and desorption of product molecules. Even though the rate was observed to decrease in some reactions, they did not observe any change in the product selectivity. After a period of time, the carbonaceous deposit was irreversibly transformed to an unreactive coke with decreased hydrogen content. On this carbon, a change in selectivity was observed.

Auger electron spectroscopy results showed that platinum surfaces were always covered with one or more monolayers of strongly bound carbonaceous deposit during steady state hydrocarbon conversion. Somorjai's group believed that in the absence of other chemical additives, the carbon had to be considered as a necessary part of catalytic hydrocarbon chemistry, and that clean platinum could not readily catalyze hydrocarbon conversion[22].

In another series of experiments, Somorjai and co-workers[23] rehydrogenated the carbon formed on the platinum surface. They found that the carbon hydrogenated in two stages: at first, C, CH, and CH_2 fragments quickly rehydrogenated, subsequently, the "coke" rehydrogenated. The latter was a slow process and continued for a long period of time.

Moore and Lunsford[25] investigated the possibility of obtaining commercial grade methane from industrial waste streams by making use of surface carbon on metals such as ruthenium and nickel. They suggested the possibility of a direct reaction between water and the surface carbon.

Webb[26] has presented a comprehensive review of reactions in which carbon has played a catalytic role, even in the presence of metals. He states that evidence exists indicating that hydrocarbon species which actually participate in catalytic reactions are not adsorbed on the metal surface but may be adsorbed on a (hydro)carbonaceous overlayer which effectively covers the metal.

Garner and Hansen[27], during a study of the adsorption and hydrogenation of ethylene on stepped tungsten, concluded that the metal surface was effectively covered by a carbonaceous layer and that reaction occurred by means of a second hydrocarbon layer adsorbed on the first layer. They also suggested that hydrogen transfer from the carbon layer was responsible for hydrogenation of ethylene. Similar results were obtained in many other studies[28-30] for a large range of supported metal catalysts, independent of the nature of the support. In many hydrocarbon conversion reactions, it was clear that

the presence of carbonaceous deposits or coke had positive effects in promoting catalyst selectivity[21,31-33].

McCarty, Hou, Sheridan and Wise[34] found very reactive carbon on nickel catalyst surfaces. They found that carbon atoms chemisorbed on nickel surfaces played a central role in the mechanisms of several nickel-catalyzed reactions. They were able to distinguish several forms of carbon of varying reactivity on the nickel surface. They also found that the temperature at which they observed a maximum rate for a particular carbon state was independent of both the amount of carbon in that state and the temperature of deposition.

Frost, Elek, Yang, Risch and Rabo[35] found that at approximately 300 °C, CO disproportionation on nickel catalysts yielded carbon dioxide and an active surface carbon, which further reacted with water or hydrogen to produce methane. The active carbon consisted in part of carbon adsorbed on nickel, C_{Ni}, and in part of an oxygenated carbon species, CO_{Ni}. In the absence of C_{Ni}, no product was observed. As the ratio of C_{Ni}:CO_{Ni} was increased, the yield of methane increased significantly, indicating the greater reactivity of the C_{Ni} species. It was suggested that the active carbon in the surface layer was partially hydrogenated.

1.5 Carbon as a Catalyst and an Inhibitor

In Sections 1.3 and 1.4, almost all the authors whose work was discussed were ambivalent about the nature of carbon. The authors who referred to carbon as a poison

which deactivated the metal catalyst or zeolite made mention of the fact that carbon was sometimes found to be catalytically active. Authors who focused on the catalytic nature of carbon referred to the fact that it also decreased the rate of the reaction being studied. This dual nature of carbon is not without precedent.

Beginning in the early 1940's and continuing until the late 1960's, many gas kinetic studies were performed in order to determine rates of decomposition or isomerization of organic compounds[36-45]. Most of these reactions were performed in static systems at low temperatures in pyrex reaction vessels. During the course of these reactions, it was noted that the rate of reaction changed and that a gray-coloured deposit was observed in the reaction vessel. Reproducible rates were obtained only if the vessel was "seasoned" prior to the commencement of kinetic studies. This procedure involved introducing an organic compound into the reaction vessel at the temperature of the reaction and allowing a carbon deposit to coat the interior of the vessel. This procedure was repeated anywhere from twenty to one hundred times or until a reproducible rate of decomposition of the particular reactant could be obtained. These films were formed using a number of different precursor compounds, the most common of which was allyl bromide. In general, this procedure lowered the rate of decomposition but gave reproducible results. It was believed, therefore that the higher initial rate was due to heterogeneous processes occurring on the walls of the reactor and that the rate obtained after seasoning was a gas-phase homogeneous reaction rate. This hypothesis was tested by packing the reactor vessel with quartz tubes as a means of increasing the surface to volume ratio in the belief that, if the reaction was heterogeneous, a corresponding increase

in the reaction rate should be observed. Such an increase was generally not observed and it was assumed that this substantiated the assumption that the reaction was homogeneous.

Laidler and Wojciechowski[46] expressed a contradictory opinion in a paper discussing the mechanism of inhibition of certain organic reactions by NO. They extended the mechanism for inhibition by NO in a general way to show how a surface could also act as an inhibitor in similar reactions. They maintained that if both chain initiation and termination occurred on the reaction vessel walls, no rate increase would be observed in a packed vessel when compared to an unpacked vessel. This did not mean, however, that the reaction was homogeneous. Laidler and Wojciechowski thus proposed that the practice of "seasoning" vessels prior to performing kinetic studies was questionable. They further stated that the carbon film, rather than possessing fewer active sites, very likely contained more active sites than clean glass surfaces and that surface processes were therefore enhanced on the carbon surface. This suggestion was further explored by Holbrook[43-45], who measured the ESR spectra of carbon deposits as a means of correlating free spins on the carbon surface with its chemical reactivity. He found that pyrolytic carbon did indeed increase the rate of certain decompositions in the very early stages of reaction, but after longer periods of time, the reactivity decreased.

From the experiments using the seasoned vessels, it seems clear that carbon acted both as accelerator and inhibitor. The reactants which were studied were mostly hydrocarbons, in some cases with halogenic groups.

1.6 Methane Conversion

1.6.1 Methane

Methane is a highly symmetric molecule. It is the most thermodynamically stable hydrocarbon. Its stability is reflected in its large negative Gibb's free energy of formation from its constituent elements, -50.67 $kJmol^{-1}$ at 300 K[48], and the large dissociation energy of the CH_3-H bond, 435 $kJmol^{-1}$. In fact, the bond dissociation energy of the C-H bond in methane is larger than that of the C-H bond in methyl or methylenic groups in higher alkanes[47] (and the C-C bond strength found in all other hydrocarbons).

In addition to its stability, methane has a low chemical reactivity. It thus becomes necessary to use very high temperatures in order to achieve measurable dissociation. The Gibb's free energy required to form ethane is approximately 34 kJ per mole of methane over the temperature range 298 K to 1000 K, and is even higher for the formation of ethylene or acetylene[48]. Thus, it is not difficult to understand why attempts to convert methane to other hydrocarbon products or derivatives involve extreme conditions. Under such conditions, radical processes are dominant and the ability to control product selectivity is greatly reduced. Once a C-H bond is broken in methane, the formation of products, such as ethane and ethylene is very rapid. At the temperatures necessary for dissociation of methane, these other products are rapidly pyrolyzed to produce carbon and hydrogen. Also, once CH_3 has been formed, it is much easier to remove each subsequent hydrogen, thereby accelerating the process $CH_3 \rightarrow CH_2 \rightarrow CH \rightarrow C$. The conversion of

methane to products having industrial applications thus presents some difficulty. At the high temperatures required to dissociate methane, higher molecular weight products are very unstable and cannot easily be recovered.

1.6.2 Natural Gas

While methane is produced by the processing of wastes and as a by-product of petroleum processing, the major source of methane is natural gas. Methane is the main constituent of natural gas, the balance comprised of light alkanes, carbon dioxide, hydrogen sulfide, nitrogen and helium.

Natural gas is located in most areas around the world, with large deposits found in Northern and Eastern portions of the former Soviet Union and in the Middle East[49]. In North America, most of the natural gas is located in the Gulf of Mexico, Alaska, the Southern United States, and Northern and Western Canada. Current world reserves of natural gas are estimated as slightly greater than 10^{14} cubic metres[50]. Canada is estimated as having reserves on the order of 2.4×10^{12} cubic metres, or approximately 2.2% of the world's proven resources, but the actual amount may be as high as 18.33×10^{12} cubic metres or 17 - 18% of the remaining discoverable areas. It is thought that the current world reserves of natural gas will last for 60 years, at the current rate of increase in demand, as opposed to a possible 30 year remaining supply of crude oil[51].

Approximately 7% of the natural gas produced in the world is used in chemical industries. The remainder is used as a fuel for heat and power. However, the low energy

content of natural gas makes it expensive to transport, with transport accounting for almost 30% of the cost. If a means of transport is lacking, the natural gas may be flared at oil sites, a process which is now illegal. In addition, accessibility to many of the areas in the world where there are currently large supplies of natural gas is limited due to geographical and political considerations.

These are only a few reasons why methane conversion is being considered as an important area of research at the present time.

1.6.3 Methane Conversion

Interest in the possibility of synthesis of higher hydrocarbons and liquid fuels from methane arose before World War II. Several methods have been studied and many processes to convert methane have been developed using a wide range of conditions. Nevertheless, as of now, no economically viable means of converting methane to products having commercial significance has been developed. The potential value of a highly selective, economic process for methane conversion and coupling to produce ethane, ethylene, acetylene and higher hydrocarbons, referred to as C_{2+}, increases as the cost of alternative hydrocarbon resources increases. Efforts in the investigation and development of both thermal and catalytic means of converting methane increased significantly during the 1970's and the 1980's. Some of the conversion techniques which have been studied and developed are described below.

1.6.3.1 Thermal Reactions

Thermal conversion of methane occurs by consecutive radical reactions in the gas phase. These reactions can be initiated by high temperatures, photo-activation or laser beams, or radicals derived from gas phase additives.

Chen, Back, and Back[52] studied the fundamental reactions involved in the pyrolysis of methane in a static system, over the temperature range 995 - 1103 K and from 25 - 740 Torr. They observed hydrogen and ethane as primary products, with ethylene, propylene and acetylene as secondary and tertiary products. Under their reaction conditions, no pressure change was seen and the rate in packed and unpacked vessels remained the same. The mechanism of formation of ethane and ethylene was given as follows:

$$CH_4 \longrightarrow CH_3 + H \qquad [1]$$

$$H + CH_4 \longrightarrow CH_3 + H_2 \qquad [2]$$

$$2CH_3 \longrightarrow C_2H_6 \qquad [3]$$

$$H + C_2H_6 \longrightarrow C_2H_5 + H_2 \qquad [4]$$

$$C_2H_5 \longrightarrow C_2H_4 + H \qquad [5]$$

Since secondary products began to form rapidly, Chen et al believed that the initial rate of methane conversion was best measured by the sum of the products ethane and ethylene.

Khan and Crynes[53] presented a summary of results pertaining to methane pyrolysis. Shock tube experiments for methane pyrolysis from 1200 - 1400 K under homogeneous

reaction conditions were represented as

$$CH_4 \rightarrow C_2H_6 \rightarrow C_2H_4 \rightarrow C_2H_2 \rightarrow C \qquad [6]$$

Methane and ethane decomposed by free-radical reactions of short and long chain lengths. Ethylene and acetylene decomposed either by molecular reactions or by radical reactions, depending on the conditions of the reaction. The overall activation energy was found to be 460 $kJmol^{-1}$, which suggested initiation occurred by Reaction [1].

Decomposition of methane in a single pulse shock tube reactor at 1656 - 1965 K, on the other hand, indicated that the high temperature homogeneous reaction of methane was not inhibited by hydrogen[54]. The following mechanism, involving formation of CH_2, was proposed to explain the major observations:

$$CH_4 \dashrightarrow CH_2 + H_2 \qquad [7]$$

$$CH_2 + CH_4 \dashrightarrow 2CH_3 \qquad [8]$$

$$2CH_3 \dashrightarrow C_2H_6 \dashrightarrow \text{Products} \qquad [3]$$

$$CH_2 + H_2 \dashrightarrow CH_3 + H \qquad [9]$$

$$H + CH_4 \dashrightarrow CH_3 + H_2 \qquad [2]$$

$$CH_2 + H_2 \dashrightarrow CH_4 \text{ (Termination)} \qquad [10]$$

Shantarovich and Pavlov[55] studied the decomposition of methane at a pressure of 0.2 Torr in the temperature range 1293 - 1373 °C. They found an overall activation energy of approximately 90 kcal, and their products were mainly ethane, ethylene, and at longer times, acetylene and higher hydrocarbons. Under their experimental conditions, they concluded that methane cracking was a heterogeneous autocatalytic reaction with Reaction [1] as the initiation step and an acceleration step of

$$CH_3 \longrightarrow CH_2 + H \qquad [11]$$

which occurred on a carbon surface.

Palmer, Lahaye and Hou[56] conducted a study of the thermal decomposition of methane in which methane, at a concentration of between 1 and 20 volume percent in helium at a total pressure of 740 Torr, was admitted into a reactor vessel. The temperature range was 1323 - 1523 K and residence times ranged from 0.1 - 0.9s. From this study, it was concluded that nucleation of carbon in the gas phase caused heterogeneous decomposition of methane on the carbon nuclei.

Thermal reactions of methane can be stimulated by the addition of gas phase additives. These form radical species which then attack methane. Such reactions, depending on the additives, form products such as higher hydrocarbons, oxygenated compounds, formaldehyde or chloromethane[57-61].

1.6.3.2 Catalytic Reactions

There appears to be no homogeneous catalytic process for large scale conversion of natural gas[49]. Some organometallic catalysts activate methane even at temperatures below 100 °C, but the conversion is low and the products formed by such reactions have few applications.

The use of heterogeneous catalysis to study methane conversion is the method that has been most studied since 1987. Products of these reactions are higher

hydrocarbons (mostly ethane and ethylene), methanol, formaldehyde and halogenated hydrocarbons. Direct conversion of methane into higher hydrocarbons appears not to be a practical commercial approach[49]. The reactions are highly endothermic and the products are favoured at high temperatures.

One commercially operable process for methane conversion is the MTG process. The MTG process involves sequential formation of syngas from methane, methanol from syngas and subsequently gasoline from methanol. This process makes use of high silica zeolite catalysts. The MTG process has been used in New Zealand since 1985. Another commercially operable process which indirectly involves methane is the Fischer-Tropsch process. The Fischer-Tropsch synthesis involves the formation of gasoline by the reaction of carbon monoxide and hydrogen, produced by steam reforming of coal or natural gas, over a catalyst bed. It is a process which has been utilized in South Africa. In general, these processes are uneconomical. The majority of the costs are associated with the generation of syngas. Thus, if methane could be converted directly, the process would be more economical.

The method of methane conversion which has been the subject of intense investigation since the late 1970's is that of oxidative coupling[62]. As mentioned, methane has a high stability

$$2CH_4 \longrightarrow C_2H_6 + H_2 \qquad \Delta G^\circ = 71.0 \text{ kJmol}^{-1} \text{ @ } 1000 \text{ K}$$

If an oxidant is introduced, the reaction becomes thermodynamically favourable,

$$2CH_4 + \tfrac{1}{2}O_2 \longrightarrow C_2H_6 + H_2O \qquad \Delta G^\circ = -121.6 \text{ kJmol}^{-1} \text{ @ } 1000 \text{ K}$$

Theoretically, higher hydrocarbons can be produced by this process; in practice, products

higher than C_2's are rarely obtained. One of the major problems associated with this process is that complete oxidation to carbon oxides readily occurs. Selectivity thus becomes an issue of great importance.

Oxidative coupling can be effected in two ways. The first is to cycle the reactants. Methane is first introduced onto the catalyst and subsequently oxygen is admitted. There is a smaller chance of explosions occurring by this method. The second method consists of cofeeding methane, oxygen and an inert gas. In general, oxidative coupling reactions occur at temperatures from 900 - 1200 K. At these temperatures, homogeneous reactions play an important role. The reaction is also affected by the reactor volume, and it is essential to minimize the empty space in the reactor.

The catalysts used in oxidative coupling are mainly metals, metal oxides and zeolites. A wide range of metals have been used, from the alkali/alkaline earth metals to the lanthanides and actinides. Much work is being done on improving the nature and the type of catalysts used[63]. Overall, it is difficult to compare the activity of different catalysts, as most studies have been performed at different temperatures and conditions.

The rate-determining step is undecided. Some believe that it could be hydrogen abstraction, while others maintain that it might be the formation of methyl radicals from methane and oxygen in the gas phase. If it is the latter, the role of surface oxides becomes uncertain. It has been found that C_2 production continues after the oxygen supply is terminated, but C_2 production stops if the methane supply is cut. It would appear, then, that the oxygen supply is not the rate-determining step, but studies performed under other conditions indicate that if the partial pressure of oxygen is less

than 20 Torr, the oxygen supply could be a limiting factor. Most data obtained at high temperatures and with the use of efficient catalysts indicates that catalytic formation of CH_3 is fast and equilibrated and subsequent homogeneous reactions will be the rate-determining step for C_2 formation. To increase C_2 yields, it is possible to increase the methane conversion or to increase the C_2 selectivity. Usually, however, if the conversion increases, the C_2 selectivity is lowered.

Alkali promoters are very good because they suppress formation of deep oxides and prevent some catalysts from acting as sinks for CH_3. The disadvantage is that at the high temperatures of oxidative coupling reactions, they may be lost due to their higher volatility.

Attempts to use oxidizing substances other than oxygen, such as NO, CO_2, NO_2, H_2O_2, and O_3, were generally unsuccessful and yielded mostly complete oxidation products.

Methane conversion has been performed over superacids in the presence of other hydrocarbons, such as ethylene. Not much work has been done in this area, although the products are C_2's and higher hydrocarbons and a high selectivity is obtained. Chlorine and chlorohydrocarbons can be used to convert methane, but the products, in general, have little commercial use.

Another potential method is electrochemical conversion, using either electrochemical oxidation or conversion of methane in hydrocarbon based fuel cells. This method is based on the dissociative adsorption of methane on metallic and metal oxide surfaces. Ultimately, the products obtained by this method are deep oxides.

At present, the role of the catalyst in oxidative coupling is to facilitate the removal of one hydrogen from methane, usually by means of the metal oxides or O^- located at the catalyst surface. Most of the hydrocarbon reaction following this step occurs in the gas phase. Certain catalysts also work to block formation of CO_x and to prevent CH_3 from being retained on the catalyst surface.

A recent method of methane conversion, involving mercury-photosensitized reactions of methane, has been reported[64], although the conversions are low. This photochemical reaction occurs via the photoexcited state of mercury atoms, Hg* ($^3P_1$, $d^{10}s^1p^1$). In a later paper, the authors[65] reported that the abstraction of a hydrogen atom from methane or ethane by Hg* is not efficient because of their poor interaction. They examined the formation of a Hg^*/NH_3 exciplex which, in turn, led to the formation of the NH_2 radical. This powerful H abstractor was capable of functionalizing methane and ethane, resulting in the formation of imines. Periana and coworkers[66] also reported the use of Hg(II) as a catalyst for the oxidation of methane by concentrated sulfuric acid to produce methyl bisulfate, water and sulfur dioxide, with a high selectivity to methyl bisulfate. It was suggested that the Hg(II) ion reacts with methane by an electrophilic displacement mechanism to produce CH_3HgOSO_3H, which readily decomposes to CH_3OSO_3H and the reduced mercurous species Hg_2^{2+}. The mercurous species is then reoxidized to Hg(II) by H_2SO_4. This reaction also occurred when the cations of platinum and gold were used in place of mercury, although conversion was poorer.

1.7 Goals of this Study

A significant amount of work has been performed to study the nature of carbon in different forms. The results show quite clearly that carbon plays a dual role under many reaction conditions. It is capable of increasing reaction rates, and in some cases, it is essential to the mechanism of the reaction. Yet equally so, it inhibits reactions and deactivates catalysts. This seemingly contradictory nature of carbon has never been examined under one set of reaction conditions. Previous studies had shown that these uniform films of carbon, of approximately 10 - 30 nm thickness, were formed on the surface of a quartz reaction vessel by pyrolysis of methane under controlled conditions. Such films are ideal for kinetic studies, and therefore, similar films were used in the present study.

As a means of understanding the nature of the reactivity of carbon, the methane conversion reaction was chosen. The decomposition of methane has also been extensively studied and the homogeneous mechanism is well-known.

It is possible that carbon will catalyze the decomposition of methane to higher hydrocarbons. The advantage to this method of conversion is that the products will only be hydrocarbons and no loss to oxygenated products will occur. As carbon is inexpensive compared to many other commercial catalysts, this could prove to be an economical method of converting methane.

Thus the fundamental goal of this project was to study the dual nature of carbon, as catalyst and inhibitor, using the methane conversion reaction as a test.

CHAPTER 2

EXPERIMENTAL

2.1 Apparatus

The pyrolysis experiments in this work were performed in a conventional static system. The apparatus is described in Figure 3. A Welch Duo-Seal rotary pump was used to evacuate the main vacuum line, which was constructed from pyrex, to ~10^{-3} Torr. A water-cooled mercury diffusion pump was initiated to evacuate the system to ~10^{-6} Torr. All the stopcocks (labelled in Figure 1 as S1 - S15) except S13 and S16 were made of pyrex and were all high-vacuum stopcocks. They were lubricated using Apiezon N grease. S13 and S16 were Nupro metal bellows valves. A liquid nitrogen bath was placed around the U-trap, T1, in order to prevent mercury vapour from entering the vacuum system. The pressure in the main vacuum line was initially determined by use of the McLeod gauge (ML), and subsequently confirmed by the use of the Penning gauge (P3). The use of the McLeod gauge was discontinued in order to minimize the possibility of contamination of the vacuum system by mercury vapour. A 10 Torr Baratron gauge, P1, and a 1000 Torr Baratron gauge, P2, were used to monitor the system pressure during experiments. These gauges were set to zero after the system pressure was confirmed as being lower than 10^{-5} Torr.

The cylindrical quartz reaction vessel was 11.5 cm in length and had an inner diameter of 4.2 cm. The mass of the reaction vessel was measured when it was empty

FIGURE 3 Vacuum Apparatus

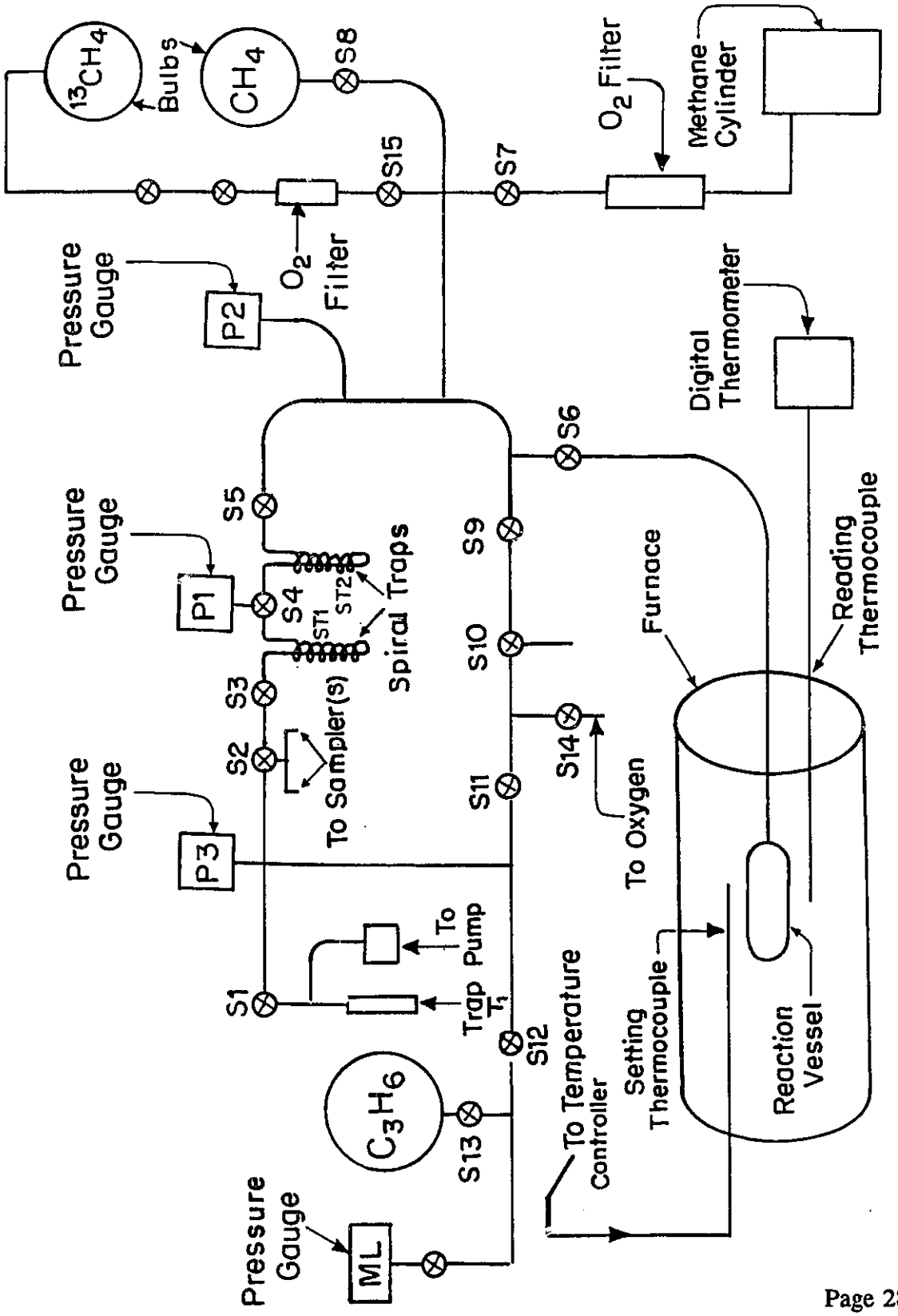

and when it was filled with water. The mass of water occupying the reaction vessel was converted to volume using the density of distilled water and it was determined that the reaction vessel had a volume of 136 mL. The vessel was constructed such that the ends of the vessel were hemispherical. Since the dimensions of the vessel were known, the surface area was calculated as being 152 cm^2. From the centre of one end of the vessel, a quartz tube connected the vessel through a graded seal to the pyrex vacuum line. The reaction vessel was enclosed in a 60 cm long quartz tube having an inner diameter of 6.7 cm. The reaction vessel was annealed prior to its insertion in the system. No further treatment was considered necessary.

The reaction vessel was heated using a 2.4 kW autoclave high-temperature cylindrical furnace manufactured by Autoclave Engineers Inc. which was connected to a Barber-Colman temperature controller. A 3 foot MgO-filled Inconel 600 sheath Type K thermocouple was connected to the temperature controller and its tip was located at the centre of the furnace beside the reaction vessel. The reaction temperature was monitored using a similar thermocouple connected to a Wahl Digital Heat-Prober Thermometer. This thermocouple was placed at the other end of the furnace and located on the other side of the reaction vessel with its tip at the centre of the furnace.

2.2 Analytical System

A Hewlett Packard 5790A Series Chromatograph with 5706A Dual Differential Electrometer connected to a Hewlett Packard 7123A chart recorder was used to analyze

hydrocarbon products. Complete separation of the residual reactant methane and the products ethane, ethylene, propylene, acetylene, and allene was obtained at room temperature (297.5 ± 0.5 °C) using a 6m x 1/4" column of 80-100 mesh Durapak, phenylisocyanate on porasil C. The carrier gas, Ultra High Purity Nitrogen (Air Products, 99.999%), was passed through a molecular sieve and a hydrocarbon trap (Chromatographic Specialties) at a flow rate of 29 $mLmin^{-1}$ before collecting the sample and reaching the flame ionization detector (FID). The separation of the hydrocarbon products on the column took approximately 30 minutes.

A Hewlett Packard F&M Scientific 5750 Research Chromatograph connected to a Hewlett Packard 7133A chart recorder was used to analyze the carbon dioxide produced by removal of the carbon films. The thermal conductivity detector (TCD) was operated at 150 mA and the carrier gas, Helium (Air Products, High Pressure Industrial Grade, 99.995%), was passed through a molecular sieve and a hydrocarbon trap (Chromatographic Specialties) to ensure its purity. Separation of the carbon dioxide from air was achieved on an 8' x 1/8" column of 80 - 100 mesh Porapak QS at 338 K with a helium flow rate of 34 $mLmin^{-1}$. The pressure of water produced from the oxidation of the carbon films was measured by expansion in a known volume at room temperature.

2.3 Materials

Research Purity Methane (99.999%) was obtained from Matheson Gas Products, Inc. It was found to contain approximately 0.1 ppm ethane.

A small trace of oxygen was removed from the methane by passing it through an oxygen trap (Oxi-Sorb, Matheson Gas Products, Inc.). The presence of this trace of oxygen was determined during the course of several reactions. This will be discussed in a later section. The ethane was not removed from the methane.

The carbon films were formed from the methane, from Research Purity propylene (99.6%), obtained from Matheson Gas Products, Inc., or from Research Grade butadiene (99.8%), obtained from Matheson Gas Products, Inc. The propylene was stored in a bulb (B2) on the vacuum line. Before use, it was condensed in liquid nitrogen and subjected to a freeze-pump-thaw cycle until the pressure was no more than 2×10^{-5} Torr.

Once the experiments requiring the use of propylene were completed, the bulb (B2) was evacuated until the residual pressure in the system was below 2×10^{-5} Torr. Air was admitted into the bulb and the bulb was again evacuated. This procedure was repeated three times and the residual pressure in the system was maintained below 2×10^{-5} Torr. Butadiene was then introduced into a storage bulb (B2). Before use, it was condensed in liquid nitrogen and subjected to a freeze-pump-thaw cycle until the residual pressure was no more than 2×10^{-5} Torr.

Methane-d_4 and ^{13}C methane with minimum isotopic purity of 99% in D atom and ^{13}C atom respectively were obtained from Merck, Sharpe and Dohme, Canada Ltd. Prior to use, they were passed through an oxygen trap (Oxi-Sorb, Matheson Gas Products, Inc.).

2.4 Experimental Procedure

2.4.1 Deposition of the Carbon Film

The furnace was maintained at the temperature of deposition of the carbon film. This temperature was 977 K when propylene was pyrolyzed to prepare the carbon film, 1223 K when methane was used, and 873 K when butadiene was used to prepare the carbon film.

A known pressure of propylene was admitted to the reaction vessel and S6 was closed. The reaction was allowed to proceed at 977 K for a fixed time, after which the contents of the reaction vessel were evacuated until the pressure was ~10^{-5} Torr.

Methane was flushed through the oxygen filter three times. A known pressure of methane was then admitted to the reaction vessel and the reaction was allowed to proceed at 1223 K for a fixed time. The subsequent procedure was identical to that for the propylene film.

A known pressure of butadiene was admitted to the reaction vessel and S6 was closed. The reaction was allowed to proceed at 873 K for a fixed time, after which the contents of the reaction vessel were evacuated until the residual pressure was ~ 10^{-5} Torr.

2.4.2 Methane Reaction

Once the carbon film had been deposited, the main vacuum line was kept under continuous evacuation and the system pressure was monitored until the carbon film was

completely degassed and the pressure was no more than 10^{-5} Torr. This was to ensure the removal of occluded hydrogen. Before any experiments were performed, the reaction vessel was isolated for approximately 30 - 45 minutes. If the reaction vessel was unable to maintain a vacuum of 10^{-5} Torr, the line was evacuated again until the vessel was capable of maintaining the vacuum. Once the reaction vessel was found to maintain the vacuum, S6 was closed. S7 was opened and the methane was flushed through the oxygen filter three times. S8 was opened, S5, S9, S15 and S6 were closed. A known pressure of methane was admitted into this volume and S7 was closed. S6 was then opened to admit this pressure of reactant into the reaction vessel. S6 was closed immediately. S8 was closed and then S5 and S9 were opened in order to evacuate the vacuum line. The reaction was allowed to proceed for a fixed time. Once the vacuum line had reached a pressure of ~10^{-5} Torr, ST2 was immersed in a dry ice/acetone bath and ST1 was immersed in a liquid nitrogen bath. When the reaction was complete, S5 and S9 were closed and S6 was opened. The pressure of the contents of the vessel was measured using P2. S5 was opened slowly in order to allow the gaseous material to pass through the two spiral traps. When all the material had been removed from the vessel, S6 was closed. S5 was closed and S4 was rotated to face the volume between S3 and S4. A liquid nitrogen bath was placed around the sampling loop and S2 was rotated to face S3. The liquid nitrogen bath around ST1 was replaced with a warm water bath, allowing the contents of the spiral trap to distill into the sampling loop. When all the contents had been transferred, the sampling loop was closed and S2 was opened again to evacuate the line. S4 was then rotated to isolate ST2. The dry ice/acetone bath was removed and P1

was used to measure the pressure as the contents were allowed to expand in ST2. The sampling loop was removed from the vacuum line and attached to a six-port valve, through which the sample was admitted to the analysis system. The entire vacuum line was then evacuated until the pressure was once again ~10^{-5} Torr.

2.4.3 Removal of the Carbon Film

S6 was closed and the reaction vessel was heated to ~1123 K. S14 was opened and oxygen (Air Products, Ultra-Pure Carrier Grade, min. pur. 99.994%) was flushed twice. S11 and S5 were closed and ~500 Torr of oxygen was admitted to the vacuum line. S6 was opened to admit the oxygen to the reaction vessel and then closed immediately. S11 and S5 were then opened in order to evacuate the system. ST2 was immersed in a dry ice/acetone bath and ST1 was immersed in a liquid nitrogen bath. After 20 minutes, S9 and S5 were closed and S6 was opened. The pressure of the contents of the reaction vessel was noted on P2. The contents of the vessel were evacuated through the two spiral traps. When the contents were completely removed, S6, S5 and S3 were closed. S4 was rotated so as to face S3. Approximately the same amount of oxygen was admitted using the same procedure described previously. After 20 minutes, the contents of the vessel were evacuated through the two spiral traps, thus adding any condensed products to those obtained with the first aliquot of oxygen. This procedure was repeated one more time. The contents of ST1 were distilled into the sampling loop immersed in liquid nitrogen. A warm water bath was used to warm up the

nitrogen. The pressure of the contents of ST2 was measured using P1. The sampling loop was transferred to an inlet system allowing the products to be analyzed by the TCD.

2.4.4 Summary of Other Experimental Procedures

In the following chapters, the experimental procedures for a particular group of experiments are described in each section in which the results are discussed. These sections describe the measurements of the yield as a function of time, the consecutive reactions, the dependence of the rate on the temperature and on the pressure and experiments designed to characterize the carbon film. Similar sets of experiments were performed in the vessel packed with quartz tubes to increase the surface to volume ratio.

CHAPTER 3

RESULTS

3.1 Introduction

In this section, the results obtained from the experimental procedures described in Sections 2.4 will be presented. In order to clarify the nature of these experiments, a short introduction, explaining the purpose of the experiment, is included. The experimental procedure is described in detail and the results obtained from this experimental procedure are summarized. A discussion section is included in order to interpret the results and where necessary, to explain why the experiments in the following section were performed. In Chapter 6, all the results will be combined and an overall interpretation will be presented.

3.2 Yield as a Function of Time

3.2.1 Introduction

As outlined in Section 1.7, the goal of this study was to determine the nature of the carbon film, by way of its reactivity, using methane conversion as a test reaction. In order to determine the extent of the influence of the carbon, it was necessary to determine the rate of reaction, as well as the product distribution, obtained in the absence of carbon.

The variation of the product yields as a function of time was measured in the quartz vessel and the product distribution was compared with results obtained by other authors. These results were then compared to results obtained when the same reaction was performed in the presence of a carbon film.

3.2.2 Experimental

3.2.2.1 In the Absence of Carbon

20 Torr of methane, purified as described in Section 2.3, was admitted into the reaction vessel maintained at 977 K. The reaction was allowed to proceed for fixed times, usually three for each condition of pressure and temperature. For these conditions the times were 15, 30 and 60 minutes, performed in random sequence. Upon completion of the reaction, the contents of the reaction vessel were evacuated through the two spiral traps, ST1 and ST2, as described in Section 2.4.2. The condensed products were removed for analysis as described in Section 2.2. After analysis, the sampler was reattached to the vacuum line and evacuated until the pressure was below 2×10^{-5} torr. The time which elapsed between the completion of the first reaction and the commencement of the second reaction was between 30 to 40 minutes. During this time, the reaction vessel was kept isolated from the remainder of the system. Before the second reaction was initiated, the reaction vessel was opened to the vacuum system and the pressure was measured. If the pressure was above 2×10^{-5} torr, the reaction vessel was evacuated until the pressure

decreased below this value. Once the system pressure was determined to be satisfactory, 20 Torr of methane was again admitted into the reaction vessel, which was at 977 K. After the third reaction, any carbon which may have been deposited was removed by the procedure described in Section 2.4.3.

The entire procedure was repeated for methane pressures of 50 Torr, 200 Torr and 640 Torr.

3.2.2.2 In the Presence of Carbon

The carbon films used in the yield-time experiments were formed from two different precursors. The films made from propylene, C_p, were formed by pyrolysis of 21.2 Torr of propylene at 976 K for 3 hours, by the method described in Section 2.4.1. The films made from methane, C_m, were formed by pyrolysis of 50.2 Torr of methane at 1218 K for three hours, by the method described in Section 2.4.1.

In the presence of carbon, the yield as a function of time was determined after 14 - 16 consecutive experiments were performed. These will be described in Section 3.3. After the consecutive experiments were performed, the reaction vessel was evacuated thoroughly. 20 Torr of methane was then admitted to the reaction vessel, and the subsequent procedure was the same as that described in Section 3.2.2.1. Upon completion of the experiments to determine the yield as a function of time, the carbon in the reaction vessel was removed by the method described in Section 2.4.3.

3.2.3 Results

Some typical plots of the yield as a function of time, on quartz as well as on C_p and C_m, are presented in Figures 4, 5, and 6. The major products were found to be ethane and ethylene. In some cases, small amounts of propylene were observed. At longer times, and at higher temperatures and pressures, some acetylene and allene were also formed.

In the absence of carbon, the overall conversion after fifteen minutes was small and varied between 0.002 and 0.05% in the pressure range of 20 to 640 Torr on quartz. In the presence of carbon, the overall conversion ranged from 0.05 for 20 Torr on C_m to 0.1% for 200 Torr on C_p.

The absolute yield of products was up to 40 times higher on the carbon surface than on quartz. The yields and the rate were higher on C_p than on C_m by a factor of approximately 5, although both rates were higher than on quartz.

The sum of the products ethane and ethylene was linear with time up to 30 minutes. At times greater than 30 minutes, the sum fell from linearity.

3.2.4 Discussion

The results obtained are consistent with those found by other groups who have studied methane conversion. Chen, Back and Back[52], whose system and conditions were similar to those used in this work, obtained yields and product distributions comparable

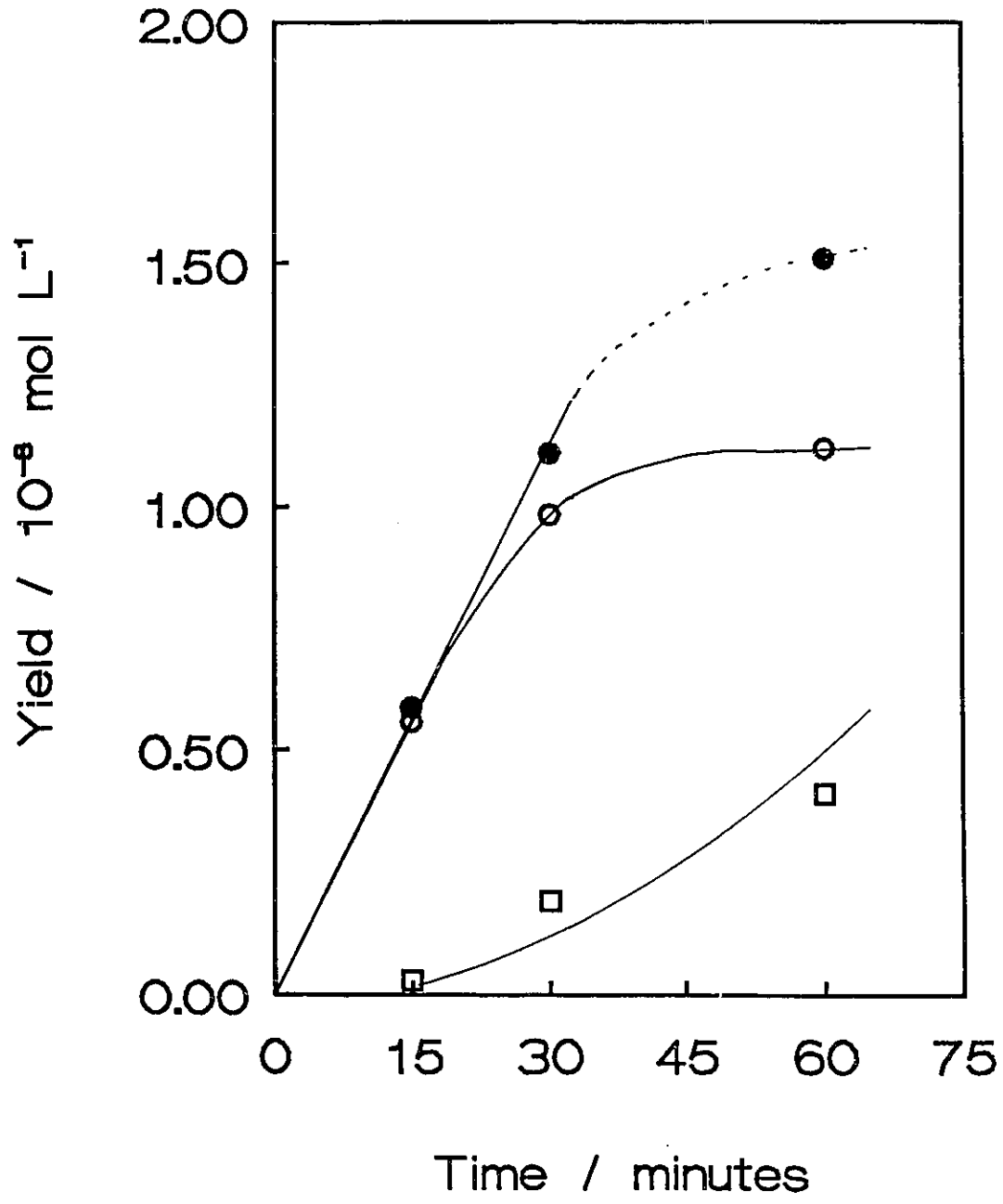

FIGURE 4 Yield as a function of time for methane decomposition using 20 Torr of methane on quartz at 977 K.
○ ethane □ ethylene ● sum of ethane and ethylene

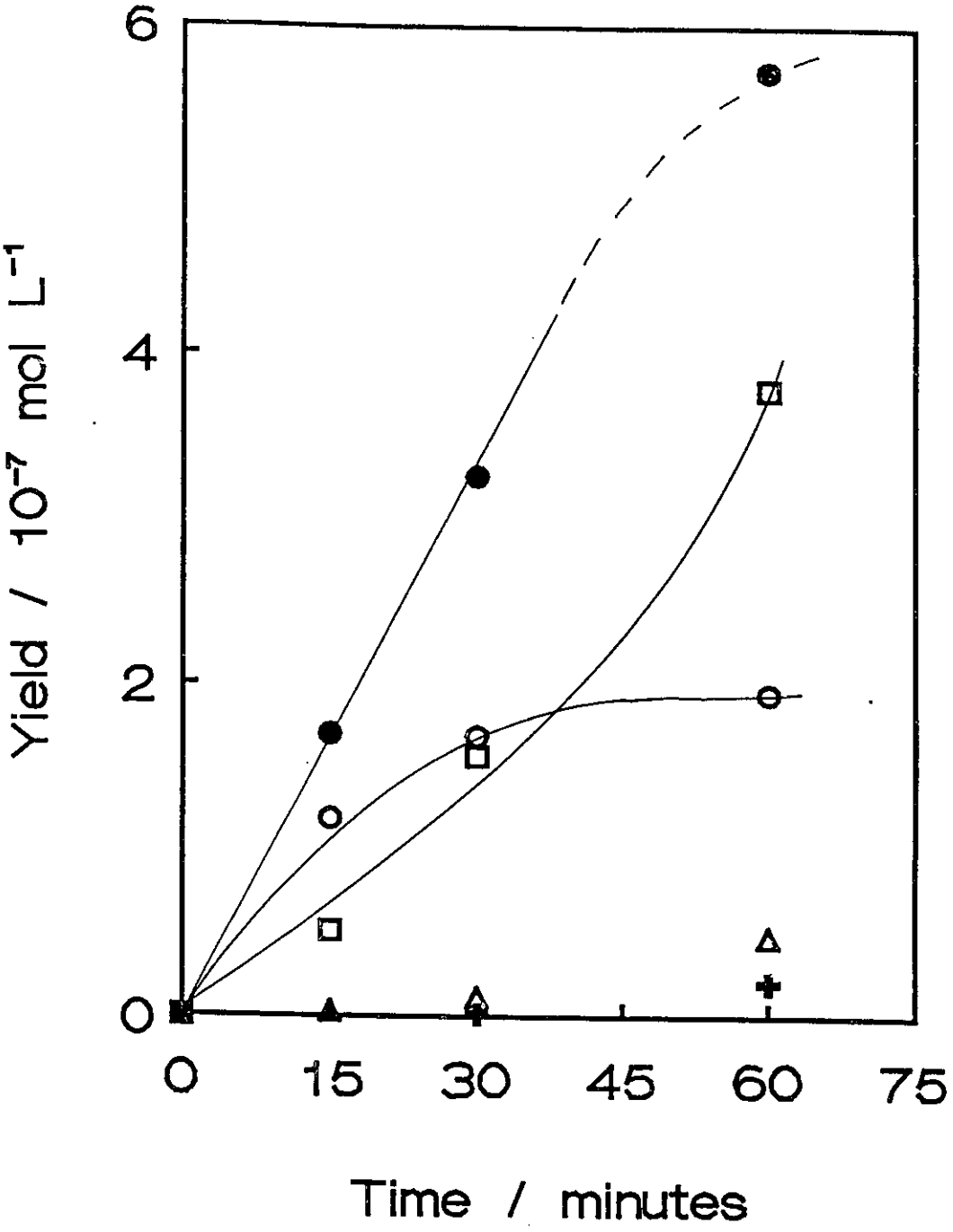

FIGURE 5 Yield as a function of time for methane decomposition using 20 Torr methane at 977 K over a carbon film formed by pyrolysis of 21.2 Torr propylene at 976 K for three hours.
○ ethane □ ethylene ● sum of C_2H_6 and C_2H_4 △ propylene
+ acetylene

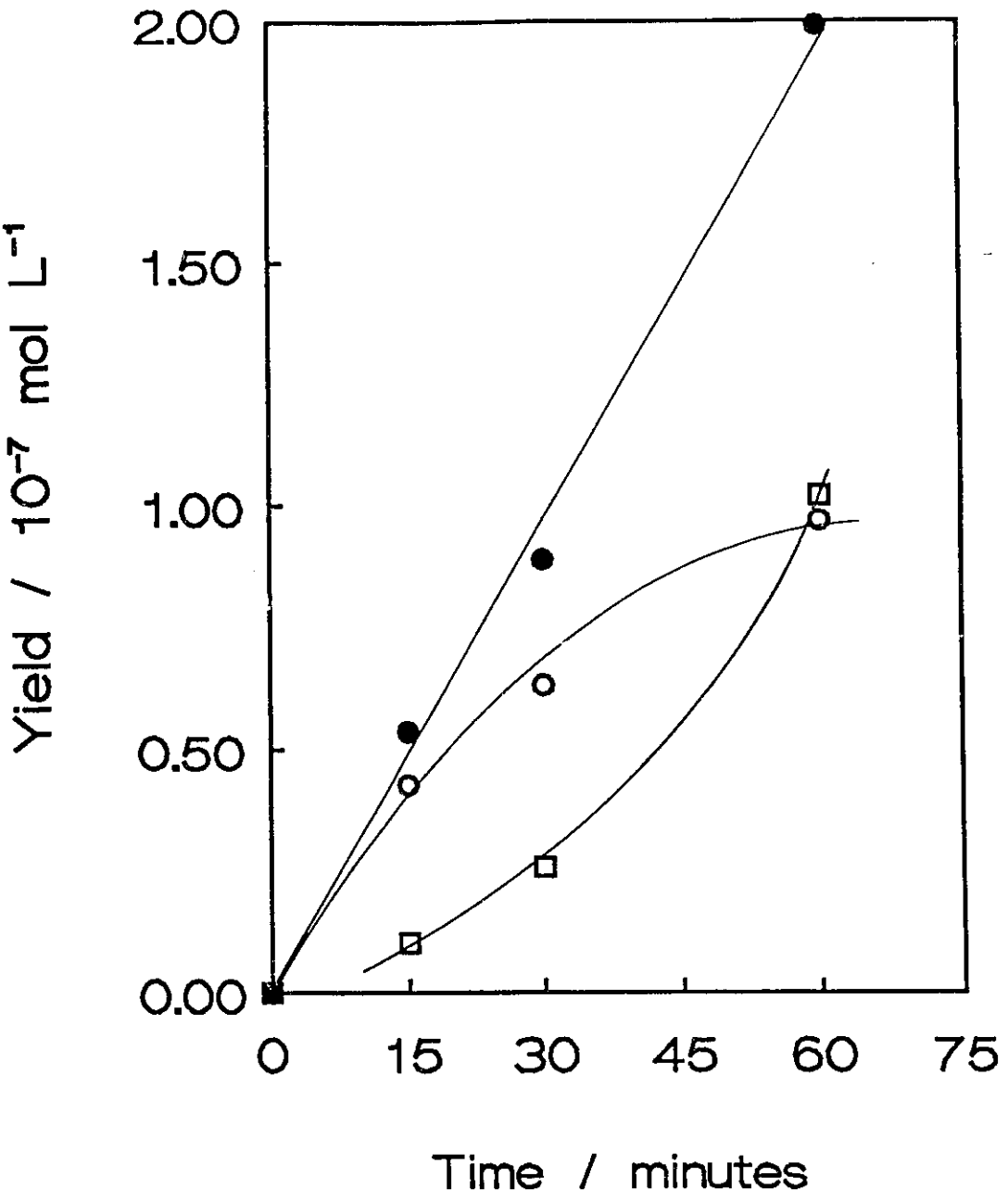

FIGURE 6 Yield as a function of time for methane decomposition using 20 Torr methane at 978 K over a carbon film formed by pyrolysis of 50.2 Torr methane at 1218 K for 3 hours.
○ ethane □ ethylene ● sum of ethane and ethylene

to those shown in Figure 4. At a temperature of 995 K and over a pressure range of 51 Torr to 640 Torr, Chen[67a] found the percentage of methane converted in a quartz vessel to be in the range of 0.002 to 0.06%. Other authors[53-57] have obtained similar products. Their product distributions, however, varied due to their respective experimental conditions and systems.

Based on the following stoichiometric equations,

$$2CH_4 \rightarrow C_2H_6 + H_2 \qquad [14]$$

$$2CH_4 \rightarrow C_2H_4 + 2H_2 \qquad [15]$$

$$3CH_4 \rightarrow C_3H_6 + 3H_2 \qquad [16]$$

$$2CH_4 \rightarrow C_2H_2 + 3H_2 \qquad [17]$$

the first order rate constant was calculated from the products as follows:

$$\frac{\Delta}{\Delta t}[2C_2H_6 + 2C_2H_4 + 3C_3H_6 + 2C_2H_2] = -\frac{\Delta CH_4}{\Delta t} = k[CH_4] \qquad [18]$$

In most cases, the amounts of propylene and acetylene produced were negligible and did not significantly affect the calculation of the initial rate.

From Equations [1] - [5], as described in Section 1.6.3.1, the rate of dissociation of methane could be equated to the initial rate of formation of ethane, as follows:

$$k_1[CH_4] = R^\circ_{ethane} = R^\circ_{hydrogen} \qquad [19]$$

where R° indicates an initial rate of formation. Experimentally, it was very difficult to measure initial rates accurately, as formation of secondary products became important at low conversions. Therefore, R° was equated to $R(C_2H_6 + C_2H_4)$, which corrected for loss of ethane by reaction [4][67a].

The initial rates were calculated using this method and the rates obtained were in close agreement with those obtained by Chen et al[52] after temperature and pressure corrections were made. This indicated that the dissociation reaction of methane on the quartz surface followed a homogeneous mechanism as long as the sum of ethane and ethylene was linear. This appeared to be valid until reaction times of 30 minutes. After this time, a deviation from linearity was observed as the rate of formation of product decreased. This decrease was not observed by Chen et al. The only significant difference in experimental procedure between this study and Chen's study was that Chen removed any carbon formed during the reaction from the reaction vessel between successive experiments. In this study, the carbon was not removed until the yield had been determined as a function of time. This suggested that some material must have been deposited on the reaction vessel walls which caused the rate to decrease.

On C_m, the rate of decomposition of methane was greater than that on quartz by a factor of eight, while on C_p, the rate was increased over that on quartz by a factor of approximately forty. The products and their distribution, however, remained the same. This led to the conclusion that the carbon was responsible for a new initiation step. The mechanism was thus rewritten to include new steps which would account for the increased dissociation of methane, as follows:

$$CH_4 + 2C(s) \rightarrow CH_3\text{-}C(s) + H\text{-}C(s) \qquad [20]$$

$$CH_3\text{-}C(s) \rightarrow CH_3 + C(s) \qquad [21]$$

$$H\text{-}C(s) \rightarrow H + C(s) \qquad [22]$$

Equations [20] - [22] precede Equations [1] - [5] and account for the increased rate of dissociation of methane while maintaining the products and their distribution. Thus, methane dissociation is accelerated by carbon, producing CH_3 and H, which may continue to react according to the homogeneous mechanism. It is also likely that in addition to the homogeneous reaction of these species, some surface reaction may occur.

The reactions which the adsorbed methane may undergo are presented pictorially in Figure 7. The methane dissociates on the surface of the carbon to form the species CH_3 and H. These species may desorb from the surface to react homogeneously in the gas phase. Alternately, a reaction may occur between two CH_3 species on the surface to produce ethane, which would then desorb. Ethylene could then be formed by homogeneous reactions in the gas phase or by surface reactions. If the CH_3 remained on the surface at an active site long enough to dehydrogenate to CH_2, a surface reaction could occur between two CH_2 groups to form ethylene, which would then desorb.

The plots of yield as a function of time were once again examined. At longer times, on quartz most noticeably and on C_p and C_m to a lesser extent, the sum of the products ethane and ethylene deviated from linearity. This effect was not as noticeable in experiments on the carbon films, as can be seen from Figures 5 and 6, due to the fact that many experiments had been previously performed on the surface of the carbon. Other results, which will be presented later, indicate that the film eventually stabilizes. It was concluded that this decrease was due to the deposition of a small amount of carbon on the walls of the reaction vessel. In order to test this conclusion, the amount of carbon recovered upon completion of the yield-time measurements was added to the sum of

FIGURE 7 Mechanism of Formation of Ethane and Ethylene

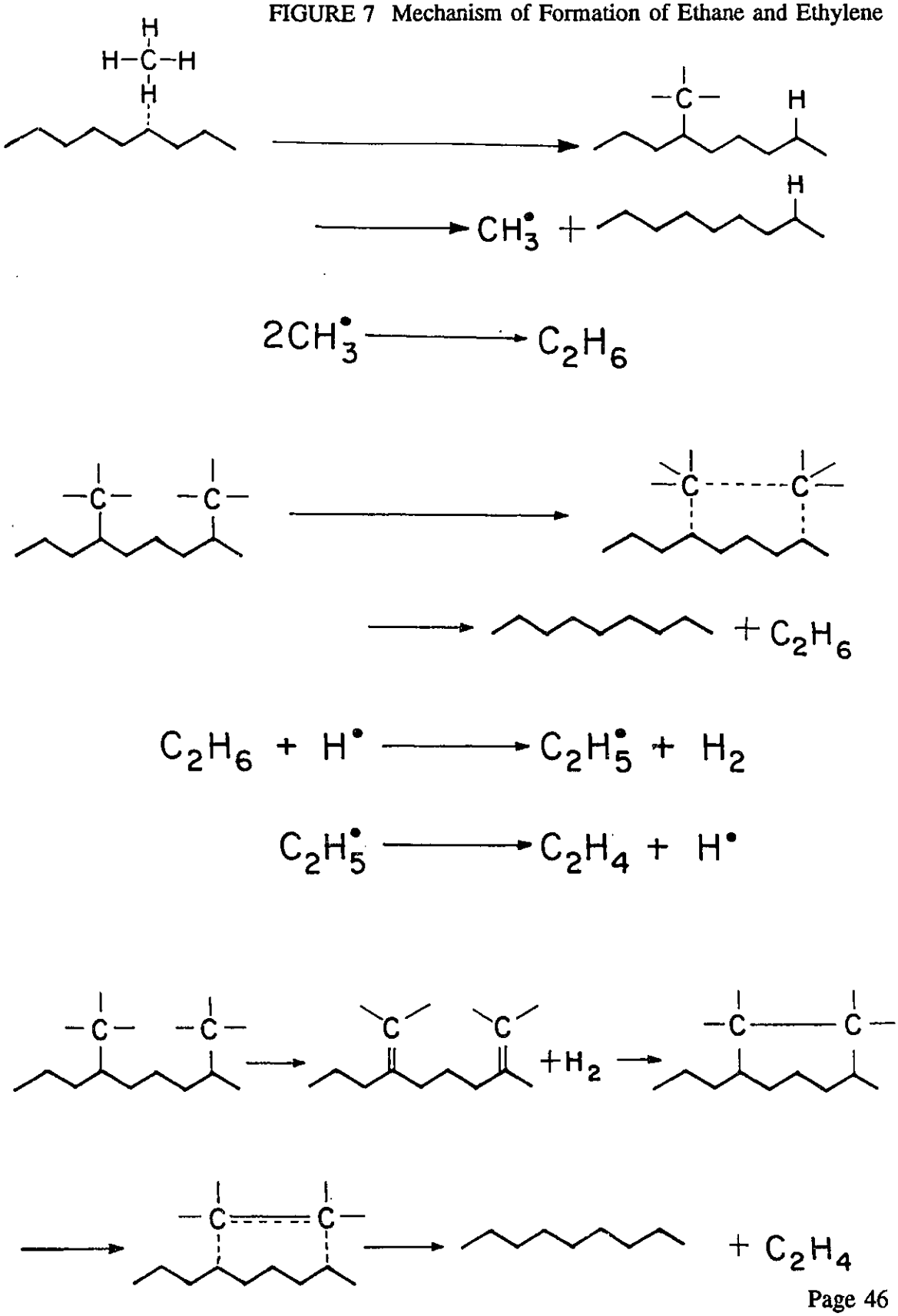

measurements, which was determined as described in Section 2.4.3, was added to the sum of products and, as shown in Figure 8, linearity of the plot was restored. This drop in the rate is important to the interpretation of the results and will be discussed in detail later.

3.2.4.1 Oxygen as a Contaminant

Throughout these experiments, extreme care was taken to prevent the intrusion of even minute quantities of oxygen into the reaction system. Figure 9 shows a plot of yield as a function of time at 976 K in which 200 Torr of methane was introduced as the reactant. Initially, before the addition of an oxygen trap to the methane cylinder, it was found that the sum of ethane and ethylene was linear but did not pass through the origin. After the oxygen trap was added to the methane cylinder, the sum of ethane and ethylene remained linear, retaining the same slope as the original line, but passing through the origin. Thus, without the presence of the oxygen trap, the sum of ethane and ethylene was increased by a small factor. This increase was undoubtedly due to the presence of a small quantity of oxygen which was present in the methane cylinder and which entered the reaction vessel along with the methane. When the methane passed through an oxygen filter before entering the reaction vessel, the oxygen was successfully removed.

Oxygen reacted rapidly with methane to form methyl radicals and thus increased the rate of formation of ethane. Oxygen itself was rapidly converted to water and was thus rendered relatively inert in this system. A possible sequence of reactions is given below, although other reactions may also occur.

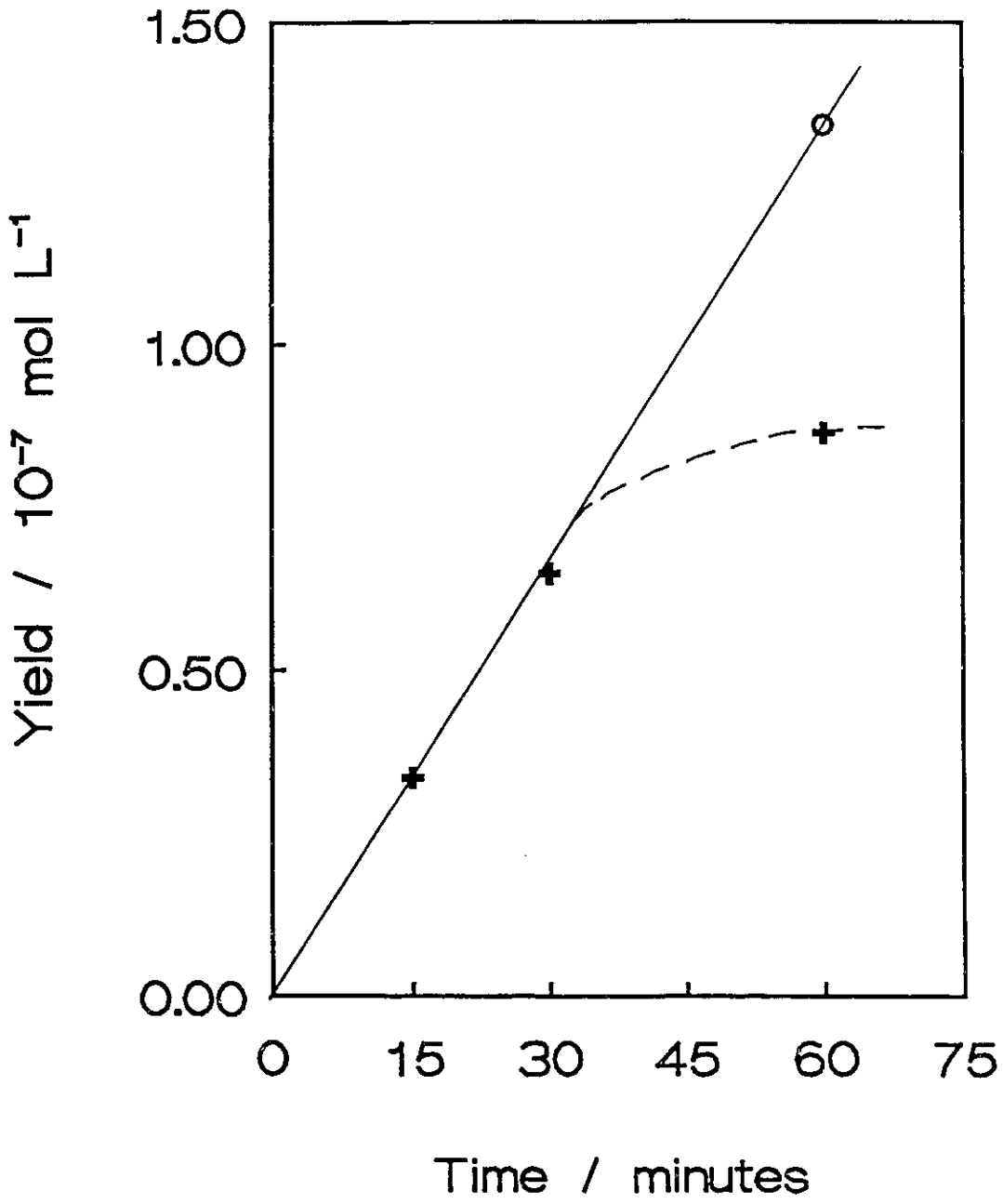

FIGURE 8 Loss of methane as a function of time using 641Torr methane at 976 K on quartz.
+ loss of methane based on sum of gas phase products only
o loss of methane based on sum of gas phase products and carbon at 60 minutes

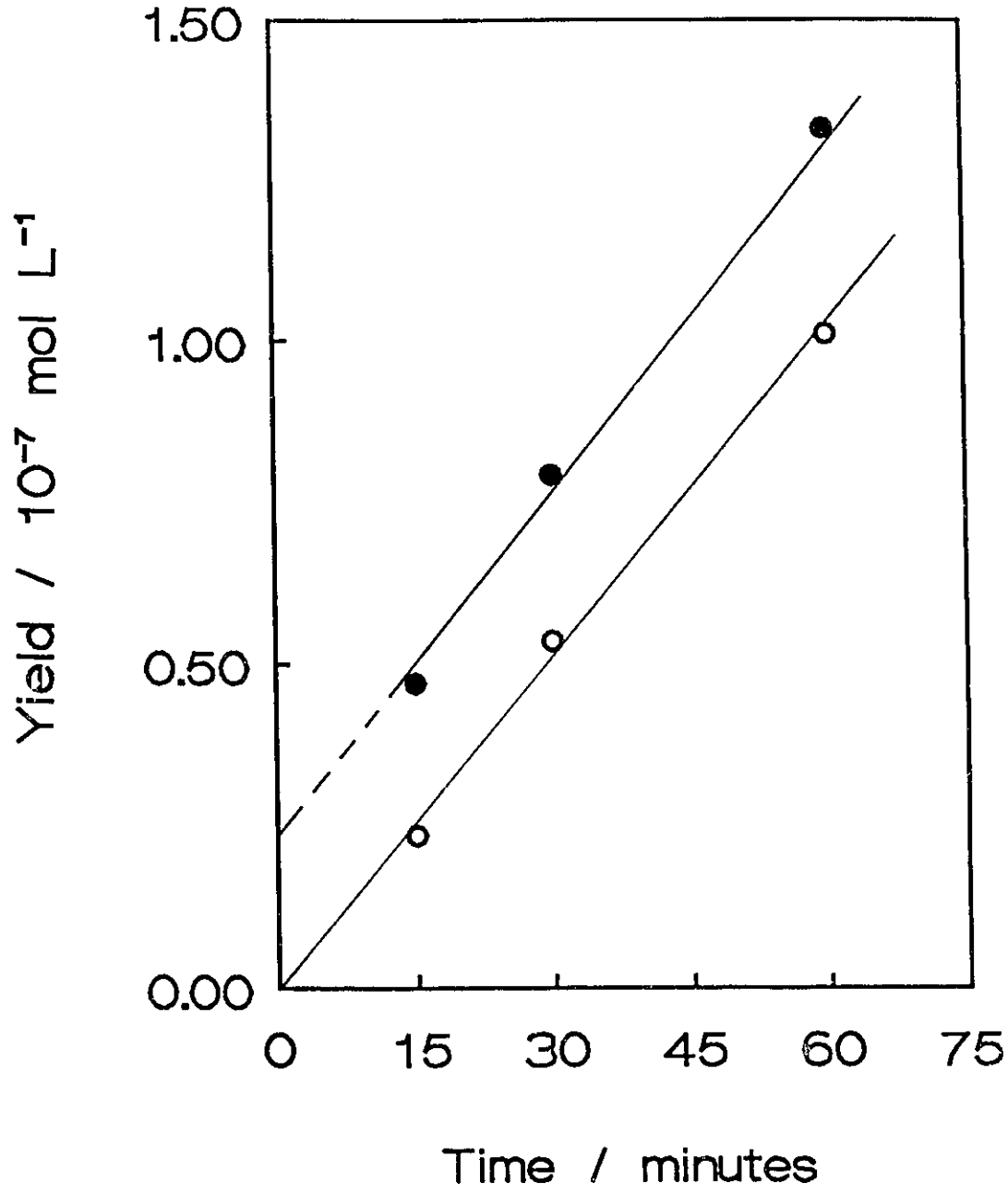

FIGURE 9 Yield as a function of time for methane decomposition using 200 Torr methane on quartz at 977 K.
- ● in the presence of oxygen impurity
- ○ in the absence of oxygen impurity

$$CH_4 + O_2 \rightarrow CH_3 + HO_2 \quad [23]$$

$$HO_2 + CH_4 \rightarrow CH_3 + H_2O_2 \quad [24]$$

$$H_2O_2 \rightarrow 2\ OH \quad [25]$$

$$OH + CH_4 \rightarrow CH_3 + H_2O \quad [26]$$

$$2\ CH_3 \rightarrow C_2H_6 \quad [3]$$

The increased concentration of CH_3 resulted in an initial rapid formation of ethane. Once the oxygen had been consumed, ethane was again formed by reactions [1] - [3]. The overall effect of this small quantity of oxygen was thus to increase the rate by a small amount initially. The subsequent rate of formation of ethane remained the same as that in the total absence of oxygen. Since each molecule of oxygen produced two molecules of ethane, the amount of oxygen present in the methane was calculated to be approximately 3 ppm. The rate of formation of ethane was thus shown to be extremely sensitive to the presence of oxygen. All results subsequent to the addition of the oxygen trap confirmed that no oxygen was present in the system.

3.3 Consecutive Experiments

3.3.1 Introduction

As shown in Section 3.2, an increase in the rate of decomposition of methane was observed in the presence of a carbon film. In order to test the reproducibility of the results, a series of experiments was performed on the same carbon film. All other

experimental conditions, such as the temperature, pressure and amount of reactant, were maintained unchanged. Each experiment was performed in the same way. The vessel was not treated in any way between experiments. This series of experiments was labelled Consecutive Experiments. If the results were indeed reproducible, a horizontal line would have been observed on plotting the rate as a function of the number of experiments, indicating no change in the activity of the carbon film.

3.3.2 Experimental

The carbon films used for the consecutive experiments performed on C_p were formed by pyrolysis of 21.2 Torr of propylene at 976 K for three hours. Consecutive experiments were initially carried out only at 977 K, but were subsequently performed over the entire temperature range studied. Methane reactant pressures of 20, 50 and 200 Torr were used and each experiment was allowed to proceed for 15 minutes. The usual time in between experiments was 30 - 45 minutes. Occasionally, the films were maintained under vacuum overnight when a large number of experiments were performed.

The films used for the consecutive experiments performed on C_m were formed by pyrolysis of 50.2 Torr of methane at 1218 K for three hours. After deposition of the film, the temperature was lowered to 977 K, at which temperature the experiments were performed. The methane reactant pressures studied were 20, 50 and 200 Torr and all reaction times were 15 minutes. As in the case of the experiments on C_p, in most cases the interval between experiments was 30 - 45 minutes, except when the film was kept under vacuum overnight.

3.3.3 Results

A few typical plots of rate as a function of number of experiments, on both C_p and C_m are shown in Figures 10 and 11. The most noticeable feature was that the rates were not constant during the series of experiments. On the contrary, the rate decreased with the number of experiments performed, although the extent of the decrease varied depending on the precursor of the carbon film. On C_p, no limiting value was observed within the 14 experiments performed and the yield continued to decrease throughout the series. On C_m, a decrease was initially observed, followed by the appearance of a limiting value, usually within 5 - 8 experiments. In both cases, the decrease in rate was not entirely uniform and several irregularities in the decrease were observed. These will be discussed later. As the pressure of methane was increased from 20 to 200 Torr, the decrease became more pronounced, as did the variations in the decrease, on both films.

3.3.4 Discussion

In this work, each experiment in the consecutive experiments series was essentially identical. Great care was taken to ensure that reaction conditions were reproducible for all the experiments in one series. Any change in reactivity could only have been due to a change in the condition of the carbon surface.

After a series of consecutive experiments, all the carbon present in the reaction vessel was removed by oxidation, as described in Section 2.4.3. The amount of carbon

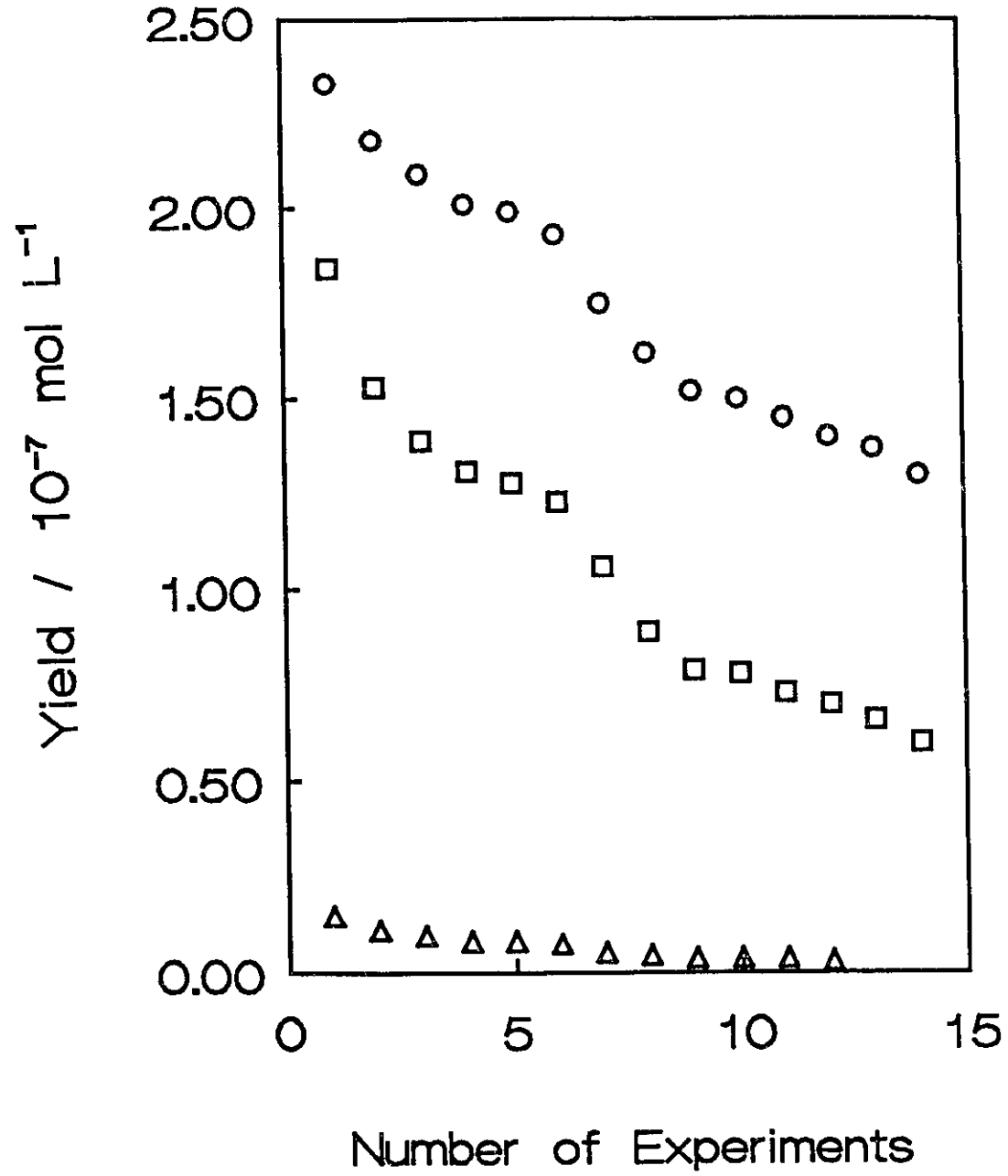

FIGURE 10 15 minute consecutive experiments using 20Torr methane at 977 K over a carbon film formed by pyrolysis of 21.2Torr propylene at 977 K for 3 hours.
○ ethane □ ethylene △ propylene

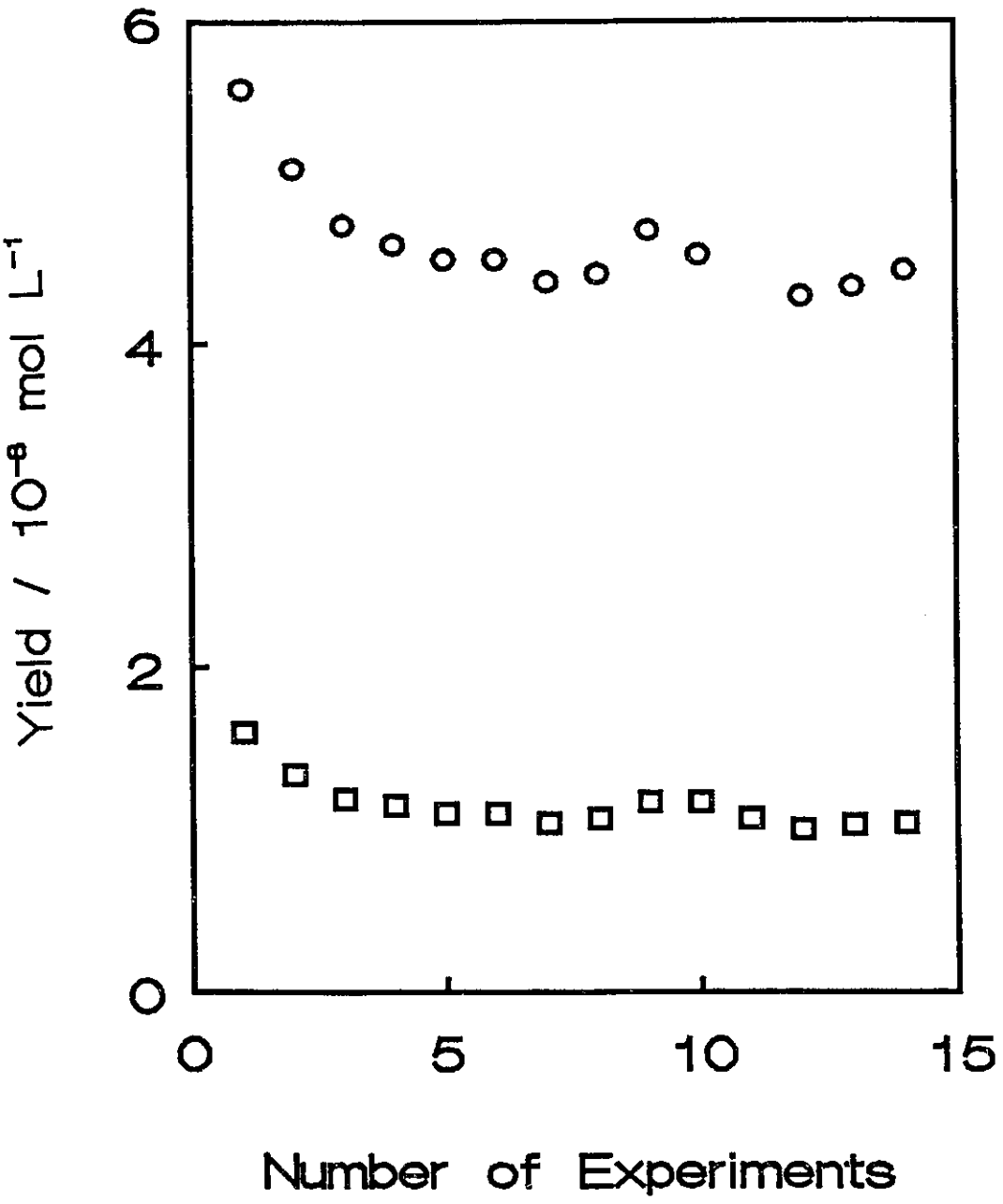

FIGURE 11 15 minute consecutive expeiments using 20Torr methane at 978 K over a carbon film formed by pyrolysis of 50.2Torr methane at 1218 K for 3 hours.
o ethane □ ethylene

recovered was consistently larger than the amount of carbon deposited initially. The difference in the initial and final amounts of carbon was not a large amount, only about $1 - 2 \times 10^{-7}$ mol, which corresponds to approximately 0.5%, and may have gone unnoticed if fewer experiments had been performed. The amount of carbon deposited in one experiment was estimated by determining the difference between the amount of carbon recovered after the consecutive experiments and the amount of carbon deposited initially in one particular series of consecutive experiments. This amount was divided by the total number of consecutive experiments performed in that series. The amount of carbon deposited in each experiment was thus estimated to be 1×10^{-8} mol or approximately 1% of a monolayer.

The deposition of carbon was unexpected for one main reason. The conversion was deliberately kept low in order to obtain low molecular weight hydrocarbons as products. None of the expected precursors to carbon formation, such as benzene or other higher molecular weight products were observed, although tests were made for their presence. Thus, carbon formation by means of polymerization and subsequent formation of highly dehydrogenated liquid droplets, or the "polyene" route, was considered unlikely.

An alternative to the formation of carbon by the "polyene" route was the formation of carbon through the dehydrogenation of hydrocarbon radicals formed on the carbon surface. The importance of this route was stressed by Murphy and Carroll[64b] in their recent study of the deposition of carbon by pyrolysis of acetylene. In the mechanism described in Section 3.2.4, methane is dissociated on the carbon surface forming a methyl radical which is initially bound to the surface. If this radical became dehydrogenated

before desorption, additional carbon would be formed on the surface. Thus, carbon may have been formed without the intermediate formation of aromatic hydrocarbons. Also while the radical remained attached to the surface, an active carbon site was blocked for further dissociation of methane. In this way, a slow inhibition of the active carbon surface may have occurred. On a metal catalyst surface, Somorjai and co-workers[21] suggested a similar mechanism for deactivation of the catalyst surface.

Studies on the pyrolytic reactions of other organic or halido-organic compounds have also shown that the rate of reaction was altered by repetition of experiments[16,17,21,36-45]. These results led to the suggestion by many researchers that use of "seasoned" vessels would reduce the extent of the observed reduction in rate. In these seasoned vessels, a hydrocarbon or a halide derivative of a hydrocarbon was pyrolyzed in order to deposit substantial amounts of carbon. Initial rates observed on these pyrolytic carbons were quite high and the rates progressively decreased with successive experiments. Such series were continued until a constant rate was obtained and it was often necessary to perform 70 -100 experiments to obtain this constant rate. This rate was much lower than the initial rate and was believed to represent a homogeneous rate of reaction. Some controversy arose over this practice of seasoning reaction vessels and Laidler and Wojciechowski[46] suggested that in fact, rather than being inactive, the carbon surface might prove to have a higher activity than the pyrex surface on which the carbon surface was deposited. Thus the inhibition by carbon may be accompanied by an accelerating effect and it is often difficult to distinguish between the two effects.

The difference in the decrease observed on the C_p and C_m films was due to the difference in the number of active sites which were present on the respective films. The two films had a different number of active sites due to the different temperatures of deposition of the two films. The C_m film was deposited at 1218 K while the C_p film was deposited at 977. The much higher temperature of deposition of the C_m film led to the formation of a more graphite-like film, that is, a film which was more ordered. In addition, significant hydrogen loss would have occurred at the higher temperature which could have affected the reactivity of the film. The hydrogen content of the films will be discussed in detail later. In order to determine whether the temperature could have affected the reactivity, a carbon film was formed by pyrolysis of 21.2 Torr of propylene at 977 K for three hours and after deposition, the reaction vessel was thoroughly evacuated. The reaction vessel was then isolated and heated to 1218 K for three hours. The temperature was reestablished at 977 K and the reaction vessel was thoroughly evacuated. A number of consecutive experiments were performed on the heat treated C_p film. The results are shown in Figure 12. While the rate on the heat-treated C_p was still 31% higher than that observed on C_m, the rate was significantly lower than that observed on the untreated film. The heat-treated C_p also resembled C_m in that the rate approached a limiting value after 5 - 8 experiments.

The variations during the decrease in the rate as a function of number of experiments were consistently observed in all the experiments performed and could not be dismissed as scatter. This result may be seen as the superposition of two different trends. The first trend is a decrease in the rate due to the loss of active sites. The second

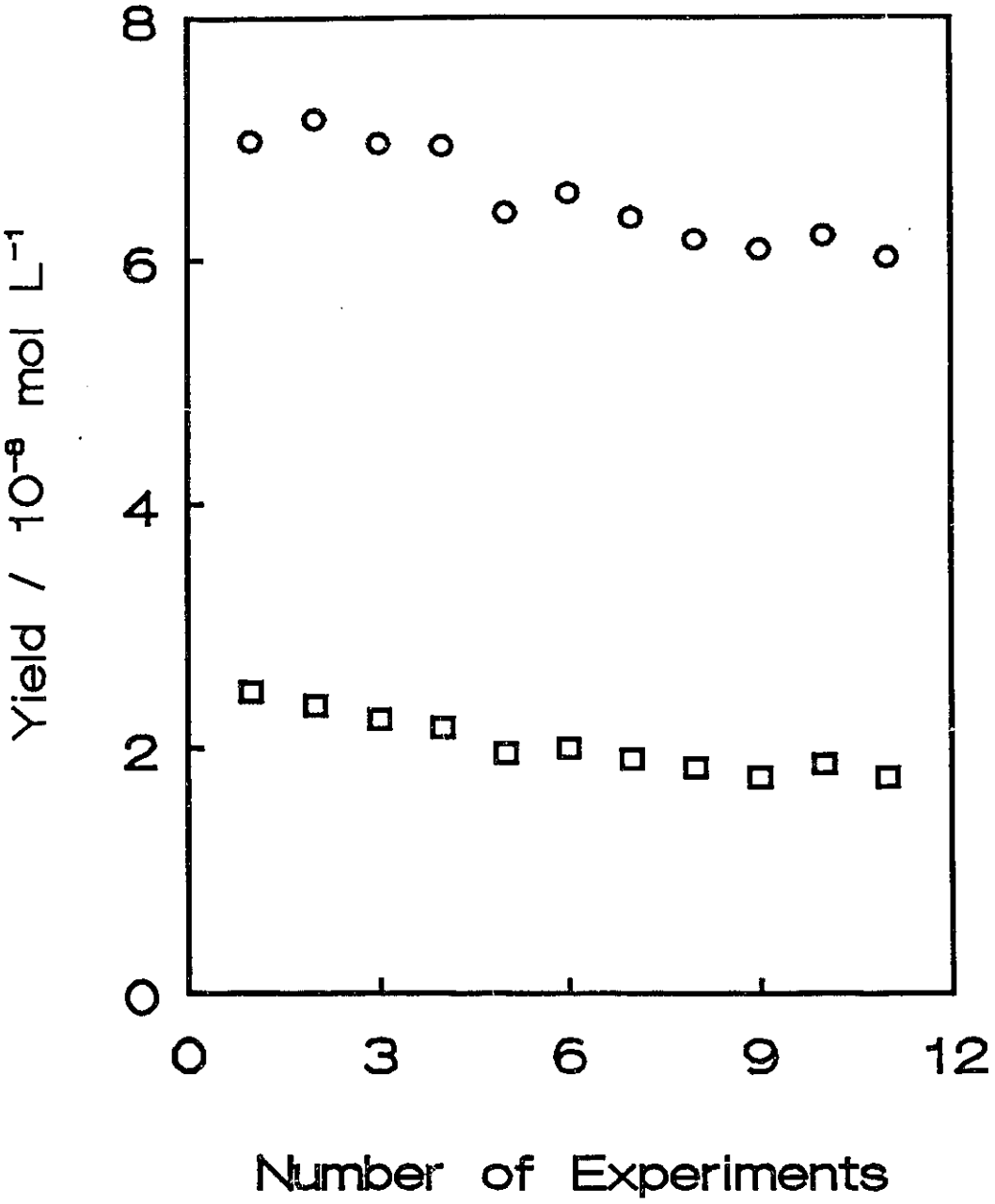

FIGURE 12 15 minute consecutive experiments using 20Torr methane at 977 K over a carbon film formed by pyrolysis of 21.2Torr propylene at 977 K for 3 hours and heated to 1219 K for 3 hours.
o ethane □ ethylene

trend is caused by an increase in the number of active sites as carbon is deposited. Initially, any imperfections in the carbon surface, which are active sites, would beblocked. This would cause a decrease in the number of active sites, and a corresponding decrease in the rate. Eventually, a point would be reached where new carbon deposited would have to start to build a new layer, which would create new active sites and the rate would no longer decrease. This could be described as a blocking and a building effect of carbon and will be described in more detail in a later section.

3.4 Rate as a Function of Amount of Carbon

3.4.1 Introduction

The results in Section 3.2 showed that the deposition of a significant amount of carbon in the form of a thin film caused the rate of conversion of methane to increase relative to the rate on quartz. However, the results obtained in Section 3.3 also showed that the deposition of very small amounts of carbon blocked active sites and decreased the rate of decomposition of methane. The question arose as to how these effects were linked. If the amount of carbon deposited was varied from the small amount deposited as a result of each experiment to the large amount deposited in the thin film, a crossover point between both effects should be observed. The rate of decomposition of methane was therefore measured as a function of the quantities of carbon which would span this wide range of amounts.

3.4.2 Experimental

All of the experiments were performed at 977 K using 20 torr of methane as the reactant. Table 1 contains the data regarding the pressure of propylene and the times of pyrolysis used to obtain each C_p film, and similar data for each C_m film. On each carbon film, a series of 4 - 8 consecutive experiments was performed. After the series was complete, the carbon was removed and the total amount of carbon was determined.

3.4.3 Results

The results obtained from this experiment are shown in Figure 13. The amount of carbon deposited ranged over four orders of magnitude and the rate resulting from this range of carbon covered two orders of magnitude. It was necessary, therefore, to use a log-log plot in order to present the results.

The deposition of a very small amount of carbon, C_p, corresponding to the amount estimated as being deposited during each experiment in a series of consecutive experiments, was achieved by careful control of the conditions for the pyrolysis. The decrease observed in the rate of decomposition of methane on the surface of the small amount of carbon relative to the rate on quartz was equivalent to the decrease observed between the first and second experiments in the series of consecutive experiments from which the small amount of carbon was estimated.

As carbon continued to accumulate, the rate noticeably increased and exceeded the value of the rate on the quartz surface. When an amount of carbon equivalent to that

TABLE 1 Rate of Decomposition of CH_4 as a Function of Amount of Carbon

Carbon Film			Amount of C	Initial Rate
Source	Deposition t (minutes)	Deposition T (K)	(mol)	(mol L^{-1} s^{-1})
-	-	-	1.64×10^{-8}	6.37×10^{-12}
50.1 Torr CH_4	60	977	4.17×10^{-8}	5.60×10^{-12}
50.1 Torr CH_4	1005	977	4.31×10^{-8}	5.30×10^{-12}
50.1 Torr CH_4	3000	977	5.18×10^{-7}	2.27×10^{-11}
72 Torr CH_4	7020	977	2.73×10^{-6}	4.82×10^{-11}
50 Torr CH_4	180	1219	7.57×10^{-5}	7.98×10^{-11}
0.80 Torr C_3H_6	10	977	7.33×10^{-8}	5.69×10^{-12}
2.0 Torr C_3H_6	15	977	3.49×10^{-7}	1.07×10^{-10}
0.49 Torr C_3H_6	10	977	3.59×10^{-7}	1.37×10^{-11}
21.2 Torr C_3H_6	180	977	3.89×10^{-5}	4.42×10^{-10}
47.3 Torr C_3H_6	180	977	1.20×10^{-4}	5.20×10^{-10}

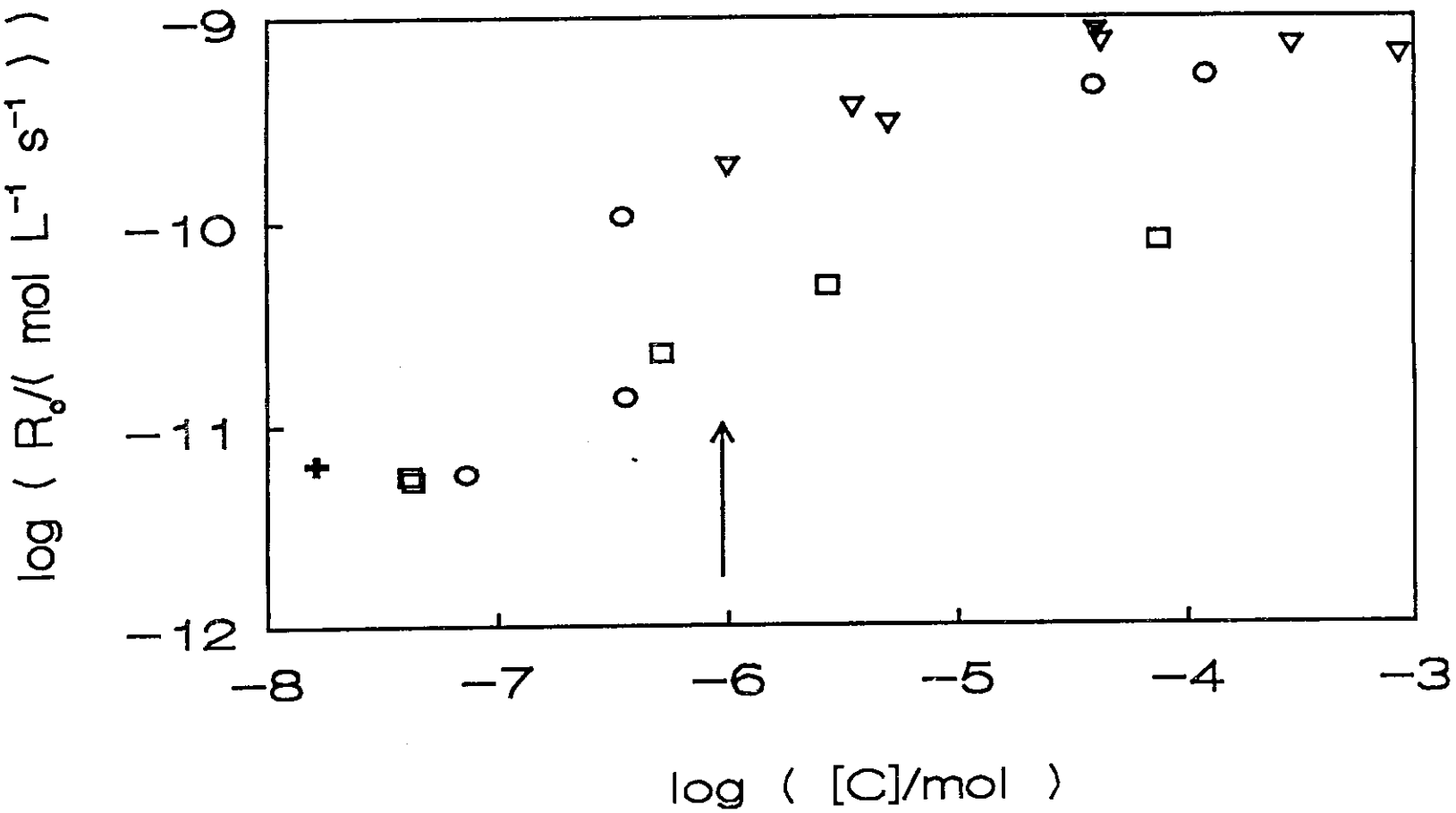

FIGURE 13 log R_o as a function of amount of carbon at 977 K
+ 20Torr methane on quartz o 20Torr methane on C_p □ 20Torr methane on C_m
▿ 200Torr methane on C_p by G. Scacchi ▼ 200Torr methane in this study
The arrow represents the equivalent of monolayer coverage in the vessel

present in a monolayer was deposited, the rate increased dramatically. Following this sharp rise, the rate reached a limiting value.

A similar trend was observed in the case of a carbon film C_m. The only significant difference between the results observed on C_p and C_m was that the limiting value on C_m was lower than the limiting value observed for C_p. In the initial stages, the rates on C_p and C_m appeared identical.

3.4.4 Discussion

A small amount of carbon clearly caused inhibition in the rate of methane decomposition. When an amount of carbon approximately equivalent to that deposited during the course of a 15 minute reaction was deposited before reaction, the decrease in rate, 11%, was the same as that observed in the consecutive reactions. It appeared that irrespective of the surface, quartz or carbon, the same decrease in rate was observed. It would seem most likely that this inhibition was due to coverage of active sites by methyl or other radicals where carbon was valence satisfied. The previously active site (carbon atoms with unpaired electrons) would no longer be active as the CH_x species would remain on the surface and block the activity of the site. Thus, the same blocking of sites observed during the consecutive experiments was also observed when an equivalent amount of carbon was deposited beforehand. The rate of decomposition of methane, which depended on the number of active sites present on the surface capable of dissociating the methane initially, thus decreased.

Hoffman et al[16,17], who were studying the pyrolysis of propylene on a commercial carbon surface, observed similar results. They measured the total number of active sites present on their carbon surface initially and then determined a rate of pyrolysis on the carbon surface. They then remeasured the number of active sites and found that the number had decreased. When the rate was measured again, it had also decreased. When the rate was normalized to the number of active sites, however, it remained unchanged, indicating that the only change in the surface was a net decrease in the total number of active sites.

As more carbon was deposited, a larger proportion of the surface was covered. As the radicals were dehydrogenated, small islands of carbon were formed on the quartz surface. The carbon, which has a reactivity higher than quartz, began to participate in the dissociation of the methane. The rate thus began to increase. At one point, the equivalent of a monolayer of carbon was formed on the surface of the quartz. The term equivalent is used since it is possible that the carbon did not initially deposit as a monolayer and there may have been discontinuities on the surface and places in which the carbon had already begun to form a second layer of carbon. This layer would have a reactivity higher than that of quartz, as shown by the yield time experiments. As enough carbon was deposited to form a second layer of carbon, or more, the carbon was attached to other carbon atoms and the observed increase in rate was due to the activity of this carbon. This carbon would have a greater activity due to the presence of unsatisfied valences and possible gaps in the layer or ring structure. This could account for the increase in the rate after the formation of the monolayer equivalent. Once the

carbon had formed a highly reactive layer, the carbon would continue to deposit in such a way that the layer structure, defects included, would propagate itself. For this reason, a limiting value was observed in the rate as the amount of carbon was further increased. The data points represented by the open triangles were performed by Dr. Gérard Scacchi[68] on C_p using 200 Torr of methane in a completely different apparatus. The data point represented by the closed triangle was performed in this study on C_p using 200 Torr. An increase in the pressure of methane used as reactant increased the limiting value slightly. The results obtained at 200 Torr in the two different apparati were comparable, indicating that the rate depended mainly on the pressure of methane and the carbon surface.

The lower value of the limiting rate for C_m as compared to C_p could be explained by the difference in preparation temperature of the two films. As explained in Section 3.3.4, the number of active sites would be much less on C_m than on C_p as the temperature of deposition of the carbon film was higher for C_m. The higher temperature of deposition caused a more graphite-like and dehydrogenated carbon to form, and the greater order in the carbon most probably resulted in a lower number of active sites.

3.5 Rate as a Function of Pressure

3.5.1 Introduction

A detailed study was made of the effect of pressure on the rate of dissociation of methane in order to shed some light on the nature of the surface. The work performed

in the previous sections indicated that the surface sites on the carbon played an important role in the dissociation of methane. This study was performed in order to obtain a better understanding of the different types of sites available on the carbon surface.

3.5.2 Experimental

Methane pressures, ranging from 0.3 Torr to 640 Torr, were reacted in a series of consecutive experiments over carbon films. These experiments were performed on quartz as well as on all three types of carbon, C_p, C_m, and C_b. The C_p films were formed by pyrolysis of 21.5 Torr of propylene at 977 K for 3 hours. The C_m films were formed by pyrolysis of 50 - 51 Torr of methane at 1220 K for 3 hours. The C_b films were formed by pyrolysis of 31.5 Torr of butadiene at 877 K for 3 hours.

3.5.3 Results

The results are shown in Figure 14. As the pressure was lowered from 640 Torr to 0.3 Torr, the rate of dissociation of methane decreased on all the carbon films. The rate was not measurable on quartz below 20 Torr. In all the experiments performed above 5 Torr, the yield of ethane was greater than that of ethylene and the rates decreased in any series of consecutive experiments. On the other hand, below 5 Torr of methane, the rate of formation of ethylene was observed to be initially greater than that of ethane, but after a few consecutive experiments, the rate of formation of ethylene decreased to

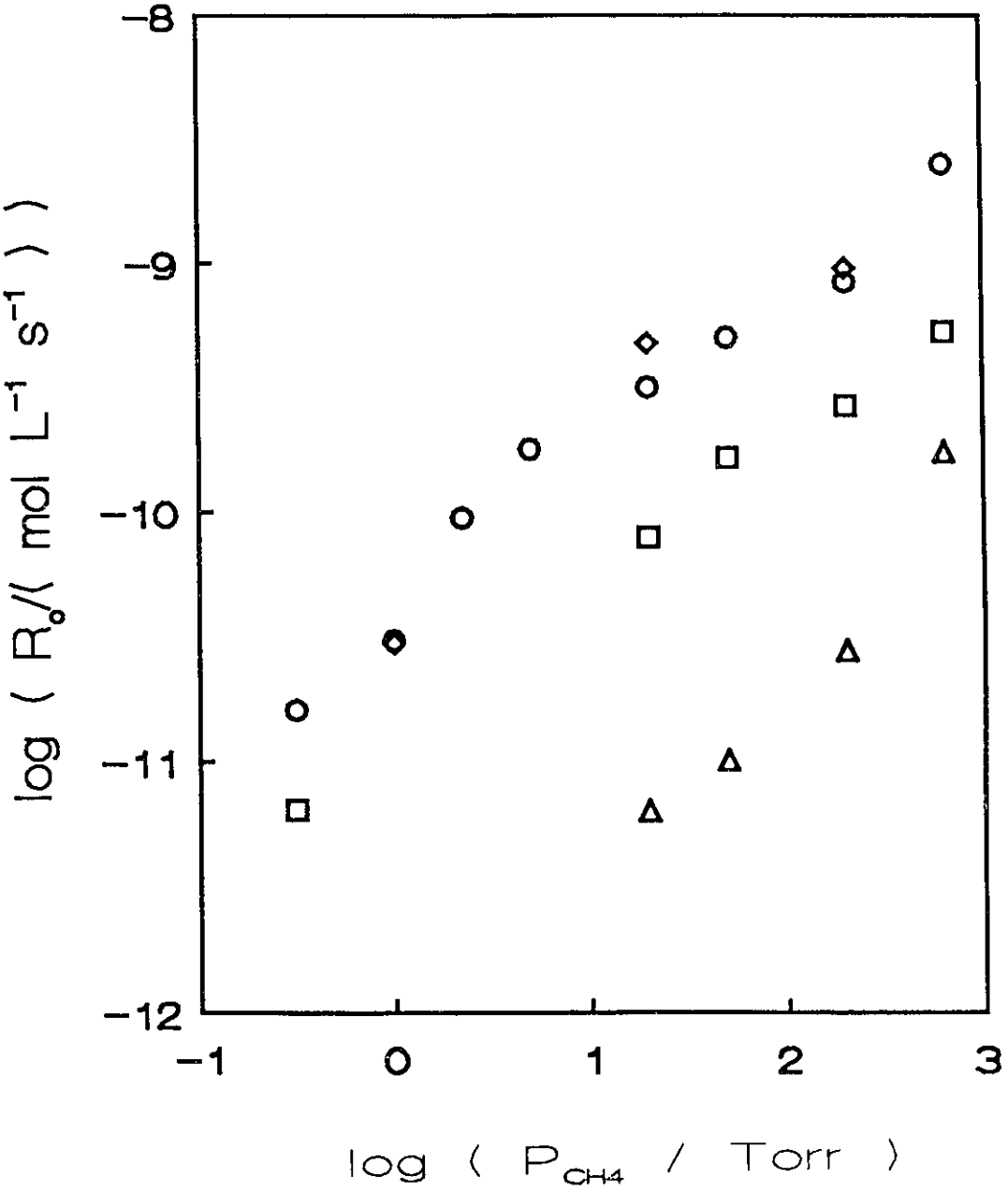

FIGURE 14 Rate of formation of ethane as a function of methane pressure at 977 K.
○ on C_p □ on C_m ◊ on C_b △ on quartz

a rate below that of ethane formation. Also, in these experiments, the rate of formation of ethane increased during the first few consecutive experiments, but then decreased after subsequent experiments.

3.5.4 Discussion

Similar behaviour was observed on all the carbon films. The increase in rate with increasing pressure indicated that the active sites on the carbon surface were not saturated with reactant. The increase in rate was, however, not regular. Since the carbon surface was known to contain a variety of types of sites, the results were not expected to follow a Langmuir-type adsorption isotherm. At low pressures, the sites of high reactivity would be occupied first and may even have been fully occupied. As the pressure of methane increased, sites of a different, and possibly lower, activity became increasingly occupied. The rate then increased due to the additional capability of the surface to dissociate the methane.

C_{III} had a lower activity than C_p, while C_p and C_b were close in activity. The difference in the films was most likely due to a difference in the number of active sites present on the respective films. The number of active sites on the carbon films was related to the temperature and conditions of formation of the carbon films. The quartz surface exhibited a different behaviour from the carbon films. This was due to the different nature of the active sites on the quartz surface, some of which may have been the result of natural impurities in the quartz itself. In all these cases, a series of

consecutive experiments resulted in a decrease in the rate as a function of the number of experiments performed. This decrease, as discussed previously, was due to the deactivation of active sites by the deposition of an inactive form of carbon. The trends observed in the rates of formation of ethane and ethylene below 5 Torr will be discussed in detail later.

3.6 Rate as a Function of Temperature

3.6.1 Introduction

In order to determine the activation energy for the dissociation process, the rate was measured over the temperature range 1023 to 573 K. The discussion is divided into two sections: temperatures above 873 K and temperatures 873 K and below.

3.6.2 Experimental

The experiments to determine the rate as a function of temperature were performed on C_p formed by pyrolysis of approximately 50 Torr of propylene at 977 K for three hours. At each temperature above 873 K, the rate was measured using methane pressures of 20, 50 and 200 Torr. Experiments were 15 minutes in length except at 1026 K where the experiments were 4 minutes in length. Below 873 K, 15 minute experiments were performed with 20 and 200 Torr of methane.

3.6.3 Results

The results are shown in Figure 15 for the three pressures at four temperatures above 873 K. The activation energy varied from 230 $kJmol^{-1}$ at 200 Torr to 303 $kJmol^{-1}$ at 20 Torr. Figures 16 and 17 show the rates of formation of ethane, ethylene and propylene over the entire temperature range studied for 20 Torr and 200 Torr of methane. The Arrhenius plots were linear from 1026 K to 873 K. Below 873 K, the rate of formation of ethane remained unchanged and the rate of formation of ethylene was very low and often could not be measured. The rate of formation of propylene decreased from 1026 to 873 K. Below 873 K, the rate of formation of propylene increased. When 20 Torr of methane was used, this increase was gradual over the range 873 K to 573 K. When 200 Torr of methane was used, the increase was very sharp and was followed by a decrease in the rate of formation of propylene to a constant value.

3.6.4 Discussion

3.6.4.1 Temperatures above 873 K

The values obtained for the activation energy were lower than that obtained for the homogeneous dissociation of methane in the limiting bimolecular region[69], which was 380 $kJmol^{-1}$, and certainly lower than the activation energy for the homogeneous dissociation of methane in the high pressure region. Since the dissociation of methane

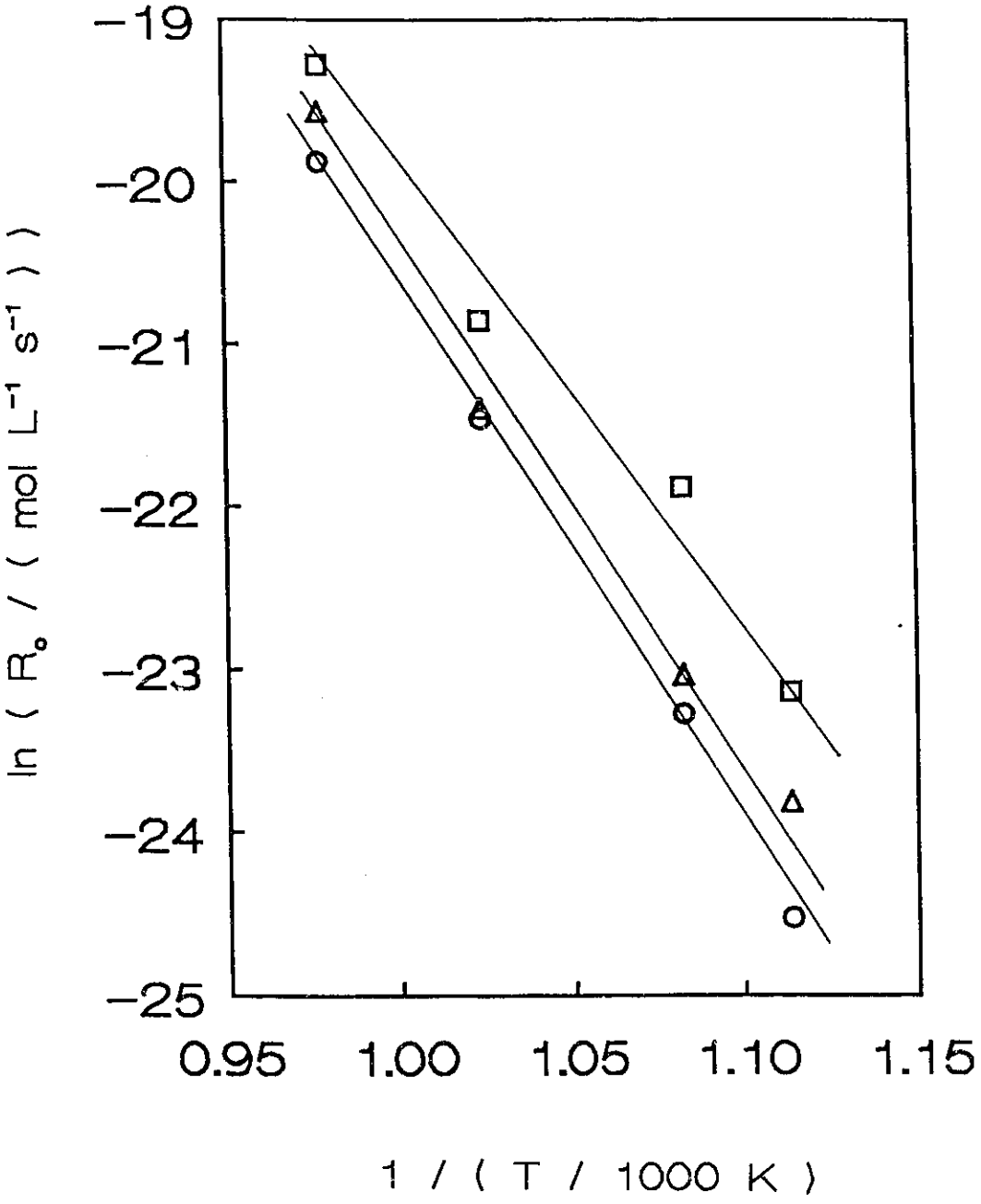

FIGURE 15 ln R_o as a function of 1/T for three pressures of methane.
○ 20Torr CH_4 △ 50Torr CH_4 □ 200Torr CH_4

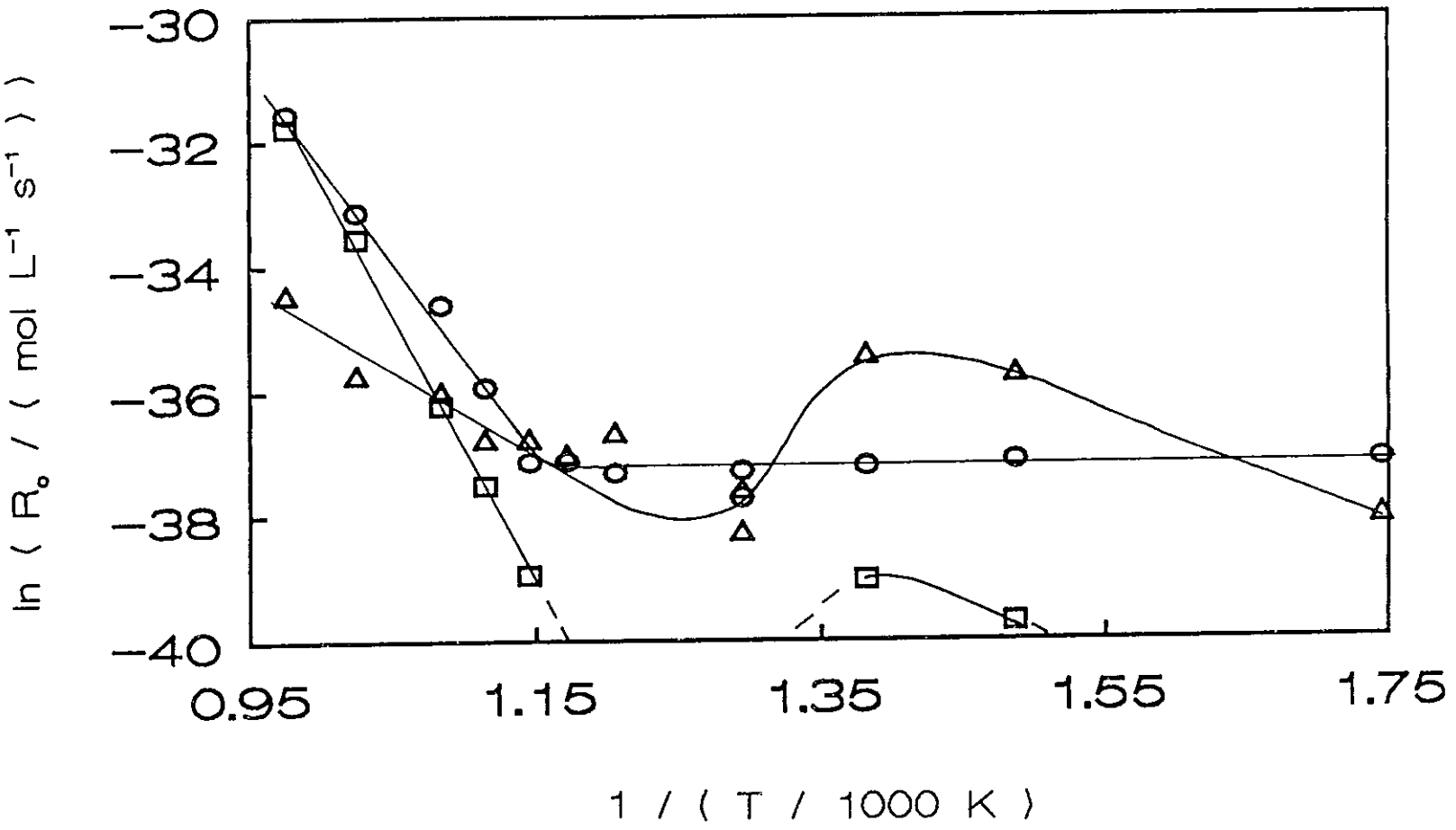

FIGURE 16 Rate of formation of products as a function of 1/T on C_p using 20Torr methane.
○ ethane □ ethylene △ propylene

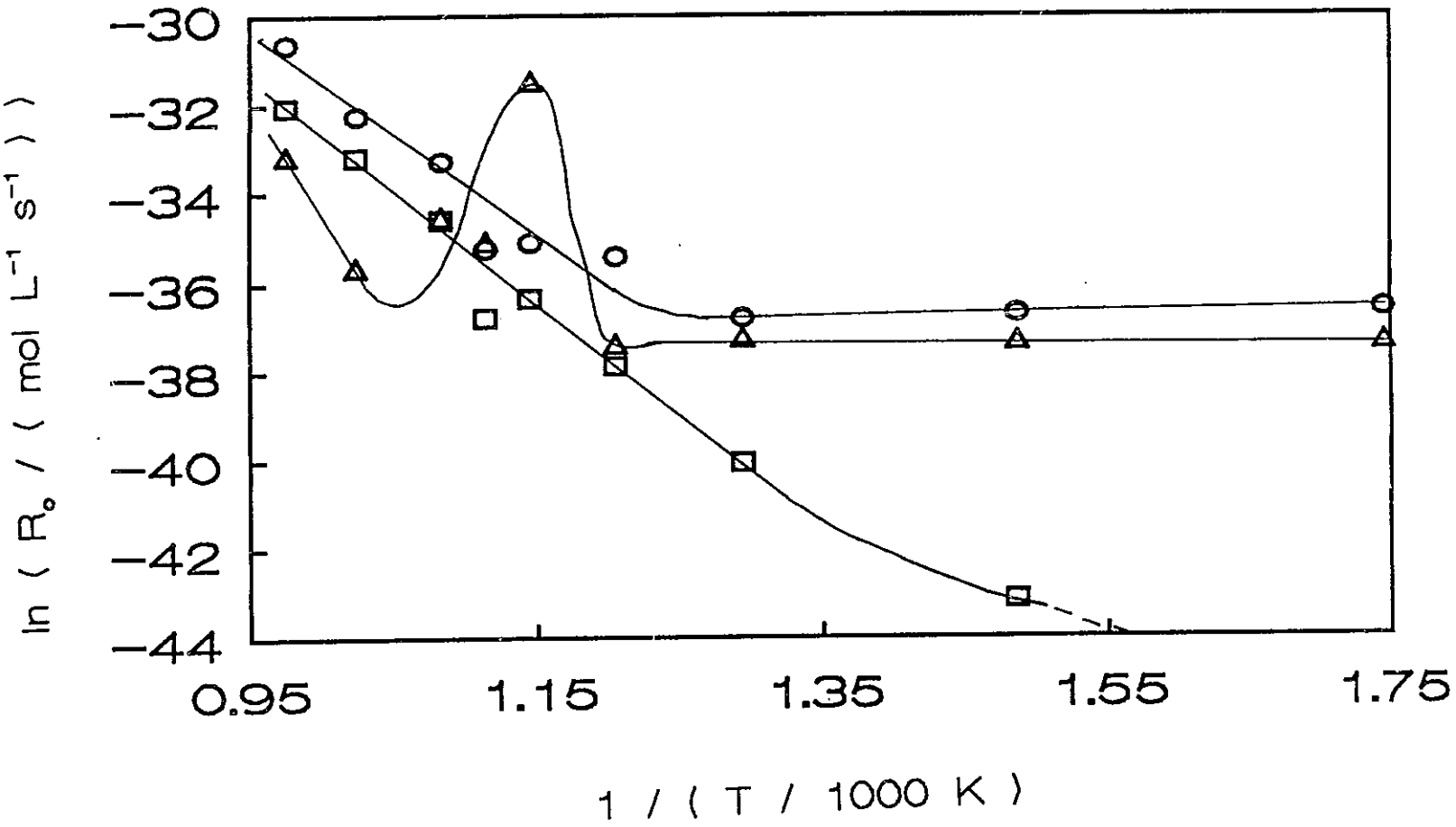

FIGURE 17 Rate of formation of products as a function of 1/T on C_p using 200Torr methane.
o ethane □ ethylene ▵ propylene

occurs mainly on the carbon surface, an activation energy lower than that measured in the homogeneous reaction was expected.

The activation energy decreased as the pressure increased and it appeared that the rates at 1023 K for 20, 50 and 200 Torr were converging. Thus, the activation energy appeared lower at 200 Torr than at 20 and 50 Torr. In actuality, this lower activation energy may be a spurious effect caused by loss of the products ethane and ethylene by catalytic decomposition on the active carbon surface. This effect should be most important at high pressures and high temperatures where the greatest amount of carbon is formed during the reaction time. Thus, with 200 Torr of methane, the rates at 977 K and 1026 K appeared less than expected from an extrapolation of the lower temperature results. The amount of carbon deposited during these consecutive reactions was, however, difficult to measure since it was only a small proportion of the total amount of carbon deposited, which was itself variable. Hence, the decrease in activation energy upon increase of methane pressure does not reflect a true change in the activation energy for dissociation, but is the result of a limitation in the experimental system.

3.6.4.2 Temperatures below 873 K

Below 873 K, the most striking result was that the products ethane and propylene, and to a lesser extent ethylene, continued to be formed at an almost constant rate. Another noticeable result was that propylene became an important product. An explanation of these results depended on the interpretation of the activation energy.

In a reaction system where surface processes occur, the five main reaction steps which must be considered are 1) diffusion to the surface 2) adsorption of reactants on the surface 3) reaction on the surface 4) desorption of products from the surface and 5) diffusion away from the surface. In the system used in this study, steps 1) and 5) were not important as there was no diffusional constraint. Adsorption was considered very likely to lead to reaction and hence step 3) was not considered to be a limiting step. Thus the measured activation energy reflected either the dissociative adsorption of the methane on the carbon surface or the desorption of the CH_3 and H species from the carbon surface. Both these steps could be used to interpret the experimental results obtained in this study. For this reason, both these cases will be considered.

A. Case I: Dissociative Adsorption of Methane

In this case, the measured activation energy is the energy required for the dissociative adsorption of methane. From the results above 873 K, this value was about 300 $kJmol^{-1}$. Below 873 K, this rate was too slow to produce the measured yields of ethane and ethylene, and hence an alternative route of formation of these products was required. It is possible that a concerted process involving the reorganization of two methane molecules, adsorbed on the surface but not dissociated, to form ethane

$$2CH_4 \rightarrow C_2H_6 + H_2 \qquad [27]$$

occurred, with the carbon surface providing a low energy pathway. This improbable pathway could require specific sites or could require that the methane molecules remained adsorbed for a slightly longer period of time in order for the concerted process to follow.

This process could also occur at higher temperatures, but its contribution to the rate would have been negligible when the higher temperature would provide sufficient energy to break the C-H bond in the methane. Once the ethane was formed on the surface, it would desorb without forming ethylene. This result is seen in Figures 16 and 17. As the temperature was further lowered, the ethane could remain on the surface long enough to dehydrogenate to ethylene, which could then desorb, or remain on the surface.

B. Case II: Desorption of the Products CH_3 and H

In this case, the measured activation energy represents the energy required for the desorption of CH_3 and H once the methane had dissociatively adsorbed on the carbon surface. At the higher temperatures, there would be sufficient energy for these species to desorb from the surface after they were formed. Below 873 K, however, these species might not have enough energy to desorb and would remain attached on the surface. Ethane would be formed by migration of CH_3 species on the surface while ethylene could be formed by dehydrogenation of the ethane, once formed, or dehydrogenation of CH_3 to CH_2 with subsequent ethylene formation. When 200 Torr of methane was reacted, the number of CH_3 species on the surface would be much larger than when 20 Torr was used and formation of ethane would predominate, as the results indicated.

The other important result was the increase in the rate of formation of propylene. This increase became more pronounced when the pressure of methane was raised. The increase in the rate of formation of propylene with reactant pressure indicated the possibility of an Eley-Rideal mechanism, whereby a molecule in the gas phase reacts directly with an adsorbed species. In both the cases discussed previously, the formation

of ethylene was possible. At lower temperatures, ethylene which had formed would be more likely to remain on the surface. The methane in the gas phase could react with the double bond of a surface-bound ethylenic species to form propylene, a process which is energetically favourable. In the second case, it is also possible that the surface ethylenic species could react with a surface CH_3 species to form propylene.

The introduction of an Eley-Rideal mechanism at lower temperatures is not unlikely. In a study of the recombination of H atoms on glass and silica[70], a comparison was made of the percentage contribution to the overall rate by the reaction of adatoms and by the Eley-Rideal mechanism. At 773 K, the contribution to the rate from the Eley-Rideal mechanism was only 2% but at 523 K, the contribution to the rate from the Eley-Rideal mechanism was 100% and it was considered that gaseous atoms were colliding with a strongly held adatom of the first layer. Such a mechanism could be extended to the consideration of an Eley-Rideal mechanism involving a gaseous methane or CH_3 species and a strongly held ethylenic species.

When 200 Torr of methane was reacted, the amount of propylene produced was very large and the propylene did not appear to be formed at the expense of ethylene, as appeared to be the case at lower temperatures. This large amount of propylene suggested a further intermediate or reaction path which was a function of the pressure as well as the temperature. One possibility was the formation of an ethylidene or an ethylidyne species, shown in Figure 18. This rearrangement would be more likely at high pressure due to a greater number of adsorbed species and subsequent lack of surface sites for the formation of a surface ethylenic species. This ethylidene or ethylidyne species might

FIGURE 18 Intermediates Ethylidene and Ethylidyne

react with methane according to an Eley-Rideal mechanism to form propylene. This process could only occur under certain conditions and the temperature window for this process would be very narrow. At higher temperatures, both ethylidene and ethylidyne would not be stable enough to remain on the surface for a long enough period of time to react with gas phase methane. Rearrangement to ethylene would be rapid. At lower temperatures, there would not be sufficient energy to form either species. In the temperature window around 873 K, there was sufficient energy to form either the ethylidene or ethylidyne species, but not so much that it would dissociate or rearrange before it could react. Thus propylene forms by this mechanism only over a narrow temperature range.

3.7 Rate Measurements in a Packed Vessel

3.7.1 Introduction

All the results obtained in the measurements of the rate as a function of time, number of experiments, amount of carbon, temperature and pressure indicated that a surface process was extremely important in the study of the dissociation of methane in the carbon-coated vessel. If the process occurred mainly on the surface, an increase in

the surface to volume ratio should lead to an increase in the rate by a factor equal to the surface to volume ratio. Since the presence of carbon on the quartz substrate increased the rate by a factor of as much as forty, a further increase in the rate by a factor of the surface to volume ratio would give rates close to those obtained with oxidative catalysts.

3.7.2 Experimental

3.7.2.1 Packed Reaction Vessel

The packed reaction vessel was constructed by placing 182 quartz tubes which were 7 cm in length, and which had an outer diameter of 2.5 mm and an inner diameter of 1 mm in a reaction vessel of the same dimensions as the previous vessel. The total surface area, determined by adding the surface areas of the inside and the outside of the tubes as well as the surface area of the reaction vessel, was 1553 cm^2. The new volume, determined by subtracting the volume of the tubes from the volume of the reaction vessel, was 84 cm^3. From these measurements, the surface to volume ratio, S/V, was approximately 20 cm^{-1}.

3.7.2.2 Experimental Procedure

The experiments performed in the unpacked vessel were repeated in the packed vessel, including experiments in the absence of carbon as well as in the presence of

carbon deposited from propylene, methane and butadiene. Details of the experimental conditions for a particular series of experiments will be provided in the section describing the results.

3.7.3 Consecutive Experiments

3.7.3.1 Experimental

Most of the consecutive experiments were performed on a propylene carbon film, C_{ppv}, formed by pyrolysis of approximately 500 Torr of propylene at 977 K for 4 hours. Some experiments were performed on a methane carbon film, C_{mpv}, formed by pyrolysis of 640 Torr of methane at 1220 K for 4 hours. A few experiments were performed on a butadiene carbon film, C_{bpv}, formed by pyrolysis of 326 Torr of butadiene at 877 K for 3 hours. The methane in all the experiments in a series of consecutive experiments was allowed to react for 15 minutes, except at 1026 K where the experiments were 4 minutes in length.

3.7.3.2 Results

From the reaction in the packed vessel, with or without carbon, the products were ethane and ethylene, with small quantities of propylene, acetylene and/or allene depending on the experimental conditions. On quartz, the rate of dissociation of methane increased

by a factor of 10. A decrease in the rate was observed as the consecutive experiments were performed, consistent with the experimental observations made in the unpacked vessel.

On the carbon surface, at low temperatures and low pressures and with less than monolayer amounts of carbon on the quartz surface, the rate decreased as the number of consecutive experiments were performed. At higher temperatures and pressures, and with amounts of carbon exceeding a monolayer coverage of the surface, the rate increased as the number of consecutive experiments were performed. At methane pressures lower than 20 Torr, the yields of ethylene exceeded the yields of ethane.

3.7.3.3 Discussion

When methane was introduced into the reaction vessel, carbon, in the form of CH_x was deposited on the surface. This carbon either formed a valence-satisfied carbon species, which blocked an active site and caused an inhibition in the rate in subsequent experiments, or formed a new active site thus building the active carbon surface. Depending on the pressure and temperature, either the building or the blocking process dominated. In some cases, the two rates were very similar and no change in the rate was observed in a series of consecutive experiments.

Carbon was likely to deposit on the most active sites on the carbon surface first. If this carbon retained its hydrogen, or dehydrogenated and became doubly bonded to the surface (in other words, remained valence satisfied) and remained on the carbon, this would block an active site. If the radical dehydrogenated forming unpaired valence

electrons, it would be building carbon. This building carbon, if deposited on an active site, would render this active site inactive but would generate a new site in its place. In this simplified picture, the number of active sites may not increase. The process of building is more complex, however, and new active sites may be formed if a carbon ring is broken, for example, or if a site of lower activity is replaced by one of higher activity.

If the building process dominated, new active sites were created. Upon introduction of methane in the second consecutive experiment, the number of active sites on the surface was greater than in the first experiment, and the rate increased, as shown in Figure 19. The increase continued until the addition of further carbon resulted in the loss of active sites rather than the gain of new sites. This could occur due to formation of completed or valence satisfied carbon rings on the surface. As newly created sites were joined together to form carbon rings, the total number of active sites diminished and the rate began to decrease. The time taken, or the number of experiments required, for this change in the nature of the deposited carbon to occur depended on the pressure and the temperature.

At low pressures, the amount of carbon deposited in each experiment was small and deposited preferentially on the sites of high activity. Thus at low pressures, a decrease in activity was seen with consecutive experiments, as mostly blocking carbon was deposited. At low temperatures, CH_3 or other surface species were more difficult to remove and any deposited carbonaceous species most likely remained on the surface as blocking carbon. Thus at low temperatures, a decrease in rate was observed with consecutive experiments. When less than a monolayer of carbon was

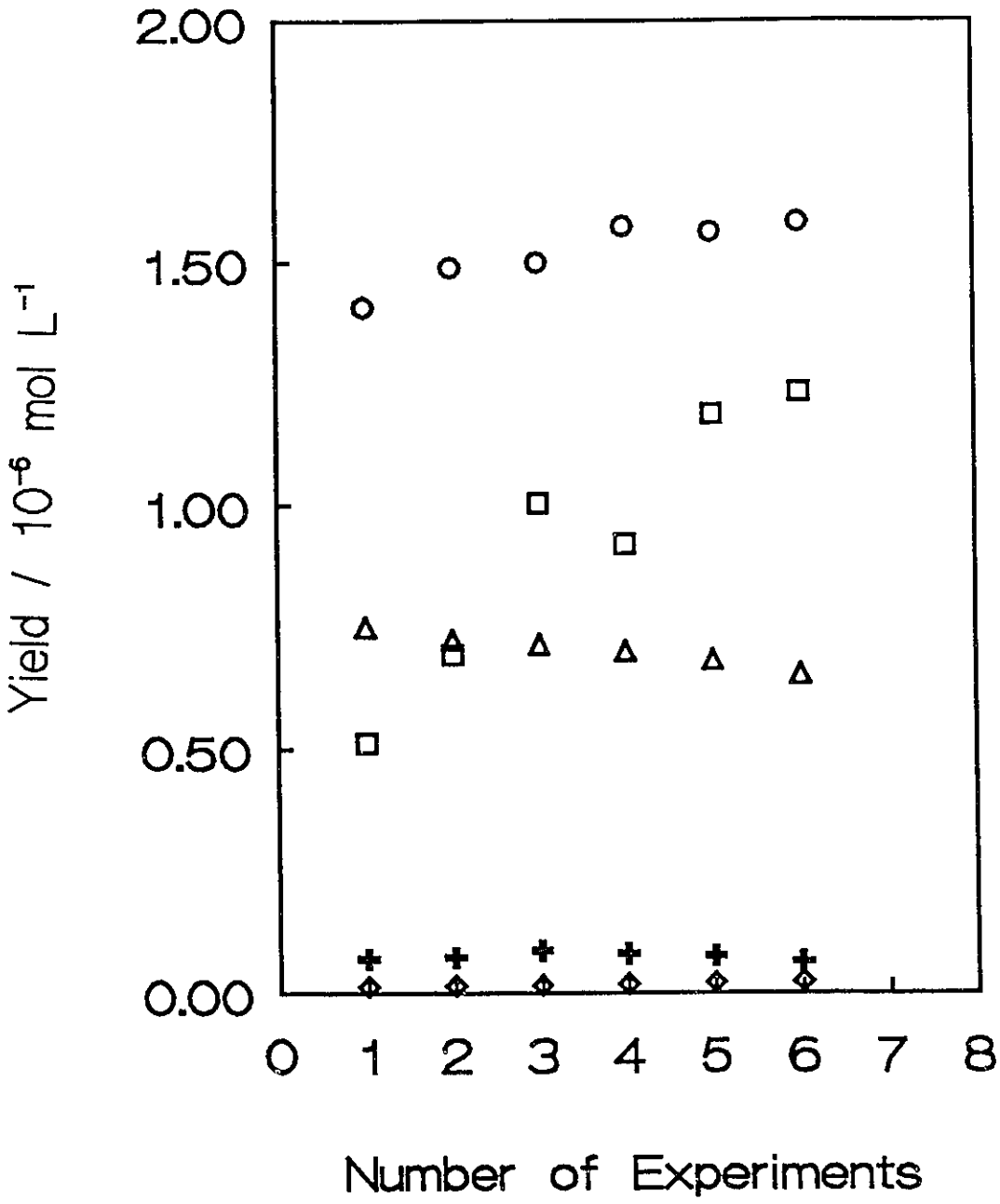

FIGURE 19 15 minute consecutive experiments using 640.9Torr methane at 977 K in the packed vessel over a carbon film formed by pyrolysis of ≈500Torr propylene for 4 hours at 977 K.
○ ethane □ ethylene △ propylene + acetylene ◊ allene

present on the surface of the reaction vessel, a decrease in the rate with consecutive experiments was observed. Carbon deposited during the reactions was incorporated into the growing carbon surface required to cover the quartz surface. Not enough carbon was yet present to observe an increase in the rate due to the building of the carbon film. At higher pressures, enough carbon was deposited that some formed new active sites on the growing carbon surface. As the pressure was increased, more carbon behaved as building carbon than blocking carbon. Products may have readsorbed and dissociated to yield further building sites. The increase in rate with consecutive experiments was most pronounced at high pressures of methane. At intermediate pressures, little change in the rate was observed, as can be seen in Figure 20.

At pressures below 20 Torr, the yield of ethylene was greater than the yield of ethane, as shown in Figure 21. This observation was also made in the unpacked vessel below 2.2 Torr. Most likely, at low pressures, the methyl radical further dehydrogenated to produce CH_2. At low pressures, the number of adsorbed species was much less and neighbouring sites would have been available to further the dehydrogenation of CH_3 to CH_2. This would result in a decrease in the ethane yield as the CH_3 species is essential to the formation of ethane whether it is formed in the gas phase or on the surface. The CH_2 species could react with another CH_2 on the surface to form ethylene, which would then desorb. Homogeneous formation of ethylene seemed unlikely due to the low pressure of methane in the gas phase. At higher pressures of methane, however, neighbouring sites would have been occupied by adsorbed species and the

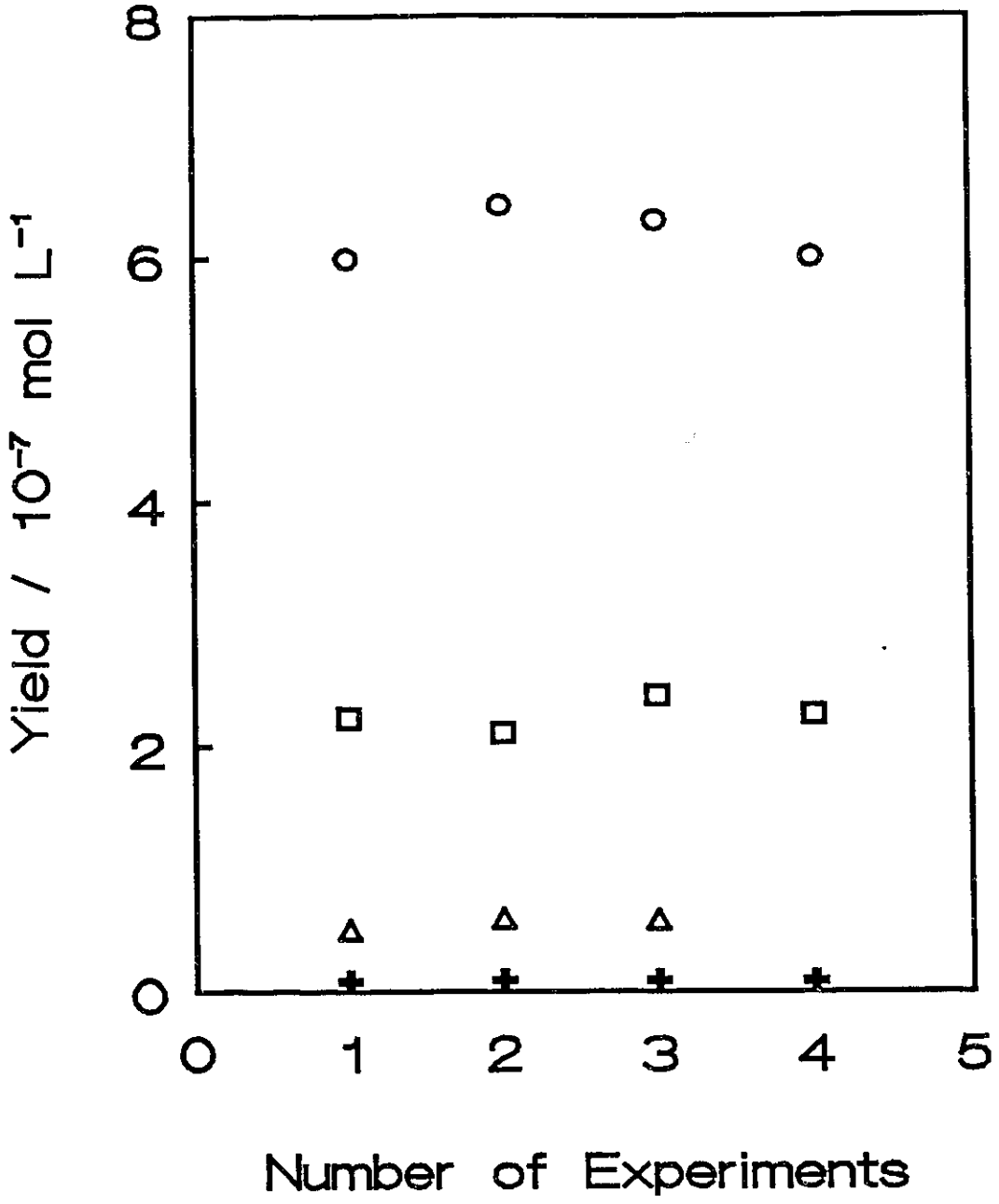

FIGURE 20 4 minute consecutive experiments using 202.3 Torr methane at 1024 K in the packed vessel over a carbon film formed by pyrolysis of ≈640 Torr methane for 4 hours at 1219 K.
○ ethane □ ethylene △ propylene + acetylene

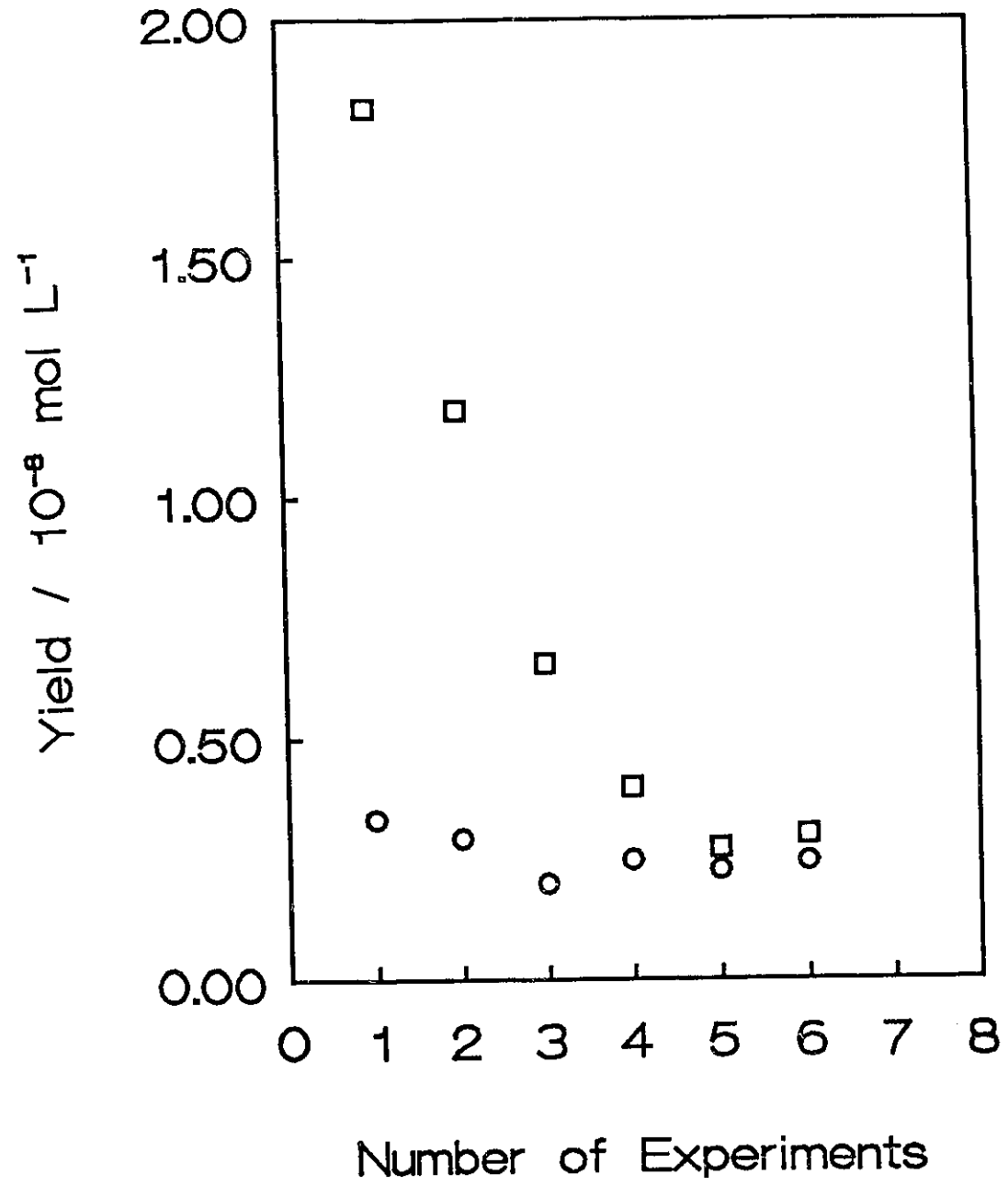

FIGURE 21 15 minute consecutive experiments using 0.513Torr methane at 977 K in the packed vessel over a carbon film formed by pyrolysis of ≈500 Torr propylene for 4 hours at 977 K.
o ethane □ ethylene

dehydrogenation of the CH_3 species would be less likely to occur before its desorption. Thus the rate of ethane formation exceeded the rate of ethylene formation at higher pressures.

3.7.4 Rate as a Function of Amount of Carbon

3.7.4.1 Experimental

The experiments to determine the rate as a function of the amount of carbon in the packed vessel were performed only on C_p. A preliminary series of consecutive experiments was performed in the packed vessel in the absence of deposited carbon. Upon completion of this series, carbon deposited during these experiments was removed and analyzed. The amount deposited in one experiment was the lowest amount used for this series of experiments. Subsequently, approximately 500 Torr of propylene was pyrolyzed at 977 K for 4 hours. This procedure resulted in the deposition of 9.0 - 9.5 x 10^{-4} mol of carbon. A series of consecutive experiments was performed on the surface of this carbon, C_{ppv}, and upon completion of the series, all the carbon was removed and analyzed. This value defined the upper limit of the amount of carbon used for the measurements. Intermediate values of amounts of carbon were chosen so as to define the variation of the rate with the amount of carbon. All consecutive experiments lasted for 15 minutes and were performed at 977 K using 20 Torr of methane as reactant.

3.7.4.2 Results

The results are shown in Figure 22. The rate obtained in the absence of deposited carbon in the packed vessel was greater than the corresponding rate in the unpacked vessel by a factor of 10. The decrease in rate in the presence of small amounts of carbon observed in the unpacked vessel was more pronounced in the packed vessel and extended over a wider range of amount of carbon. Increasing the amount of carbon deposited caused the rate of dissociation of methane to rise above the rate observed in the unpacked vessel. However, as the amount of carbon was further increased, the rate decreased to a value lower than that obtained in the unpacked vessel.

3.7.4.3 Discussion

The rate in the packed vessel in the absence of carbon showed a large increase over the rate observed in the unpacked vessel in the absence of carbon. The two rates differed by a factor of 10. This was also the factor by which the actual surface area increased in the packed vessel. If the number of active sites on the quartz surface was proportional to the area, then the rate should have increased by the same factor. After the series of consecutive experiments was performed in the packed vessel in the absence of any deposited carbon, all carbon which may have deposited during the course of the consecutive experiments was removed and analyzed. The amount of carbon recovered was found to be greater than the amount recovered from the corresponding experiment

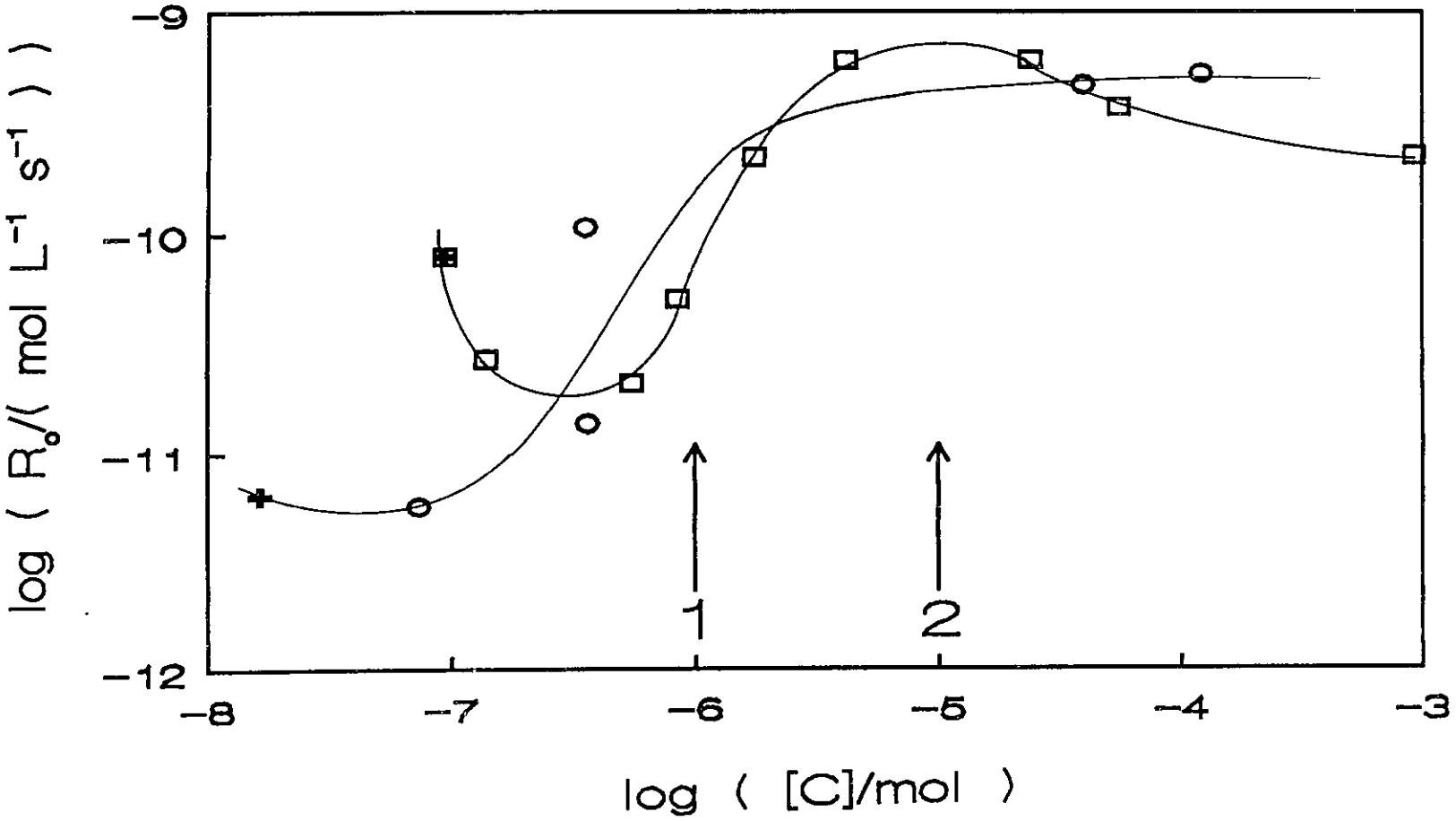

FIGURE 22 log R_o as a function of amount of carbon at 977 K in the packed and unpacked vessels.
+ 20Torr methane on quartz o 20Torr methane on C_p
⊞ 20Torr methane on quartz in packed vessel □ 20Torr methane on C_{ppv}
The arrows marked 1 and 2 represent approximate monolayers in the unpacked and packed vessels respectively

in the unpacked vessel. Since the rate had increased in the packed vessel, more methane would have dissociated and subsequently more carbon deposited on the active sites. Hence, the amount of carbon recovered from the quartz surface was greater in the packed vessel than in the unpacked vessel, as shown in Figure 22. As with the unpacked vessel, deposition of a small amount of carbon caused the rate to decrease, due to coverage of the most active sites on the quartz surface. This decrease was more pronounced in the packed vessel. Since the surface of the packed vessel was much larger than the surface of the unpacked vessel, much more carbon had to be deposited in order to observe the subsequent increase in the rate. As the amount of carbon approached the equivalent of a monolayer in the packed vessel, the rate increased above that observed initially on the quartz surface, as well as above the maximum rate observed in the unpacked vessel. The rate did not, however, increase by the expected factor of the surface to volume ratio and actually decreased to a value below that observed in the unpacked vessel as more carbon was deposited. The reason for this was a limitation of the experimental system. The inner diameter of the tubes used to pack the reaction vessel was small enough that diffusional constraints were introduced to the system. Thus, although the products were formed at an increased rate, diffusion through the tubes was slow. Since the deposited carbon presented a highly active surface, the products, unable to diffuse rapidly through the system, were readsorbed on to the active sites of the carbon surface. Because ethane and ethylene are more reactive than methane, rapid decomposition to carbon would occur. Since the rate was measured by the yields of ethane and ethylene, loss of ethane and ethylene gave an apparently lower rate of decomposition of methane. An alternative

explanation involving loss of methyl radicals on the surface and reformation of methane was considered less likely.

3.7.5 Rate as a Function of Pressure

3.7.5.1 Experimental

The pressure dependence in the packed vessel was examined over the pressure range 0.5 Torr to 640 Torr on C_{ppv}, C_{mpv} and C_{bpv}. The films C_{ppv} were prepared by pyrolysis of about 500 Torr of propylene at 977 K for 4 hours. The films C_{mpv} were prepared by pyrolysis of 640 Torr of methane at 1220 K for 4 hours. The films C_{bpv} were prepared by pyrolysis of 326 Torr of butadiene at 877 for 3 hours. All reactions were 15 minutes in length and were performed at 977 K.

3.7.5.2 Results

The results are shown in Figures 23 and 24. In the packed vessel in the absence of deposited carbon, the rate initially increased by a factor of 10 relative to the rate in the unpacked vessel as shown in Figure 23. On C_{mpv}, the ratio of rates in the packed and unpacked vessels was slightly less than 10, as shown in Figure 24. On C_{ppv} and on C_{bpv}, little increase over the rate in the unpacked vessel was observed. The rates observed on all three carbon films in the packed vessel were very similar and were not remarkably different from the rate obtained in the unpacked vessel. Figure 25 shows a comparison

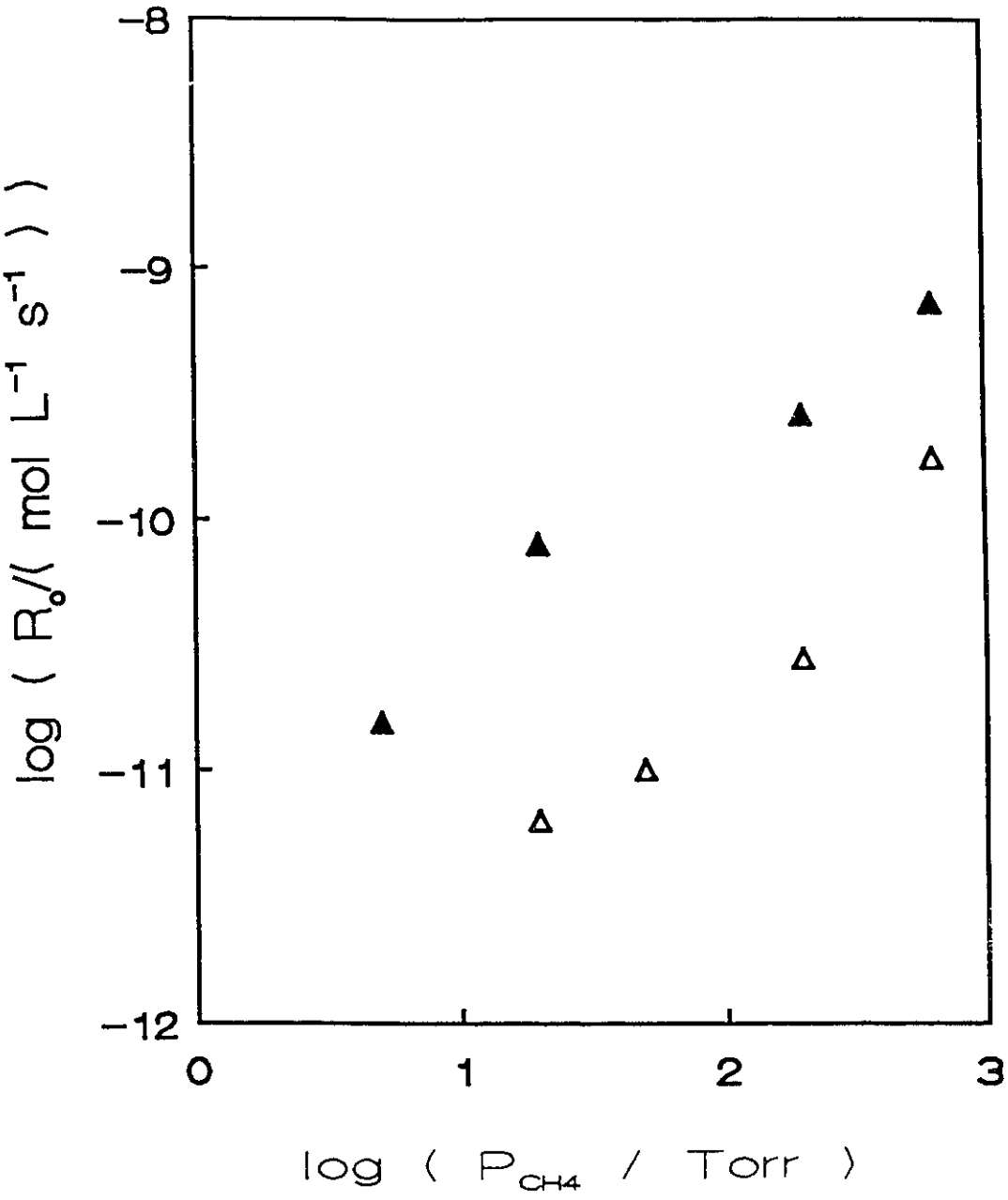

FIGURE 23 Rate of formation of ethane as a function of methane pressure at 977 K in packed and unpacked vessels.
△ on quartz ▲ on quartz, packed vessel

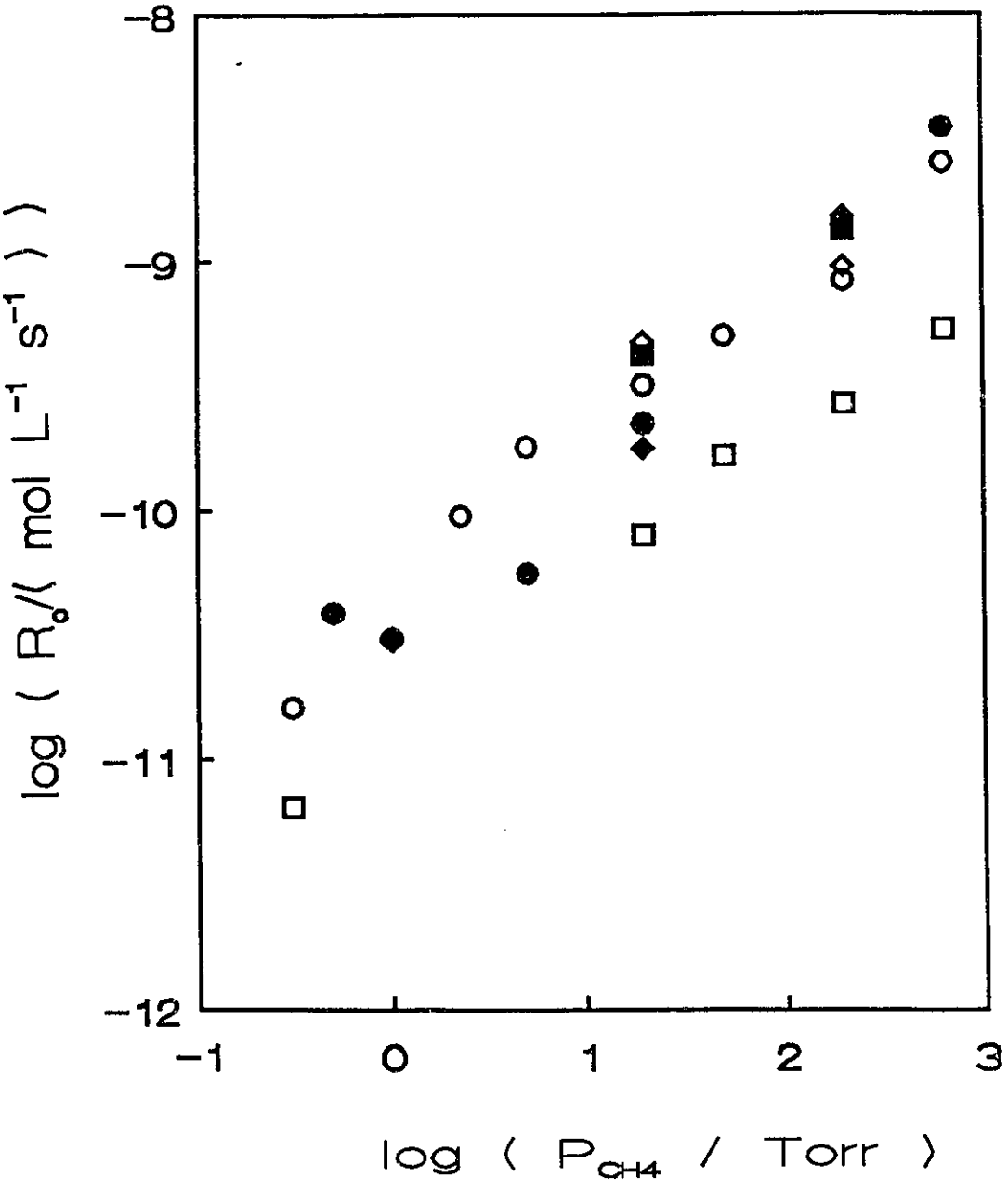

FIGURE 24 Rate of formation of ethane as a function of methane pressure at 977 K in packed and unpacked vessels.

○ on C_p □ on C_m ◊ on C_b

● on C_{ppv} ■ on C_{mpv} ♦ on C_{bpv}

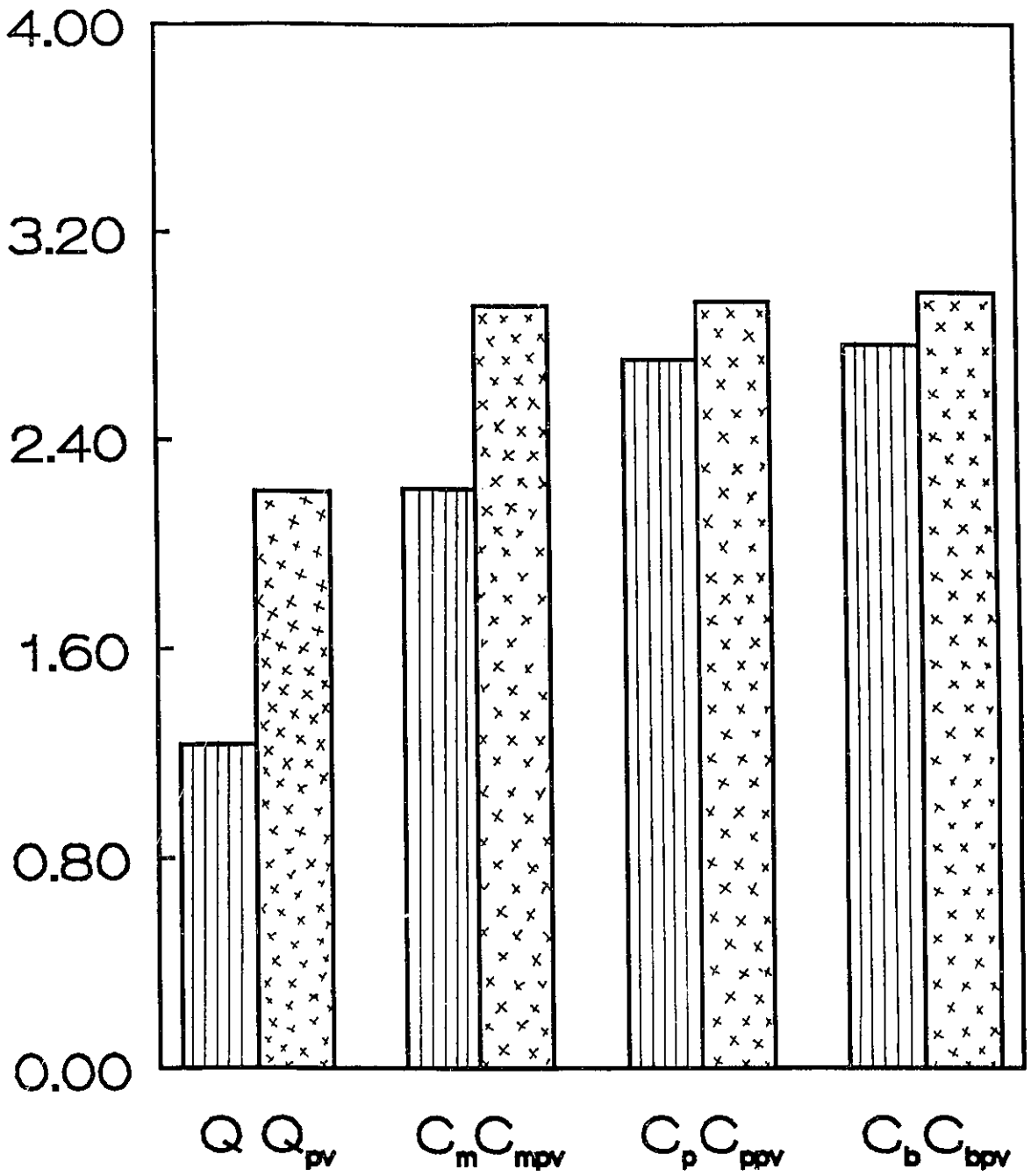

FIGURE 25 Comparison of the rates obtained using 200 torr methane on quartz, C_p, C_m, and C_b in the packed and unpacked vessels.

of the rates at 200 Torr in the packed and unpacked vessels on all the surfaces on which the rate was studied.

3.7.5.3 Discussion

On the quartz surface, the rate at low pressures increased by a factor of 10, which was the factor by which the actual amount of surface had increased in the reaction vessel. As the pressure of methane was increased, the increase in the rate was not as pronounced. This was most likely due to the increased deposition of carbon as the methane pressure was raised. The most active sites on the quartz were quickly blocked by valence-satisfied carbon atoms. The rate was observed to decrease and it is possible that the products ethane and ethylene were beginning to readsorb on the vessel surface.

On C_{mpv}, the rate was also found to increase by a factor slightly less than 10. The carbon formed by pyrolysis of methane, C_m, was the least active of the three carbon films studied. An increase in the total surface nonetheless resulted in an increase in the total number of active sites present on the surface and the rate of formation of ethane and ethylene was increased.

On C_{ppv} and C_{bpv} the rate did not increase significantly over the rate obtained in the unpacked vessel. In fact, there appeared to be a limiting value over which the rates did not increase. This was very clearly seen in Figure 25, where the rates on all three carbon films were almost identical. This indicated that irrespective of the method of formation of carbon, the rate did not increase above a certain value. The relative increase

in yield between the different surfaces studied showed that the least active surfaces showed the greatest increase in rate while the most active surface showed the least increase in rate. This supported the conclusion that the apparent inactivity of C_{ppv} and C_{bpv} was not due to inherent lack of activity of the film itself, but to the diffusional constraint imposed by the experimental system, as mentioned in the previous section. Below 20 Torr of methane, the rate did not vary much with a decrease in pressure. The rate approached a limiting value at lower pressures.

3.7.6 Rate as a Function of Temperature

3.7.6.1 Experimental

The rate of methane dissociation was studied over a temperature range of 1026 K to 573 K. The rate was determined on a methane carbon surface as well as a propylene carbon surface. The methane carbon film, C_{mpv}, was formed by pyrolysis of 640 Torr at 1220 K for 4 - 5 hours. The propylene carbon film, C_{ppv}, was formed by pyrolysis of about 500 Torr at 977 K for 4 - 5 hours. The experiments were performed using 200 Torr of methane as reactant and they were 15 minutes in length, except at 1026 K where the experiments were only 4 minutes in length.

3.7.6.2 Results and Discussion

3.7.6.2.1 Temperatures above 873 K

The observed products were ethane and ethylene, with small quantities of propylene, acetylene and allene at the higher temperatures.

The activation energy observed on C_{ppv} using 200 Torr of methane was comparable to that observed on C_p using 20 Torr of methane and had a value of 313 $kJmol^{-1}$. The activation energy observed on C_{mpv} using 200 Torr of methane was 234 $kJmol^{-1}$, which was comparable to the value obtained on C_m using 20 Torr of methane.

These results showed that the activation energy was dependent on the type of carbon and so the results for the activation energy for C_m and C_p, both in the packed and unpacked vessels, were different. On any one type of carbon, however, the activation energy was essentially the same even for different pressures of methane and in spite of the greater surface in the packed vessel, as shown in Figure 26. This further illustrates the picture of the carbon surface as composed of a range of sites of different energies and activities. Each type of carbon has a different proportion of the different types of sites. The products and their distribution remained the same and this also indicated that the mechanism after dissociation probably remained unchanged.

As the temperature was lowered to 873 K, the rate on C_{ppv} decreased below the rate on C_p. Since C_{ppv} had a much larger number of active sites than C_p, a lower rate suggested that radicals formed on the surface may not have had sufficient energy to

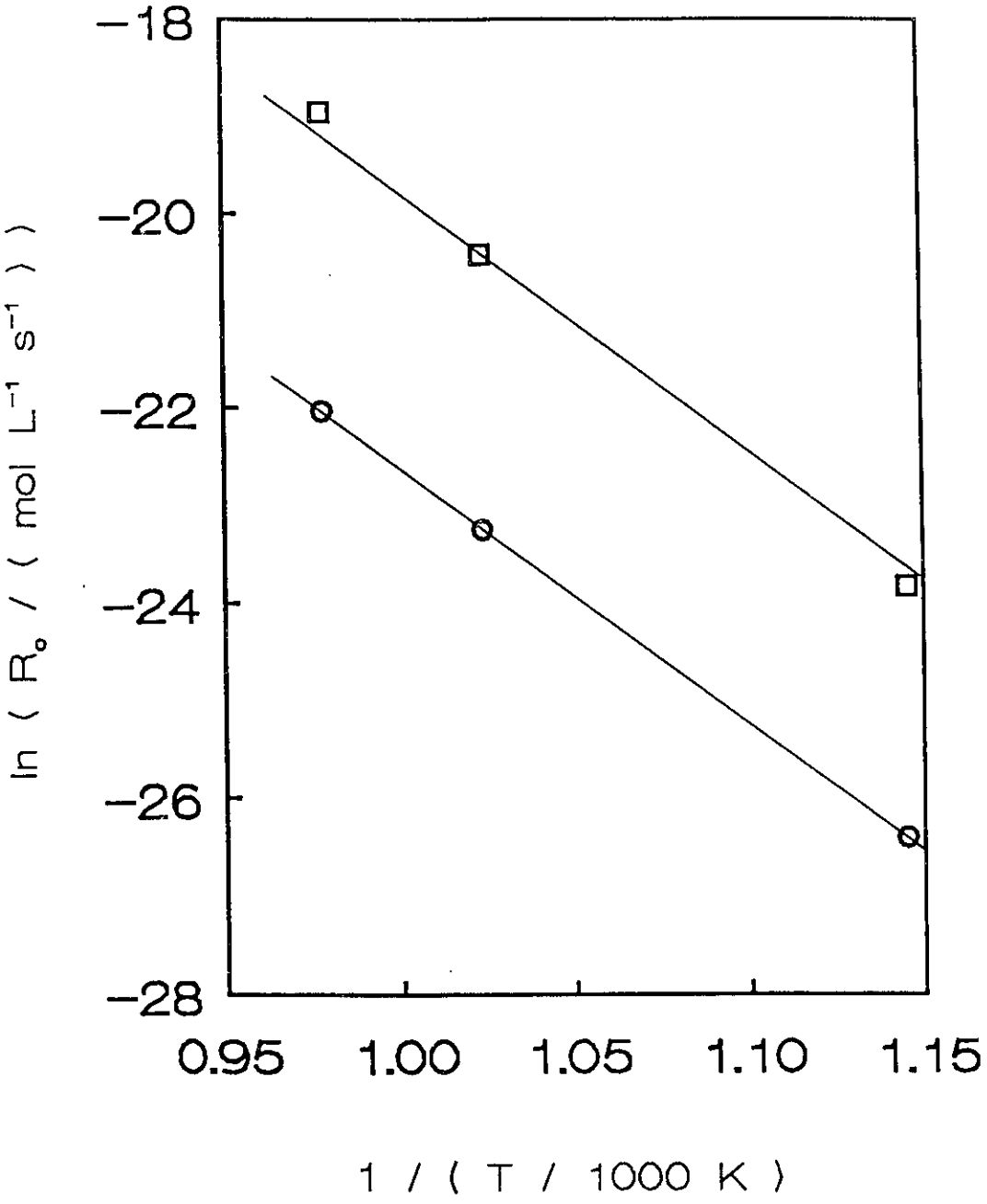

FIGURE 26 ln R_o as a function of 1/T on C_m and C_{mpv} above 873 K.
o 20Torr CH_4 on C_m □ 200Torr CH_4 on C_{mpv}

desorb from the surface and may have dehydrogenated to carbon. The proportion of adsorbed species which would have enough energy to desorb or form products which would desorb was much lower at 873 K than at 1026 K. A similar trend was observed on C_{mpv} and C_m.

3.7.6.2.2 Temperatures 873 K and below

The observed product distribution began to change below 873 K. The yield of ethane remained essentially unchanged while the amount of ethylene produced decreased to the detection limit. The amount of propylene began to rise and then fell gradually as the temperatures approached 573 K. This change in product distribution was only observed on C_p and C_{ppv}, and not on C_m or C_{mpv}. The results for the packed vessel are shown in Figure 27.

Over a range of temperature in the lower end of the temperatures studied, an increase was observed in the rate of formation of propylene. This increase was also observed on C_p at 20 Torr of methane and C_p at 200 Torr of methane. As explained in Section 3.6.4.2, the increase in the rate of formation of propylene was most likely caused by addition to a surface-adsorbed ethylenic species, either by a CH_3 species already on the surface or by methane in the gas phase via an Eley-Rideal mechanism. Although the rates were higher, the shape and the temperature dependence of the rate of formation of propylene at 200 Torr methane in the packed vessel resembled those obtained in the unpacked vessel at 20 Torr methane. A closer comparison of these results showed that

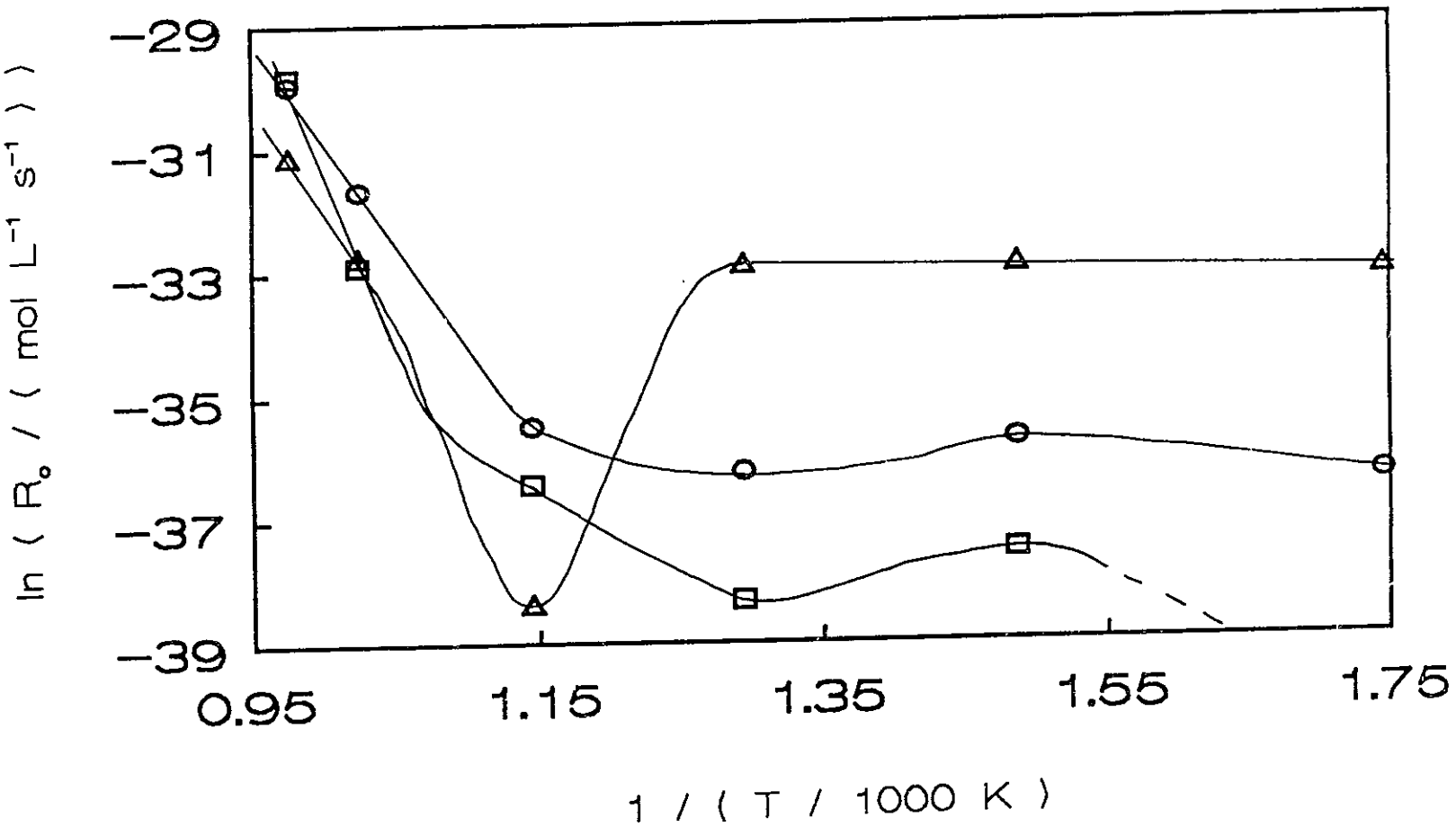

FIGURE 27 Rate of formation of products as a function of 1/T on C_{ppv} using 200Torr methane.
○ ethane □ ethylene △ propylene

while the pressure in the packed vessel was greater by a factor of 10, the available surface in the packed vessel also increased by a factor of 10. This could explain the resemblance between the two sets of results. 200 Torr of methane would not be a high enough pressure, given the large surface of the packed vessel, to have complete occupation of all the surface sites. Thus, formation of ethylidene or ethylidyne would be less likely than the formation of a surface ethylenic species.

CHAPTER 4

CARBON CHARACTERIZATION

4.1 Introduction

Up to this point, the inhibiting nature of the carbon film at small amounts of carbon and the catalytic nature of the carbon film at large amounts of carbon had been characterized reproducibly over a range of quantities of carbon. Further experiments were done to explore the source of the reactivity of the carbon in the films. The hydrogen content was determined as a function of the amount of carbon in the films and as a function of the precursor of the film. A comparison was made of the reactivity of the three carbon surfaces C_m, C_p, and C_b. Tests were made to determine the presence of fullerenes. Additionally, some reactivity studies were performed using labelled methane. In order to distinguish whether the activity of the carbon film was due to the presence of active sites inherent in the carbon lattice or whether the activity was due to unusual physical characteristics of the carbon surface, some experiments were performed to characterize the carbon film. These experiments included study by scanning electron microscopy (SEM), transmission electron microscopy (TEM), X-ray diffraction (XRD), and Fourier transform infra-red spectroscopy (FTIR).

4.2 Hydrogen Content of the Carbon

4.2.1 Introduction

The carbon films used in all of the experiments performed in this study were made by pyrolysis of hydrocarbons. Consequently, the films contained only carbon and hydrogen. The amount of carbon was determined by oxidation of the carbon film to produce carbon dioxide and water. The carbon dioxide was analyzed by gas chromatography and the amount of carbon in the films was quantitatively measured. The amount of hydrogen in the films was difficult to analyze. On oxidation the hydrogen formed water. Gas chromatography, however, was not a sufficiently sensitive method of determining the small amounts of water formed by the hydrogen in the films, and hence a measure of the hydrogen content of the films could not be obtained by this method.

The determination of the hydrogen content of the films was necessary in order to have a better understanding of the reaction mechanism. In most studies of reaction on a carbon surface, the carbon used is a commercial graphite, such as Graphon[16,17]. Generally, when such bulk carbons are used, the hydrogen content of the carbon is not determined. However, the studies of Somorjai and coworkers[20-24] of hydrocarbon reactions on metal surfaces have indicated that almost coincident with the commencement of reaction on a metal surface, a hydrocarbonaceous layer was deposited on the metal surface. This carbon was found to be necessary for the catalytic activity of the metal due to the capacity of the carbon to act as a hydrogen transfer agent. As the carbon

progressively dehydrogenated to form unreactive carbon or coke, the catalytic activity of the surface decreased.

Thus the presence of hydrogen was important in the reactivity. The hydrogen contained in the carbon films deposited in this study was considered to be an important factor in determining the change in reactivity observed in the carbon. A simple method was developed to measure the hydrogen content of the carbon films which was applicable even when the amount of carbon deposited was small.

4.2.2 Experimental

The carbon film was oxidized according to the procedure described in Section 2.4.3. The products of the oxidation, CO_2 and H_2O, were trapped separately in the two spiral traps, ST1, which was maintained at 77 K and ST2, which was maintained at 195 K. After the oxidation procedure was complete, the contents of ST1 were condensed into a removable sampler for analysis, and ST1 was evacuated. The contents of ST2 were allowed to expand quickly into a calibrated volume. The pressure was monitored constantly using a 10 Torr Baratron gauge and the maximum pressure was noted. This operation was performed as quickly as possible because water is rapidly lost by adsorption on the walls of the pyrex apparatus. Tests showed that by reading the maximum pressure, errors due to this loss were reduced to a few percent. If a large amount of hydrogen was present or if the pressure was too high to register on the Baratron gauge, an additional calibrated volume was adjacent to ST2. Thus a large range of amounts of water, from 5×10^{-9} to 7×10^{-5} mol, could be accurately measured.

4.2.3 Results and Discussion

Figures 28 and 29 show plots of the log of hydrogen amount and the H/C mole ratio respectively as functions of the log of carbon amount over a large range of carbon amounts from films deposited by pyrolysis of propylene in both the packed and unpacked vessels. When the amount of carbon deposited was large, the total amount of hydrogen was roughly proportional to the amount of carbon. As the amount of carbon deposited decreased, however, the amount of hydrogen in the carbon films did not decrease proportionately. As a result, the relative amount of hydrogen increased. This is more clearly seen in Figure 29. This trend in the H/C mole ratio with amount of carbon may be compared with the results obtained in Figure 13, in which the reactivity of the carbon is plotted as a function of the carbon deposited on the surface of the reaction vessel. The minimum in the H/C ratio occurs at an amount of carbon corresponding approximately to the amount of carbon required to form a monolayer on the reaction vessel surface. This is also the point at which the reactivity rises rapidly. It thus appears that the hydrogen content of the carbon may be a factor in the reactivity of the carbon film.

This method of determining the hydrogen content of the carbon films was found to be reproducible and consistent for a particular carbon film over four orders of magnitude in carbon amount. The relation between the hydrogen content of the carbon films and their reactivity will be discussed in the following section.

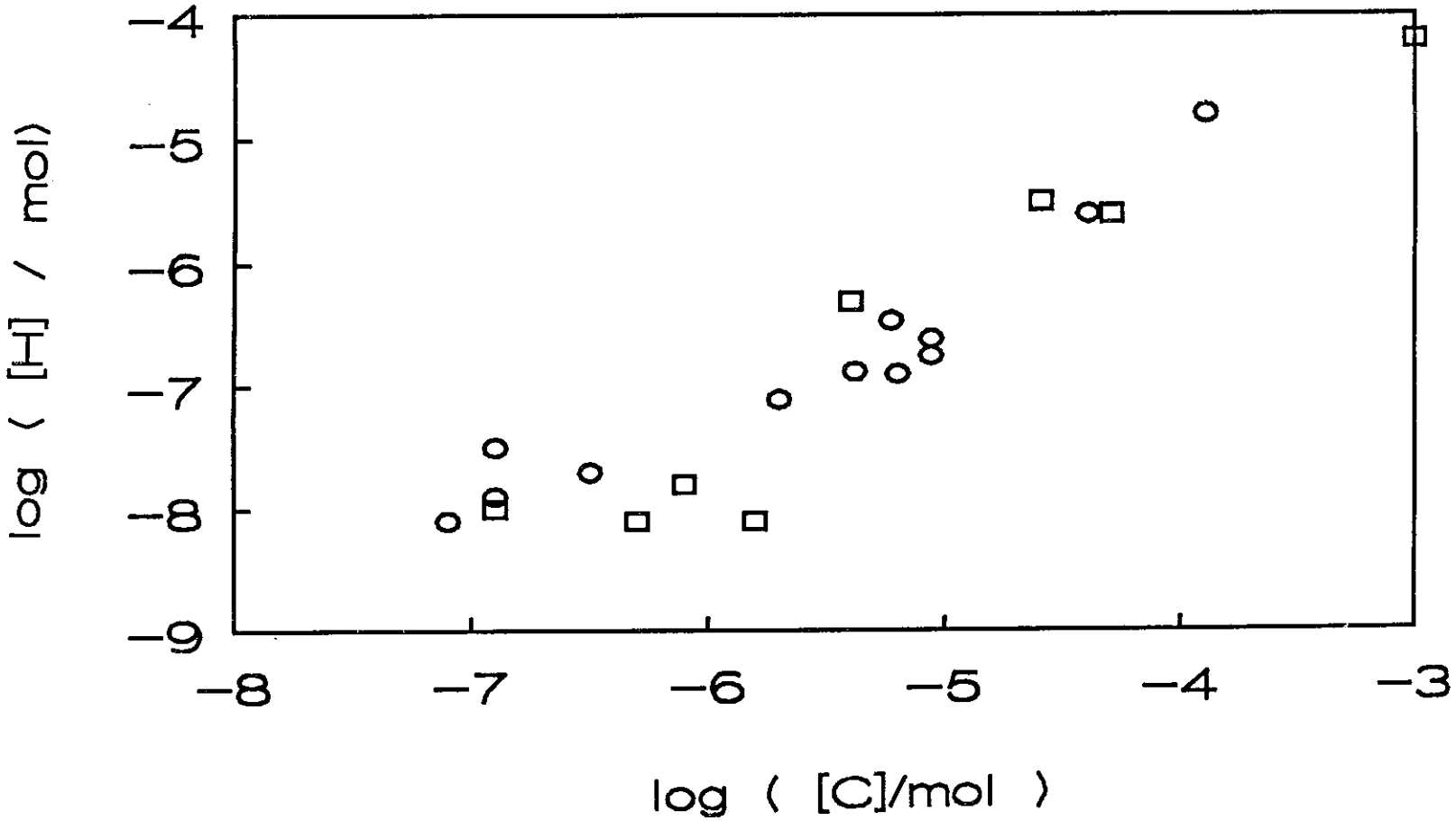

FIGURE 28 log [H] as a function of log [C] for carbon films formed by pyrolysis of propylene.
o unpacked vessel □ packed vessel

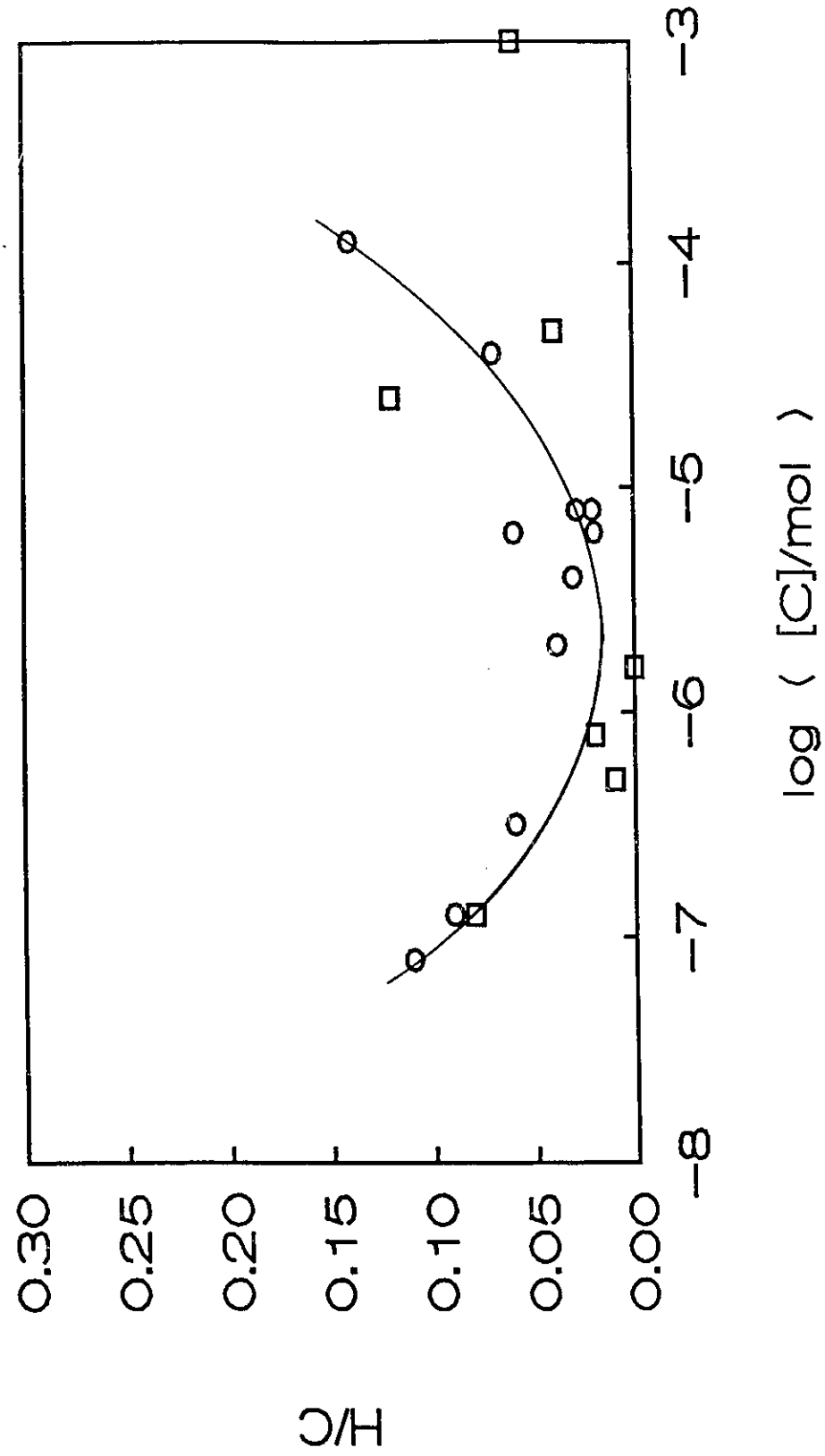

FIGURE 29 Hydrogen to carbon mole ratios as a function of log [C] for carbon films formed by pyrolysis of propylene.
o unpacked vessel
□ packed vessel

4.3 The Reactivity of Carbon as a Function of the Carbon Precursor

4.3.1 Introduction

As mentioned in Section 3.3.4, the rate of methane dissociation on C_p was higher than the corresponding rate on C_m. The main difference between these two films was the temperature at which they were deposited. A higher temperature of deposition of the carbon film resulted in a film which had a lower reactivity. To examine this effect further, carbon films were formed by pyrolysis of butadiene at a lower temperature than was used for the formation of the propylene carbon films.

4.3.2 Experimental

In order to obtain an amount of carbon comparable to that obtained in the propylene and methane carbon films, 31.5 Torr of butadiene was pyrolyzed at 877 K for 3 hours. The reactivity of the butadiene film, C_b, was tested at three temperatures, 1026, 977, and 877 K using 21 Torr of methane. All experiments were 15 minutes in length except for the experiments performed at 1026 K which were 4 minutes in length.

4.3.3 Results and Discussion

The results obtained on C_b are compared to the results obtained on C_p and C_m in Figure 30. The rate of dissociation of methane follows the order $C_b > C_p > C_m$ at 877 K.

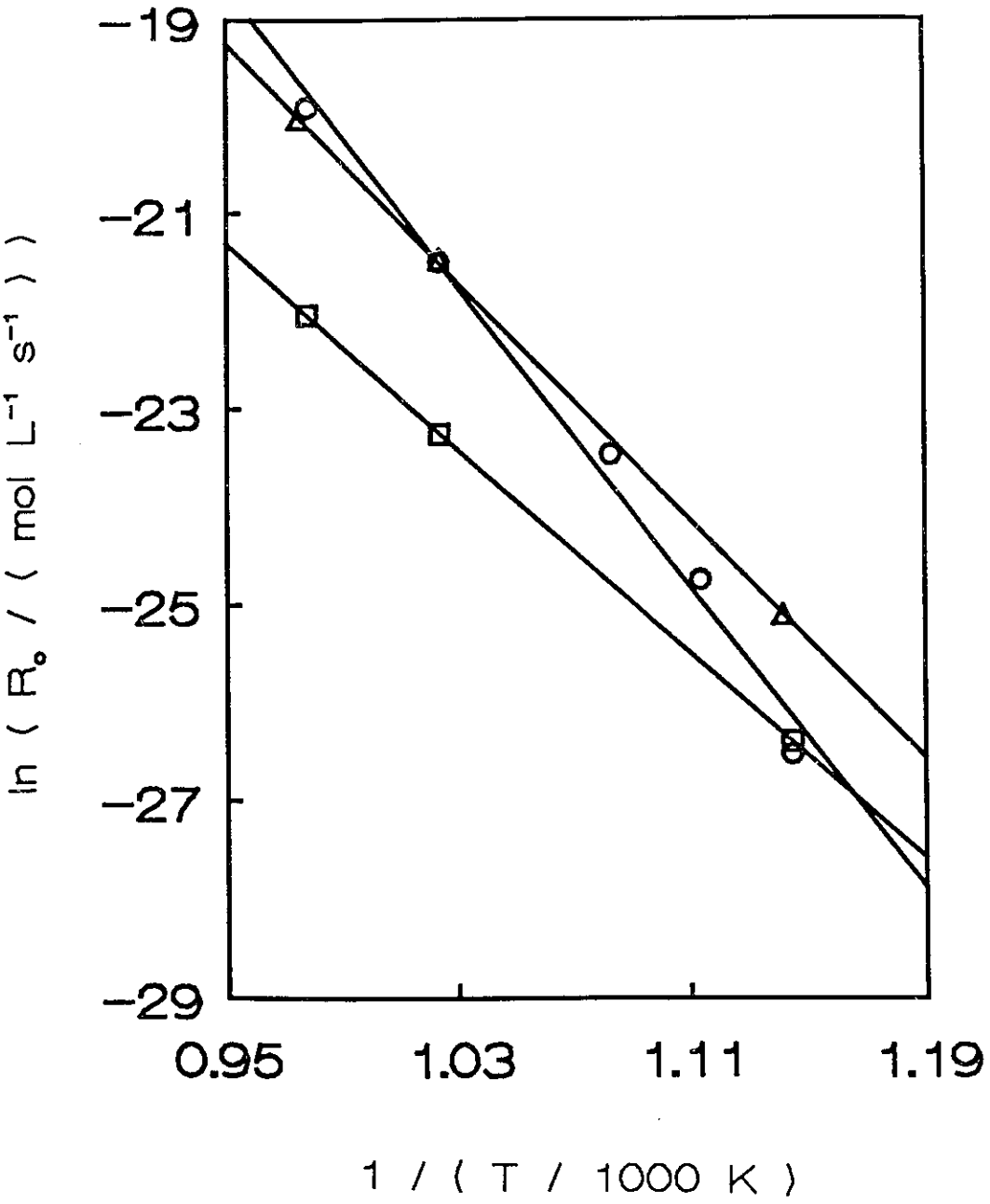

FIGURE 30 ln R_o as a function of 1/T on different carbon films using 20Torr methane.
○ on C_p □ on C_m △ on C_b

At 977 K, the rate on C_b and C_p are very close, and at 1026 K, the rate on C_b is slightly lower than the rate on C_p.

When C_p was heated above the temperature at which it was deposited, its activity decreased. A similar effect was observed on C_b as the temperature of reaction was raised above the temperature of deposition of the film. At the temperature of deposition of C_b, however, the rate of methane dissociation on C_b was significantly higher than on C_p and C_m. This provided additional support for the premise that the difference in reactivity between C_p and C_m was due to a difference in deposition temperature of the two films. While the deposition temperature would have affected the degree of graphitization of the carbon to a small extent, the temperature would have had a significant effect on the hydrogen content of the films. Table 2 shows hydrogen to carbon mole ratios for the three different films at the three temperatures studied.

TABLE 2

	1026 K		977 K		877 K	
	H/C ($\times 10^{-2}$)	R_o (Torr s^{-1})	H/C ($\times 10^{-2}$)	R_o (Torr s^{-1})	H/C ($\times 10^{-2}$)	R_o (Torr s^{-1})
C_b	9.1	1.22×10^{-4}	7.7	2.89×10^{-5}	25	7.61×10^{-7}
C_p	10	1.37×10^{-4}	4.3	2.83×10^{-5}	13*	2.88×10^{-7}
C_m	1.5	1.64×10^{-5}	1.2	4.87×10^{-6}	1.1	2.09×10^{-7}

* this H/C value was measured on C_p at 777 K; the rate was measured at 877 K

At 877 K, C_b has the largest amount of hydrogen in the film and also has the highest reactivity. The hydrogen content of C_p at 877 K is intermediate to that of C_b and C_m, as is its reactivity. At 1026 K, the hydrogen contents of C_b and C_p are very similar but C_p is slightly larger. The rates on these carbons followed the same trend. The values at 977 K are different with C_b having almost twice as much hydrogen as C_p, but both films having the same reactivity. The main difference at this temperature is that only a few consecutive experiments were performed on C_b at this temperature but many consecutive experiments were performed on C_p at 977 K. The carbon deposited during these reactions most likely contained enough hydrogen to raise the H/C ratio significantly. It thus appears that the rate on the three films C_p, C_m and C_b correlates reasonably well with the H/C ratios of the films.

4.4 Analysis of Carbon for Fullerenes

4.4.1 Introduction

It is known that fullerenes, which are three-dimensional truncated icosahedral clusters containing sixty carbons or more are formed upon carbon arc vaporization of graphite[1]. It was not expected that any fullerene-type structures would form under the conditions used in this study. In order to ensure that no fullerenes were present, however, a mass spectrometric analysis was made of three different carbon films.

4.4.2 Experimental

Carbon was deposited by pyrolysis of propylene at 977 K for a particular series of experiments. After the experiments were complete, the reaction vessel was evacuated, isolated by means of a stopcock, and cooled to room temperature. After it was completely cooled, air was admitted into the reaction vessel. The carbon film was extracted using a small amount of methylene chloride. Any fullerenes would have dissolved during this process, although the carbon itself, which is not soluble in methylene chloride, remained suspended in the solvent. A similar procedure was followed for a carbon film deposited by pyrolysis of methane at 1220 K and a carbon film formed by pyrolysis of propylene at 977 K and then heated to 1220 K for three hours.

The samples were then submitted for mass spectrometric analysis by Fast Atom Bombardment (FAB) on the Kratos Concept IIH. The source was operated at 8 kV in order to maximize the sensitivity and the ions were produced by a cesium ion gun running between 12 and 15 kV. The methylene chloride was evaporated quickly and a drop of 3-nitrobenzyl alcohol (NBA) was used to redissolve the samples.

4.4.3 Results and Discussion

A sample spectrum is shown in Figure 31. The peak at mass 132.9 corresponds to the cesium ion beam while the peak at mass 154 corresponds to the protonated solvent

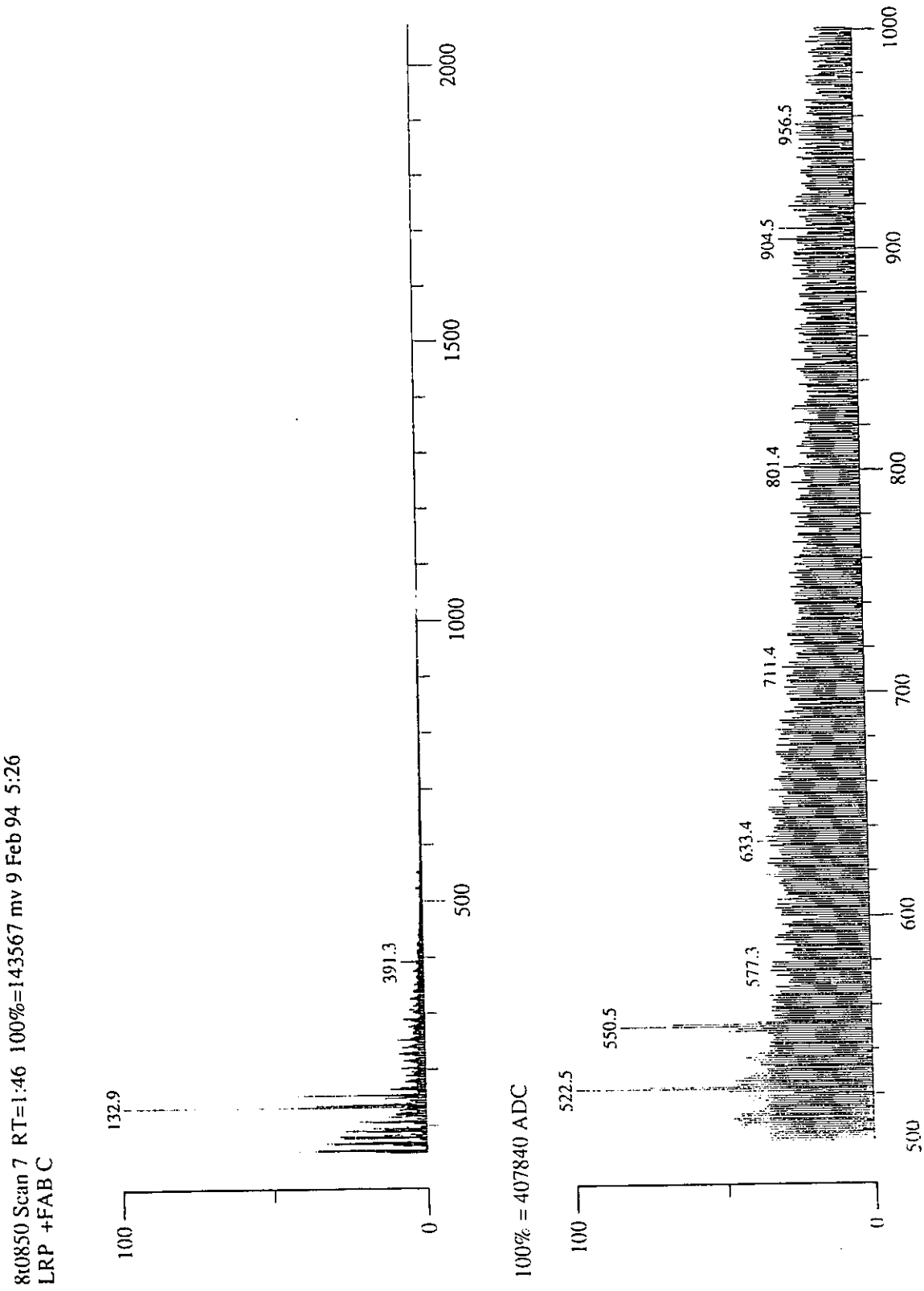

FIGURE 31 Sample Mass Spectrum analyzed for the presence of Fullerenes

3-NBA. These were the two major peaks observed in all the spectra. Other than these two peaks, a number of small peaks at almost every mass between 50 and 350 were observed, corresponding to the different fragments produced upon dissociation of the carbon suspended in the solvent. No peak was observed at mass 720 or 721 which would have corresponded to C_{60} or protonated C_{60}. These spectra confirmed that there were no fullerenes present in the carbon films formed by pyrolysis of the hydrocarbons used in this study.

4.5 Study of the Carbon Film by Electron Microscopy

4.5.1 Introduction

The carbon film was found to have both catalytic and inhibitive effects. The experimental work up to this point dealt with the chemical reactivity of the carbon films and possible mechanistic explanations for this reactivity. It was necessary, however, to ensure that the different effects of the carbon film on methane conversion were not due to unusual physical characteristics. For example, the formation of filamentous carbon would result in a larger surface area than simple coverage of the vessel surface would predict. The formation of filaments could also increase the number of surface defects and the surface roughness, both of which would contribute to possible rate acceleration. Thus, the morphology of the carbon surface was an important factor in its catalytic activity. In order to determine the nature of the carbon surface, analysis of the film was made using a scanning electron microscope (SEM). Additional studies were made using a transmission electron microscope (TEM).

4.5.2 Experimental

Device quality silicon wafers were cut into pieces approximately 5 mm x 10 mm. The first sample was prepared by placing one wafer in a quartz boat which was placed in a quartz tube. The tube was evacuated and placed in a furnace heated to 977 K for three hours. Subsequently, the tube was evacuated to remove any materials which had been adsorbed on the silicon surface. Carbon films were made by admitting the reactant to the tube, and allowing it to react for the required time. After reaction, the tube was evacuated and allowed to cool to room temperature. Air was admitted to the tube, and the sample was removed with tweezers and placed in a container for analysis by SEM and TEM. Three samples were prepared under the conditions described in Table 3:

TABLE 3

Reactant	Pressure	Temperature	Reaction Time	Second Temperature	Reaction Time
	Torr	K	Hours	K	Hours
(1) C_3H_6	52.1	977	3	-	-
(2) CH_4	50	1223	3	-	-
(3) C_3H_6	52.1	977	3	1223	3

4.5.3 Results

Analysis by SEM indicated only an amorphous surface. Bright field cross-sectional TEM images with a resolution of 2.5 Å were taken on a Philips EM430T operating at 250 kV near the <110> zone axis. To minimize sample preparation artifacts, samples were prepared by the small-angle cleavage technique[71]. Each sample was of uniform thickness. Samples 1 and 3 varied in thickness from 26 - 30 nm while sample 2 was 40 - 45 nm in thickness. The cross-section of the samples indicated a smooth, non-porous, evenly-layered, featureless surface at a magnification factor of 1.78×10^6. No filaments were observed.

4.5.4 Discussion

These results showed that the carbon was indeed deposited uniformly on the vessel surface. A sample transmission electron micrograph is shown in Figure 32. No filamentous formation was observed under conditions identical to those under which the reactions were performed. The surface was uniform and devoid of any remarkable characteristics. No distinction could be made between the films formed by pyrolysis of propylene and methane. The heat treatment of the propylene carbon did not seem to alter the appearance of the film. The difference in thickness between the propylene and methane carbon films could probably be explained by the higher temperature of pyrolysis of the methane carbon film. The reactivity of the carbon films was therefore due to the

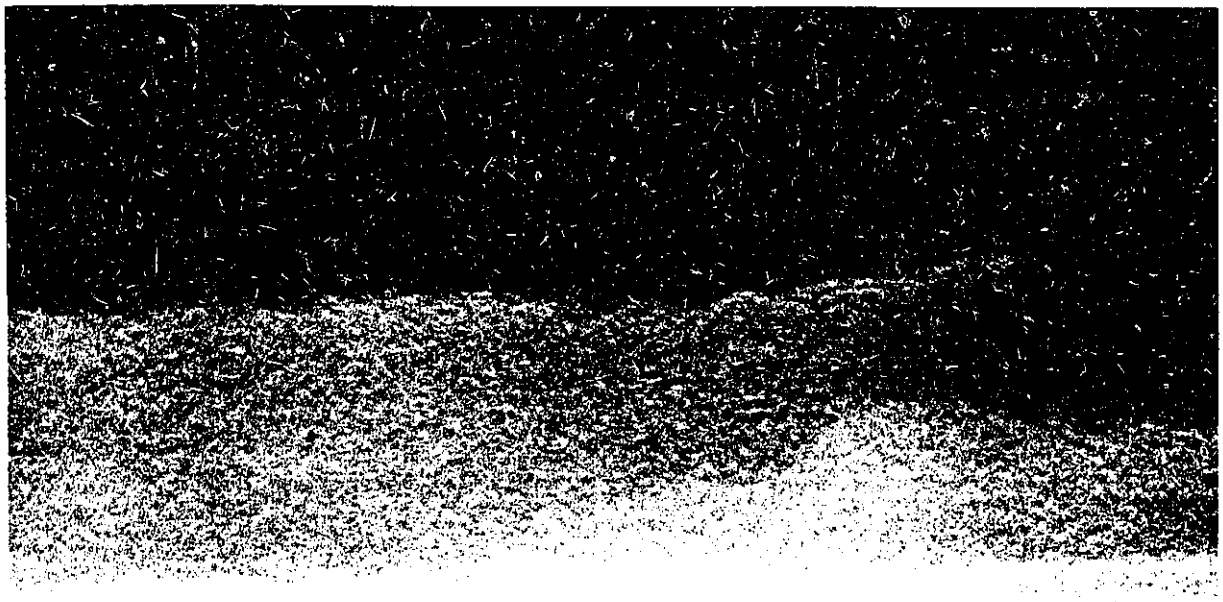

FIGURE 32 Transmission Electron Micrograph of Carbon Film. The bottom portion of the photograph (white) is the silicon on which the carbon was deposited, and the thin portion above the silicon is the native oxide on the silicon. The shaded portion above the native oxide is the carbon film. The black portion above the film is air. The scale is such that 1.8 cm represents 10 nm.

inherent chemical properties of the carbon itself and not the presence of some unusual physical characteristic of the carbon film or its surface.

4.6 X-Ray Diffraction Studies of the Carbon Film

4.6.1 Introduction

X-rays lie in the electromagnetic spectrum between ultraviolet and gamma radiation and have wavelengths ranging from 0.1 to 100 Å. They are usually produced by fast moving electrons whose energy of motion is converted into quanta of radiation. The wavelength of the radiation produced depends on the energy of the electron.

Shortly after X-rays were discovered by Wilhelm Röntgen in 1913[72], it was suggested that they might be diffracted if passed through crystals since their wavelengths were comparable to the separation observed in lattice planes.

In a three-dimensional lattice , the unit cell is a volume element which may be defined as a parallelepiped whose edges are successive grid lines[73]. If an X-ray beam is incident on two parallel planes with interlayer spacing d such that the beam forms an angle θ with the surface, as shown in Figure 33, the electrons at the points of impact, O and C, of the beam on the planes will be forced to vibrate by the oscillating field of the incident beam. Consequently, they will radiate in all directions. For a particular direction where the two parallel beams, 1' and 2', emerge at the same angle θ as the incident beam, as if the beam had simply reflected off the surface, the diffracted beam would

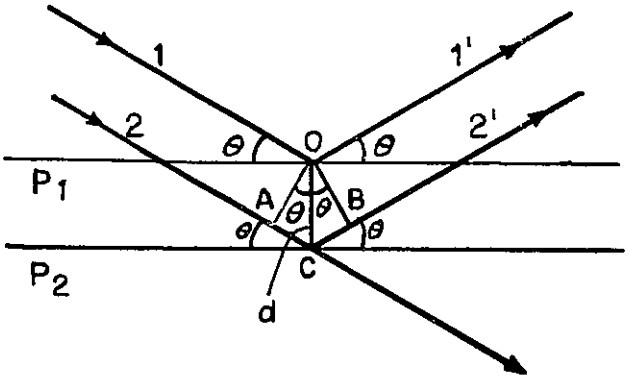

FIGURE 33 Illustration of Bragg's Law

reach a maximum intensity when the waves represented by the two rays were in phase. This situation would occur if AC + BC or 2AC was equal to an integral number of wavelengths. Since AC/d is equal to sin θ, the relationship

$$2d \sin\theta = n\lambda \qquad [27]$$

can be obtained, where n is an integer. This relationship is known as Bragg's Law and forms the basis for X-ray diffraction techniques. In modern work, it is customary to absorb n into d and write the Bragg law as

$$2d \sin\theta = \lambda \qquad [28]$$

thus regarding the nth order reflection as arising from the (nh, nk, nl) planes. Once the angle θ corresponding to a reflection has been determined, d may readily be calculated.

In experimental X-ray diffraction studies, the X-rays are formed from electrons which are accelerated by an electric field and directed against a metal target. The metal chosen as the target depends on the type of crystal structure being examined. Copper produces x-rays[74] of wavelength 1.5418 Å which are sufficiently penetrating to be

diffracted by the crystal. When used with a diffraction apparatus, copper as a target metal is capable of providing more than enough data to adequately determine the structure.

4.6.2 Experimental

Sample films were formed by pyrolysis of methane and propylene. Two samples of each type of carbon were prepared. The first sample was approximately the thickness deposited before most of the reactions performed in the unpacked vessel. The second sample contained approximately ten times that amount of carbon. The sample preparation conditions are provided in Table 4.

TABLE 4

Sample	Reactant	Pressure	Temperature	Deposn. Time
		Torr	K	hours
A	C_3H_6	54.6	976	3
B	C_3H_6	329.0	977	4
C	CH_4	52.0	1219	3
D	CH_4	329.0	1219	3

After preparation, the samples were sent to Dr. M. S. Seehra of the physics department at the West Virginia University for analysis.

4.6.3 Results and Discussion

The carbon films A, B and C were too thin to observe any significant results. Carbon film D yielded a spectrum in which a peak other than the peak corresponding to quartz was observed. Since a quartz blank was supplied along with the samples, the data for the quartz was subtracted from the spectrum of sample D and the resulting spectrum is shown in Figure 34. The raw spectrum was curve-fitted and the results are shown in Figure 35.

The peak was observed at a value of $2\theta = 25.6$. The θ value was thus determined as 12.8. The wavelength at which the measurements were made was that of copper, 1.54 Å, and the diffraction was measured from the 002 plane. The value of n was therefore known to be 2. From Bragg's Law, the value of d, the interlayer spacing was calculated as being 3.44 Å. The x-ray diffraction from sample D was subject to structural analysis using the model of Dahn et al[75,76] by Dr. Seehra's group. The structural parameters provided by Dr. Seehra were determined by the analysis model they used. A value of the parameter a, where a, b, and c define distances in the x, y and z directions respectively, was given as being 2.427 Å. An estimation of the value of a was made using the structural parameters for a synthetic graphite obtained from the JCPDS database[77]. By proportionately scaling the appropriate parameters for the graphite and using the value of d obtained by Dr. Seehra's group, a value of a closely resembling the value of a provided by Dr. Seehra was obtained.

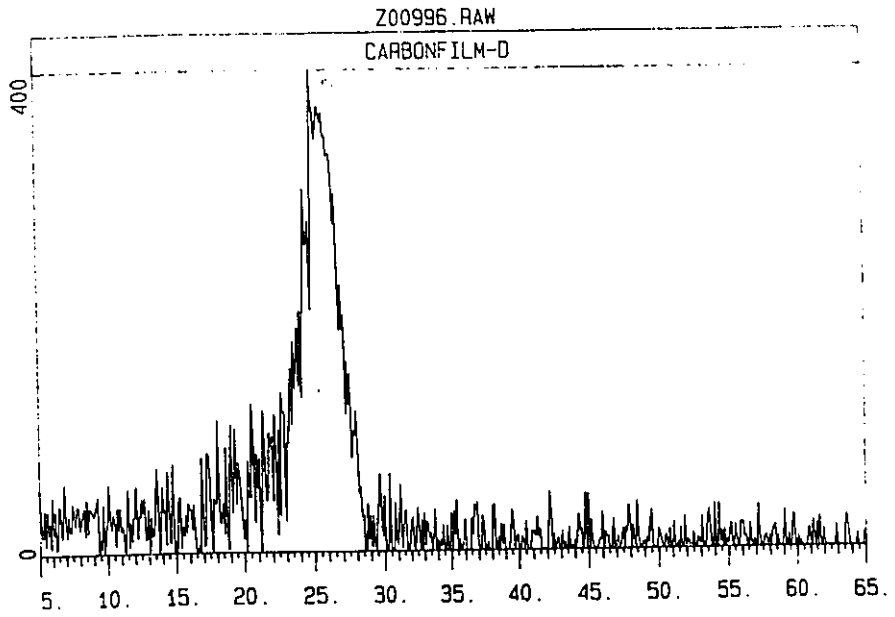

FIGURE 34 Experimental Results of XRD Analysis of Carbon Film

A00996.RAW- Sample D.

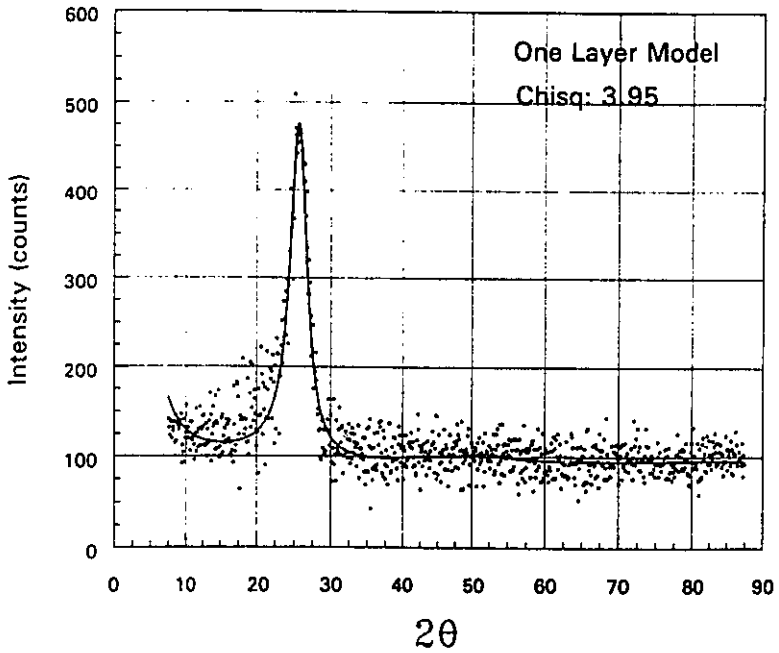

FIGURE 35 Curve-Fitted Results of XRD Analysis of Carbon Film

The interlayer spacing for graphite is known to be 3.35 Å[2] and the interlayer spacing for amorphous or microcrystalline carbon is known to be greater than the value for graphite. The value of d obtained upon analysis of sample D was 3.44 Å, indicating the presence of non-graphitic carbon.

4.7 Analysis of Carbon Films by Fourier Transform Infra-Red Spectroscopy

4.7.1 Introduction

Infra-red light is low energy radiation which has wavelengths ranging from just below the visible, at 700 nm, to just above the microwave region, at 3 mm. The energy required to produce vibrations in molecules also lies in this range. Thus, infra-red radiation is ideal for studying the vibrations of molecules or functional groups in molecules, and infra-red spectroscopy plays an important role in chemical analysis. The vibrational spectra of different groups in a molecule act as fingerprints for that group since the contribution of the normal modes of a group is often similar even if the group occurs in different molecules[72]. Thus the identity of a particular molecule or group can be determined by studying its infra-red spectrum and comparing the bands obtained to tabulated vibrational frequencies.

4.7.2 Experimental

The same films prepared for the XRD study in Section 4.6 were used in the FTIR study as well. This analysis was also performed by Dr. Seehra at West Virginia University.

4.7.3 Results and Discussion

Figure 36 shows a sample spectrum of a type of coal called vitrinite[78a]. Although the infrared spectrum of amorphous carbon is different from that of coal[78b], the important groups can be identified from the spectrum shown in Figure 36. The region 3800 to 3200 cm^{-1} is characteristic of various OH and NH stretching modes. Aromatic CH groups have stretching bands between 3100 and 3200 cm^{-1}, while aliphatic CH stretching bands lie between 2700 and 3000 cm^{-1}. The region 1500 to 1800 cm^{-1} is characteristic of aromatic ring modes and carbonyl and carboxylic acid groups. The region 1000 to 1400 cm^{-1} is complicated and consists of a number of overlapping bands which reflect highly mixed and coupled vibrations. Although it is difficult to assign bands to specific functional groups, vibrations involving CC stretching, OH bending, and CH_2 bending should appear in this region. Between 700 and 1000 cm^{-1}, vibrations may be assigned to CH out-of-plane bending modes.

Figure 37 shows the infrared spectrum of the carbon film in sample A, after subtraction of the quartz blank. The peaks observed between 3500 and 4000 cm^{-1} correspond to water, while the peak between 2300 and 2500 cm^{-1} corresponds to carbon dioxide. The water and CO_2 were most likely present in the air. Between 2800 and 3000 cm^{-1}, two small negative peaks may be seen. This is the region where CH stretches are observed but, as can be seen in Figure 37, no positive peaks were observed. This may have been due to impurities, such as grease from handling, on the quartz blank. Subtraction of the blank from the carbon spectrum may have cancelled the positive peak

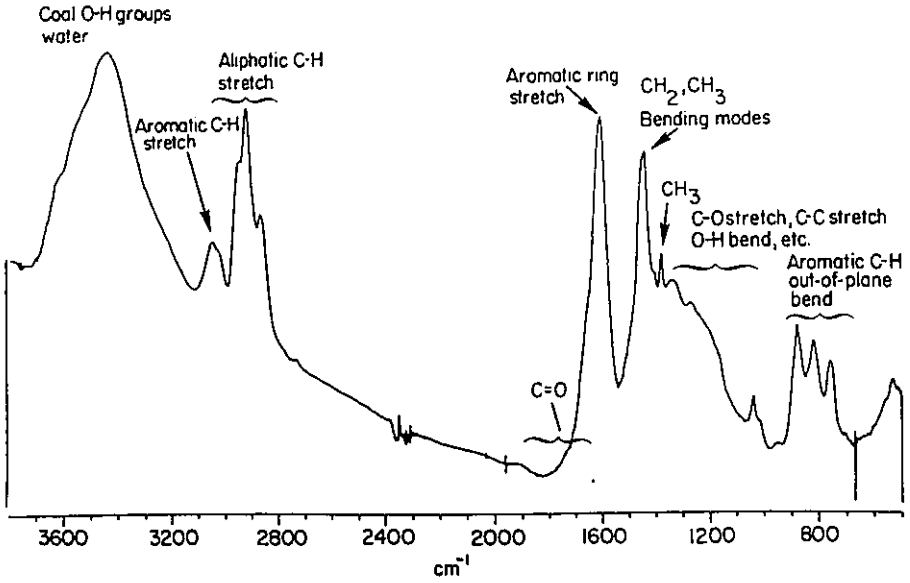

FIGURE 36 Sample FTIR Spectrum of Vitrinite Concentrate (PSMC 52)

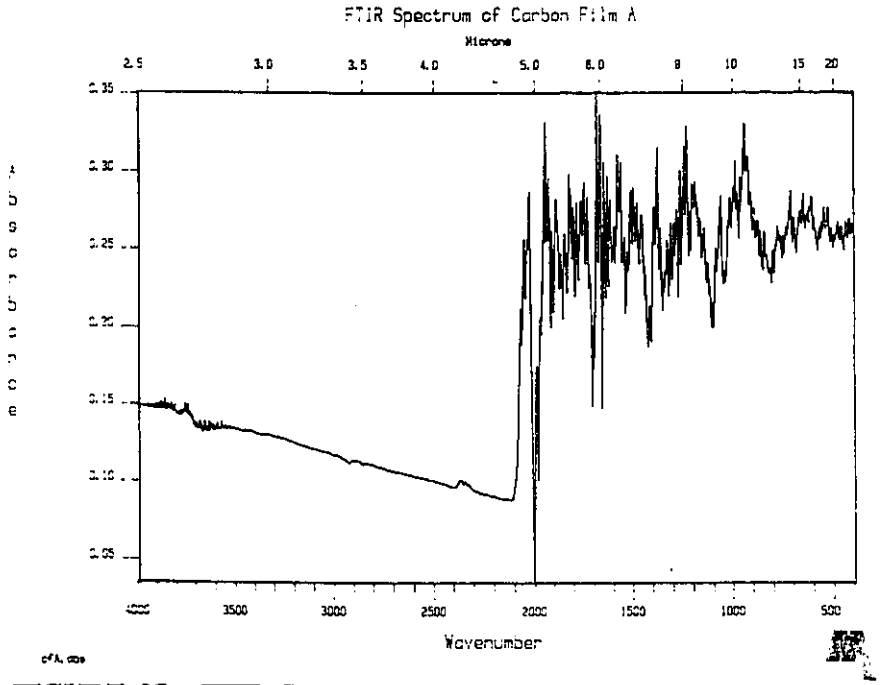

FIGURE 37 FTIR Spectrum of Carbon

from the sample and, in fact, could account for the presence of a negative peak. Below 2000 cm^{-1}, the quartz is opaque and no characteristics may be identified.

Infrared spectroscopy proved to be an inconclusive means of characterizing the carbon surface. If the carbon had been deposited on a surface which was not opaque in the region 700 - 1000 cm^{-1}, it may have been possible to observe CC stretching or CH_2 bending.

4.8 Study of Carbon Reactivity using Labelled Methane

4.8.1 Introduction

A key question in the matter of the heterogeneous processes occuring on the surface was how the surface carbon participated in the formation of the products. Was the carbon which was part of the original film hydrogenated during the course of the reaction to form the hydrocarbon products, or did the carbon participate only as a catalyst for the dissociation of methane. In an effort to clarify these questions, a study was undertaken using labelled methane, $^{13}CH_4$.

4.8.2 Experimental

4.8.2.1 $^{13}CH_4$ as a Reactant

As in previous studies, a carbon film was deposited by pyrolysis of propylene, $^{12}C_3H_6$. $^{13}CH_4$ was used as the reactant. If carbon from the surface participated in the

reaction, a mixture of labelled and unlabelled products would be observed. The products expected were ethane and ethylene based on the product distribution obtained in similar experiments. If the surface carbon did not participate in the reaction, the products would contain only ^{13}C, but if surface carbon was part of the reaction, $^{13}C^{12}CH_6$ and $^{13}C^{12}CH_4$ would be observed. Products containing exclusively ^{12}C could be: a) released from the surface as one or more surrounding surface active sites on the carbon were removed by reaction; b) formed by surface rearrangement or migration; c) formed by direct hydrogenation of the carbon surface. While these mechanisms were inherently unlikely, the spectra were examined for indication of these products.

4.8.2.2 Experimental Procedure

22.1 torr of propylene (Matheson, 99.9% purity) was admitted into the quartz vessel, having a volume of 136 mL, at 977 K. After a period of three hours, the vessel was evacuated and the system pressure was lowered to 10^{-6} torr (as confirmed by the McLeod gauge) where it was maintained for the duration of the experiments. The resultant carbon film contained only carbon and hydrogen and was free from impurities. Tests were made to determine whether hydrocarbons, particularly ethane or ethylene, were degassed from the film in the absence of the reactant CH_4. Such a reaction would be a source of $^{12}C_2H_6$ and $^{12}C_2H_4$. No traces of these products were observed from the films at the temperatures of the reaction. Preliminary experiments indicated the presence of traces of oxygen in the sample of $^{13}CH_4$. These traces were eliminated by insertion of an

oxygen filter. Following this treatment, the oxygenated species in the products were not detected.

20 Torr of $^{13}CH_4$ was then admitted into the vessel containing the carbon film which was at 977 K, and after a period of fifteen minutes, all products were removed through two spiral traps. The first trap was immersed in a dry ice/acetone bath and the second was immersed in a liquid nitrogen bath, in order to differentiate between lighter and heavier hydrocarbon products. The products in the second spiral trap immersed in liquid nitrogen were then condensed into a sampler fitted with an o-ring seal for connection to the mass spectrometer. The sample was then admitted via the gas inlet system and analysed by mass spectrometry on the AEI MS-902 Mass Spectrometer (MS-9). A total of six to eight such reactions were performed over the same carbon film and the products from all the reactions were analysed in a similar manner.

Upon completion of the desired number of experiments in the series, the reaction vessel was heated to 1023 K and ~200 Torr of oxygen was admitted for 20 minutes. The reaction vessel was evacuated through two spiral traps, similar to the procedure used during the reaction series. Oxygen was admitted to the reaction vessel two more times and the evacuation procedure repeated, each time storing the products in the spiral traps. After the third time, the products in the liquid nitrogen trap were distilled into the sampler, and analyzed on the MS-9. The expected product was carbon dioxide, some with m/z 45 ($^{13}CO_2$) and most with m/z 44 ($^{12}CO_2$). The total amount of carbon in the film ranged from 3×10^{-5} to 4×10^{-4} moles depending on the amount of propylene pyrolyzed.

In order to understand the mechanism more clearly, another reaction series was commenced at lower temperatures where ethane was the only expected product. The carbon film on which the reaction was performed was prepared by pyrolysis of 50 Torr of propylene at 977 K for three hours. After evacuation of the vessel, the temperature was lowered to 854 K. 20 Torr of $^{13}CH_4$ was then admitted to the vessel and the reaction proceeded for 120 min. The products were evacuated, and the analysis was carried out as before.

4.8.3 Results

4.8.3.1 Interpretation of the Data

In order to determine the relative peak heights of the ions in the fragmentation pattern of the reaction products, samples of methane (m/z 16), methane-^{13}C (m/z 17), ethane (m/z 30), ethylene (m/z 28), and propylene (m/z 42) were analyzed on the MS-9. The relative ratio of the peak heights of the fragment ions was determined by assigning the largest peak in each spectrum a value of 100%. In the subsequent analysis of the spectra it was assumed that the fragmentation pattern did not change substantially upon substitution of ^{13}C for ^{12}C. Sample spectra of $^{12}C_2H_6$ and $^{12}C_2H_4$ are shown in Figures 38 and 39. The major peaks in these spectra and their relative amounts are given in Tables 5 and 6.

In a previous similar series of experiments at 977 K using 20 Torr of methane, the products were ethane and ethylene and small amounts of propylene. Analysis of the

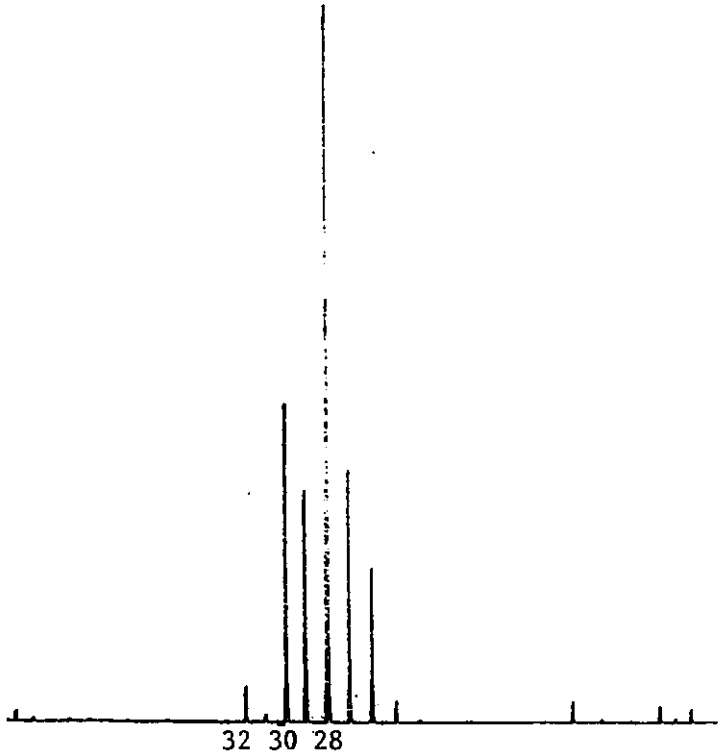

FIGURE 38 Mass Spectrum of $^{12}C_2H_6$

TABLE 5 Expected Distribution of Peaks for $^{12}C^{13}CH_6$ and $^{13}C_2H_6$ based on $^{12}C_2H_6$

Peaks for $^{12}C_2H_6$	Peaks for $^{12}C^{13}CH_6$	Peaks for $^{13}C_2H_6$	Percentage
(m/z 30)	(m/z 31)	(m/z 32)	%
28	29	30	100
30	31	32	35.8
27	28	29	27.5
29	30	31	26.0
26	27	28	16.5
25	26	27	2.2

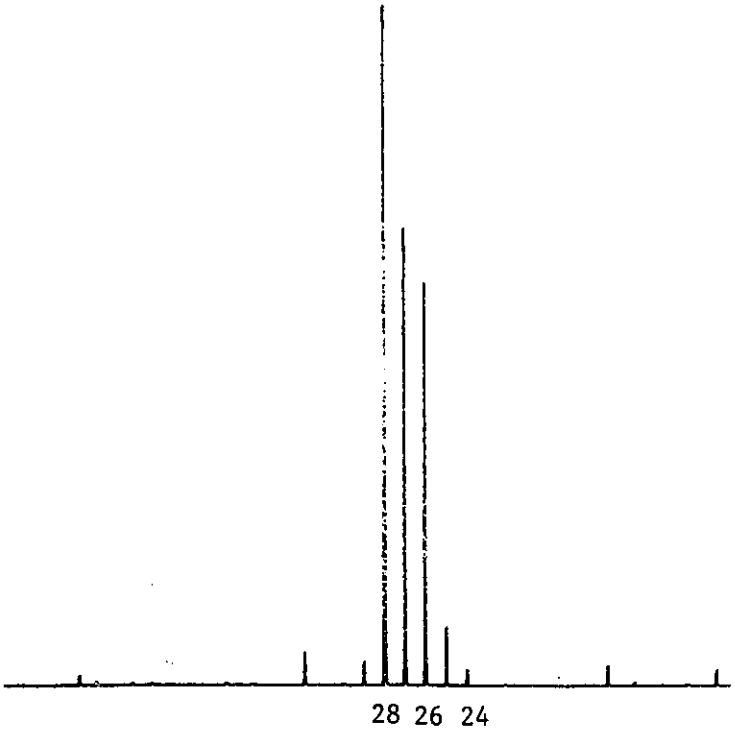

FIGURE 39 Mass Spectrum of $^{12}C_2H_4$

TABLE 6 Expected Distribution of Peaks for $^{12}C^{13}CH_4$ and $^{13}C_2H_4$ based on $^{12}C_2H_4$

Peaks for $^{12}C_2H_4$	Peaks for $^{12}C^{13}CH_4$	Peaks for $^{13}C_2H_4$	Percentage
(m/z 28)	(m/z 29)	(m/z 30)	%
28	29	30	100
27	28	29	51.7
26	27	28	43.9
25	26	27	5.8
24	25	26	3.3

spectra indicated that amounts of propylene were too small to be distinguished from the background. Consequently, only ethane and ethylene were analyzed.

The relative amounts of the four products, ethane ($^{13}C_2H_6$), ethane ($^{13}C^{12}CH_6$), ethylene ($^{13}C_2H_4$), and ethylene ($^{13}C^{12}CH_4$), were determined in the following manner. Figure 40 illustrates a typical mass spectrum of the reaction products of a fifteen minute reaction of 20 Torr of $^{13}CH_4$ at 977 K over a carbon film formed by pyrolysis of 22 Torr of propylene for three hours at 977 K. The heights of the peaks in Figure 40 are listed in Table 7. The peak at m/z 32 shows the presence of O_2 (from air in the background of the MS-9) as well as the presence of $^{13}C_2H_6$. However, the mass of O_2 is slightly lower than that of the ethane and the MS-9 was capable of resolving the two masses. As there are no other reaction products or background materials having m/z 32, the high-side of the m/z 32 peak can be attributed only to $^{13}C_2H_6$. This highest mass peak for $^{13}C_2H_6$ corresponds to 29% of the largest peak for this product, which is at m/z 30. The largest peak can thus be found for $^{13}C_2H_6$. Once this peak is known, the other peak heights for $^{13}C_2H_6$ can be found using the known fragmentation pattern. If the determined peak heights for $^{13}C_2H_6$ do not completely account for m/z 31, what remains can only be due to the presence of $^{13}C^{12}CH_6$ and it must be 29% of the largest peak for this product which is m/z 29. In a manner similar to that used to determine the peak heights for $^{13}C_2H_6$, the peak heights for $^{13}C^{12}CH_6$ can be determined.

After accounting for $^{13}C_2H_6$ at m/z 30, the remaining portion of m/z 30 is attributed to $^{13}C_2H_4$ for which m/z 30 constitutes the 100% peak. Again, the fragmentation pattern is used to determine heights for the peaks corresponding to $^{13}C_2H_4$.

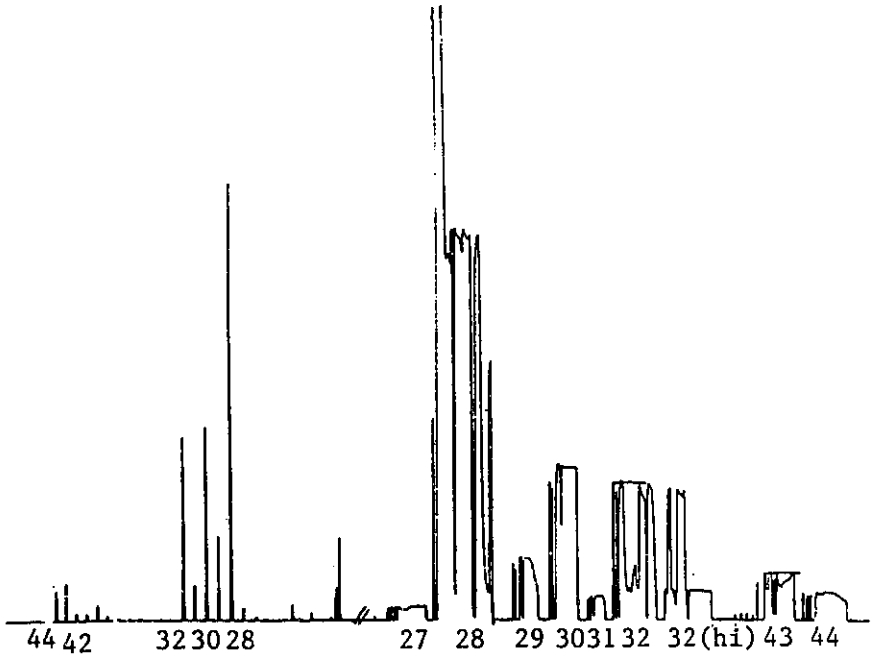

FIGURE 40 Mass Spectrum of Products after Reaction with $^{13}CH_4$

TABLE 7 Product Distribution after Reaction with $^{13}CH_4$

m/z	Peak height (arbitrary units)
32(high side)	4
31	3.5
30	22.5
29	14.5
27	2

This procedure is repeated for m/z 29 which is the largest peak for $^{13}C^{12}CH_4$. If any m/z 27 remains unaccounted for, some $^{12}C_2H_3$ (from $^{12}C_2H_4$) is likely present. Generally, the labelled products account for all the peaks.

The spectrum of the carbon removed by oxidation from the reaction vessel contained mainly a large peak at m/z 44 with a smaller peak at m/z 45. 1.1% of the peak height of m/z 44 (the natural abundance of ^{13}C in the carbon) was subtracted from the height of the peak corresponding to m/z 45. It was concluded that the amount remaining of m/z 45 was ^{13}C which had remained on the carbon surface after reaction.

4.8.3.2 Observed Results

Two series of fifteen-minute experiments were performed at 977 K using 20 Torr of $^{13}CH_4$. The results of the first series showed that no oxygenated products were produced and hence the filter had removed the oxygen impurity. Six fifteen-minute experiments were performed in the second series for the purpose of determining the ratios of the products. The peaks in the range m/z 27 -32 were interpreted according to the method described above. As expected, the major products were $^{13}C_2H_6$ and $^{13}C_2H_4$, and in all of these experiments evidence of mixed products was obtained. In each experiment, within experimental error, a few percent of the ethane was the mixed isotope, $^{13}C^{12}CH_6$ was detected. In addition, anywhere from one-quarter to one-half of the ethylene produced was the mixed product $^{13}C^{12}CH_4$.

Oxidation of the carbon film revealed that, natural abundance having been accounted for, approximately 1% of the carbon in the film was ^{13}C. In all five sets of experiments, the same proportion of ^{13}C was observed in the film after the series of reactions.

4.8.4 Discussion

These results were consistent with the proposed mechanism for the reaction of the methane. Upon admission to the vessel, methane was immediately adsorbed on the surface of the carbon film, probably completely covering the surface. The active carbon atoms on the surface (those at edge sites) acted as a hydrogen-transfer agent for the removal and transfer of the hydrogen from the methane molecule, resulting in the formation of a methyl radical. This methyl radical could subsequently desorb into the gas phase, or remain on the surface and react further. The methyl radical could also react with a carbon atom from the carbon film to yield ethane or ethylene. The results obtained in this series of experiments indicated that the ethane was mostly formed homogeneously and in the gas phase, but that the ethylene formed was a mixture, partially formed in the gas phase and partially formed on the surface. These results suggest that the carbon, in addition to being a catalyst, may actually participate in the reaction.

CHAPTER 5

THE REACTIVITY OF CARBON-IRON FILMS

5.1 Introduction

5.1.1 Gasification Reactions

Gasification reactions of carbonaceous materials, such as coke, coal and graphite, have become increasingly important as a means of producing clean, gaseous fuels[79]. Fundamental studies have been made of the reactions of these various forms of carbon with oxygen, hydrogen, carbon monoxide, carbon dioxide and water[80-82]. Although numerous such studies have been performed, the ideas on the mechanisms are still speculative[83].

Water vapour gasification of coals and cokes has been studied for more than sixty years as this reaction formed the basis for the first production of synthesis gas on an industrial scale[84]. In the interim period, this technology was less intensely researched due to the large-scale availability of petrochemical raw materials. Recently, however, the study of steam gasification of carbon has again become important due to the anticipated shortage of petrochemical products and the availability of coal. In general, this reaction is slow except at very high temperatures, hence more attention has been focussed on the catalyzed steam gasification of carbon. While many studies of catalytic steam gasification

reactions have been made, the kinetics of these reactions has received less attention compared with that of noncatalytic gasification[85]. When the catalyst is a solid at the working state, it is essential to have good contact between the two solids, in this case the carbon and the catalyst. While this seems to be the most important factor for the effectiveness of the catalyst, an essential point in such gasification systems is that the state of contact between the solids gradually changes as the reaction progresses.

5.1.2 Catalysts for Steam Gasification

Steam gasification has been studied using many types of catalysts, but the best catalysts were found to be the alkali and some transition metals[84]. The alkali metals have been studied under a range of pressure and temperature conditions and in the presence of various other metals[86-90]. Most attention, however, has been devoted to the transition metals, and in particular, iron[79,83,84,91-96]. Reasonable carbon monoxide and methane selectivity and low carbon dioxide formation, even at elevated pressures, are only some of the advantages that iron possesses compared with other steam gasification catalysts, especially the alkali metals[83].

In an early study by McKee[91], iron, nickel and cobalt were found to promote rapid reaction between graphite and moist hydrogen even at 973 K. The metals were also found to be catalytic only when they were present in a reduced state, as the metal oxides were generally found to be inactive. McKee believed that the metal acted as a catalyst for the initial dissociation of water, leading to the formation of chemisorbed oxygen and

hydrogen atoms. Metals such as copper, lead and silver formed less stable oxides and hence did not promote the dissociation of water. On the other hand, metals such as chromium and manganese had such an affinity for the oxygen that the subsequent reaction with the carbon to transfer the oxygen, and release carbon monoxide, did not occur.

Hüttinger and coworkers[79,83,84,92-94] performed an impressive range of studies on the steam gasification of carbons and coal. They also found that the iron was only active as long as it remained present in a reduced form. They also performed surface studies on the carbon after deactivation occurred and found that another cause for loss of activity of the catalyst was agglomeration of the iron particles as carbon was removed from the surface. They also found that beyond a certain concentration of iron in the carbon, addition of further iron did not increase the rate of reaction. In fact, in the application of iron as a steam gasification catalyst, one of the major problems to be overcome is the uniform dispersion of the iron, or catalyst material, on the carbon or coal surface.

5.1.3 Methods of Catalyst Preparation

Several methods have been used to incorporate iron and other elements into the carbon structure, for example, by heat and pressure treatments and by electrochemical reactions. The main purpose of these methods was the preparation of carbon with improved physical properties such as strength or electrical conductivity. Carbon containing iron as a catalyst has usually been prepared in one of two ways.

The first method of preparation of the catalyst involves physical mixing of a solution of the iron salt with finely divided carbon. Different iron salts, ranging from inorganic salts, such as $FeCl_3$ and $Fe(NO_3)_2$, to organometallic salts, have been used as the iron source and the solution is usually sprayed over the carbon surface or mechanically ground with the fine carbon particles. Following the impregnation of the carbon with the metal, the carbon is dried, and depending on the final state of the catalyst, the catalyst is pretreated such that the metal is in a reduced state. Although significant catalytic activity has been observed using this method, a disadvantage is that the reactivity often decreases markedly over a period of time, an effect which has been attributed to the agglomeration of the iron on the surface, as mentioned previously. It is also acknowledged that poor dispersion of the iron leads to the problem of agglomeration.

The second method of preparation of the catalyst involves intercalation of the metal into a graphite matrix. Many studies have been performed on the structure and resultant activity of graphite with the intercalation of different metals. The regular structure and the unique electronic properties of these intercalated compounds makes them highly active and stereoselective materials for catalysts[97]. In many of the cases studied, however, the gasification rates obtained were the same irrespective of the method of addition of the metal. The rate was determined by the total metal surface exposed in the catalyst, and this surface did not depend on the method of insertion of the metal into the carbon.

5.1.4 Novel Method of Iron Catalyst Preparation

In order to improve the gasification rates, it was necessary to improve the contact of the iron with the carbon. This involved the development of a better means of dispersion of the iron within the carbon. The method of impregnation yielded good rates until agglomeration of the iron particles began to occur. If a method could be found whereby the iron could be kept from agglomerating, the catalyst should remain active.

In an attempt to improve both the dispersion of the iron within the carbon and the bonding characteristics of the iron to the carbon, a chemical method of preparation of a mixture of carbon and iron was explored. A mixture of a hydrocarbon, propylene, and an organometallic compound containing iron, ferrocene, was pyrolyzed under conditions where a carbon film was deposited on the surface of a quartz reaction vessel. The purpose of the co-pyrolysis was to obtain a carbon deposit with iron atoms dispersed on an atomic level and chemically bonded to the carbon.

The pyrolysis of metallocenes has not been studied extensively. Some work has been performed by Dyagileva and coworkers[98,99] on the thermal decomposition of metallocenes for the purpose of forming thin metal films. They found that it was possible to measure the rate of decomposition of ferrocene above 773 K. They also found that the solid products of the pyrolysis of ferrocene, which contained both iron and carbon, were catalytic in nature and accelerated the decomposition process of the metallocene. This effect was not observed with the other metallocenes studied. In fact, the solid pyrolysis products were so active that the decomposition could be studied at a temperature 200 degrees lower than possible in the absence of the iron-carbon-containing solid.

S.-I. Hirano and coworkers[100] synthesized carbon fibrils, spheres and polyhedra containing finely dispersed iron. These carbons were formed by pressure pyrolysis of a copolymer prepared from divinylbenzene and vinylferrocene at temperatures lower than 953 K and pressures of 125 MPa. The carbon consisted of cementite and magnetite, two forms of iron carbide. Studies performed on the bond dissociation energies in ferrocene by Lewis and Smith[101] also indicated that the pyrolysis products formed a catalytic coating. Attempts to obtain similar results with nickelocene were unsuccessful. Additionally, they were able to calculate that, given the second bond energy they had calculated, the species FeCp should be stable and should be functional as a catalyst below 550 K. Mass spectrometric studies performed by Hedaya[102] on the cyclopentadienyl radical and its dimer indicated that upon thermal decomposition of nickelocene, the three thermal products obtained were C_5H_5, $C_{10}H_{10}$, and C_5H_5Ni. The last product was described as being cyclopentadienylnickel based on its low ionization potential, which was close to that of nickel, its spectrum in the presence of nickel isotopes and its reactivity with allyl, which is especially significant since nickel is well known to form strong bonds to unsaturated ligands.

5.1.5 Goal of this Study

The aim of this study was to develop a new method of preparing carbon films which contained iron in a well dispersed and bonded form. The reactivity of the iron-carbon film formed by co-pyrolysis of propylene and ferrocene was tested using first

water and hydrogen mixtures and then using methane. The reactivity on the iron-carbon film was compared with the reactivity on a carbon film in the absence of any iron.

5.2 Experimental

5.2.1 Deposition of a Pure Carbon Film

Research grade propylene (Matheson Gas Products Inc., Minimum Purity 99.6%) was thoroughly degassed and approximately 7 Torr was admitted into the reaction vessel at room temperature. The reaction vessel was a quartz cylinder with plane windows inclined slightly towards the centre of the vessel. The vessel, centrally placed in a furnace (Autoclave Engineers), was heated to the desired temperature (the temperature of reaction). The amount of carbon deposited was measured by monitoring the transmittance of a laser beam (He-Ne Melles Griot) with a phototube and Keithley Electrometer connected to a recorder (Perkin Elmer R100). As the film was deposited, the transmittance of the light decreased and was continuously monitored. The thickness of the film was controlled by the amount of time allowed for deposition. After deposition, the carbon film was degassed at the same temperature for 1 - 2 hours. This method of deposition and measurement of carbon is described in greater detail in the work of Ahmed and Back[103].

5.2.2 Calibration of the Quantity of Carbon in the Film

The carbon film deposited in the reaction vessel was calibrated using optical density measurements. The reading on the Keithley Electrometer before the laser beam was turned on was recorded as the dark current. The transmittance of the laser beam through the reaction vessel before deposition commenced was recorded as I_o. This value was recorded for some time allowing the beam to stabilize. Subsequently, the transmittance was monitored as the carbon deposited. When deposition was stopped, the transmittance was recorded as I_t and the optical density was calculated as log I_o/I_t with both values corrected for the dark current. The carbon was then removed using excess oxygen and the carbon dioxide formed was measured. The value of the optical density was thus related to a number of moles of carbon. Several values of I_t were measured and a calibration curve was obtained. From the surface area of the vessel and the density of carbon[104,105], 1.9 g/cm^3, the thickness of the carbon films was found to lie between 15 and 20 nm.

5.2.3 Deposition of a Carbon Film containing Iron

A few grams of ferrocene (98% Ferrocene, Aldrich Chemical Company) were placed in a small tube using a glove bag filled with helium (Air products, UN1046). A small piece of glass wool was placed on top of the ferrocene and the tube was quickly attached to the vacuum line.

Ferrocene was admitted into the reaction vessel at its vapour pressure at 295 K (≈ 0.005 Torr). Subsequently, approximately 7 Torr of propylene was added and the two gases were allowed to mix in the isolated reaction vessel overnight (16 - 17 hours). The reaction vessel was then heated to the desired temperature, as described in Section 6.2.1, and the deposition of the carbon was monitored continuously by the transmittance of the laser beam. Assuming all of the ferrocene was decomposed, the percentage of iron in the films was ≈0.29%.

5.2.4 Preparation of the Hydrogen/Water Mixture

All the work performed previously with iron as a catalyst indicated that the iron had to remain in a reduced state to exhibit catalytic activity. In order to ensure that the iron remained reduced even in the presence of water, the water was mixed with hydrogen, which would act as a reducing agent.

After several degassing cycles, water was admitted to a 2 L mixing flask, designed with minimum connecting tubing, at its vapour pressure at 295 K. Hydrogen gas (Air Products, UN1049), was passed through a palladium thimble heated to between 573 and 673 K. Approximately 300 Torr of the purified hydrogen was then admitted into a 1 L storage bulb. From this bulb, a known pressure of hydrogen was added to the mixing flask containing the water vapour, and the two gases were allowed to mix for at least 2 hours. The ratio H_2/H_2O was about 4:1. This procedure was performed carefully to ensure that no oxygen was present in the system. Although the H_2/H_2O mixture was used for more than one reaction, the mixture was prepared frequently.

5.2.5 Reaction Procedure

The reaction was initiated by admitting the H_2/H_2O mixture to the reaction vessel. The total initial pressure in the vessel was between 80 and 100 Torr. The rate of disappearance of carbon was monitored by the change in I_t. As I_t increased, carbon was removed by reaction and the amount of light from the laser beam, which passed through the reaction vessel before reaching the photometer, increased. After the desired reaction time, reactants and products were removed through two cold traps, at 175 K and 78 K respectively, and the non-condensible gases were collected in a gas sampler.

The products were analyzed on a gas chromatograph (Hewlett-Packard Model 5750) using thermal conductivity detection. The non-condensible products were analyzed using a 10' x 1/8" Carbosieve II column at 298 K. The products collected from the trap at 78 K were analyzed on the same column at 403 K. The products collected from the trap at 175 K were analyzed using a 6' x 1/8" Porapak Q column at 403 K.

After the reaction products were removed, excess oxygen (Air Products, UN1072) was admitted to the reaction vessel for removal of the remaining carbon. When the transmittance of the laser beam returned to its original value, the carbon film was judged to have been completely removed. The carbon dioxide produced was condensed at 78 K and then expanded into a known volume to determine its pressure.

5.2.6 Analysis of the Reaction Vessel for Iron

The reaction vessel was cooled to room temperature and removed from the furnace. It was rinsed with three 5 mL aliquots of a mixture of three parts HCl to one part HNO_3, and two 5 mL aliquots of distilled water. The syringe which was used to drain the vessel was then rinsed with a 2 mL aliquot of distilled water. The total volume of each rinse was 30.6 mL. A blank was prepared in a similar manner using the same quantities of acid and water without passing them through the reaction vessel. After a few days, the vessel was rinsed again to test for remaining iron. The analysis for iron was performed on a Direct Current Plasma Atomic Emission Spectrophotometer (Beckman Spectraspan 5, Sequential, 371.994 nm background correction).

5.3 Results and Discussion

The experiments were performed at three temperatures: 1343 K, 1103 K, and 1053 K. At 1343 K, there was almost no reaction of the pure carbon film with the H_2/H_2O mixture, even after 16 hours. The iron-containing film reacted very slowly and only after an induction period of approximately one hour. At 1103 K, the carbon film produced no reaction after 3 hours, but the film containing iron reacted immediately, with no induction period. The carbon was consumed in about 20 minutes. At 1053 K, a slow but measurable rate was obtained with the carbon film. The carbon film containing iron was consumed in about 1 minute. The traces showing the consumption of carbon for the two films at 1053 K is provided in Figure 41.

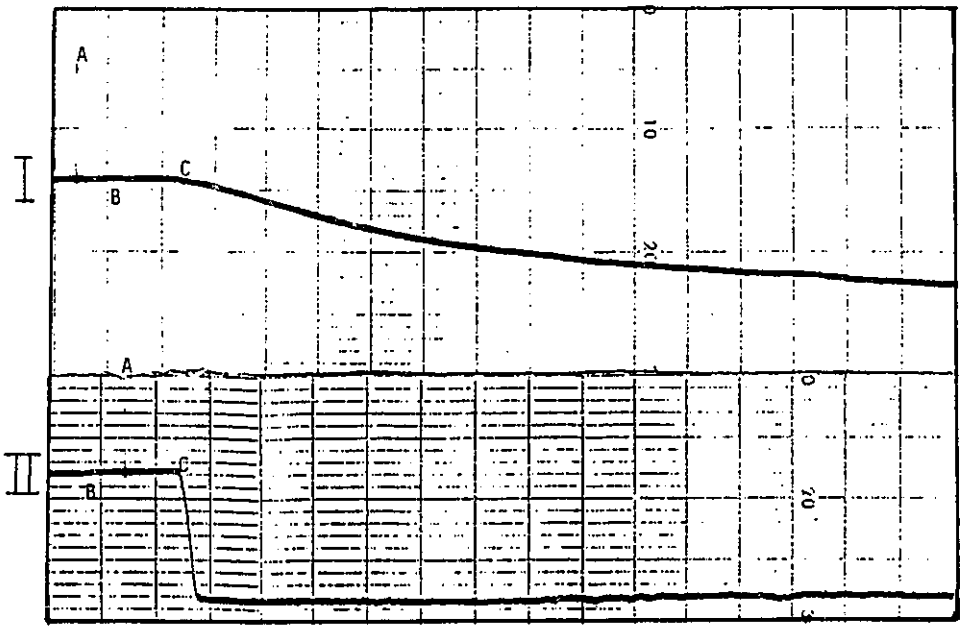

FIGURE 41 Traces showing the Change in Absorbance of the Carbon Film during Reaction with the H_2/H_2O mixture at 1053 K. Curve I represents Reaction with pure Carbon and Curve II represents Reaction with Carbon Containing Iron. Point A indicates the value of the Dark Current. Point B represents I_t of the Carbon Film at the Beginning of the Reaction. Point C indicates the start of the Reaction. The time is the same for both curves. Each interval represents 2 minutes.

The measured optical density of the carbon film in each experiment (log I_o/I_t) was converted into total moles of carbon, as described in Section 6.2.2, and a rate of consumption of carbon was estimated. At 1053 K, the rate of disappearance of carbon for the uncatalyzed reaction was found to be approximately 1.6×10^{-8} mol s^{-1}, while that of the catalyzed reaction was found to be about 8.2×10^{-7} mol s^{-1}. The rate was estimated in the following manner: the total number of moles of carbon which reacted was calculated using the difference in optical density between the initial amount of carbon in the film and the amount remaining after a specified time, as illustrated in Figure 41. The catalyzed reaction rate was therefore about 50 times greater than the uncatalyzed reaction rate under these conditions. This difference in rate was observed in all the trial experiments.

Although much work has been done on the steam gasification of carbon, few values of the rate have been reported using mixtures of hydrogen and water vapour in a static system with the type of catalyst used in this work. These conditions have been most closely approached in the work of McKee[91]. Under similar conditions at 1053 K, extrapolated rates of loss of carbon from McKee's work were found to be approximately 3.5×10^{-7} mol s^{-1} with 0.09 wt% iron and 1.0×10^{-6} mol s^{-1} with 0.32 wt% iron. Thus, even the first attempts to prepare a film containing carbon and iron by co-pyrolysis appeared to produce reactivity at least comparable to previous methods.

In both the catalyzed and uncatalyzed reactions, CO and CO_2 were obtained as products. Hydrogen was not measurable in this system. Unreacted water was also

measured. The ratio of CO/CO_2 was between 20 and 40 for both the catalyzed and uncatalyzed reactions. Some other minor products were observed in some reactions.

Analysis of the iron recovered from the reaction vessel following removal of the carbon was inconclusive. In spite of many successive rinses of the reaction vessel, iron continued to be recovered, as shown in Table 8. Subsequent examination of the reaction vessel showed that the excess iron was introduced into the vessel during the process of sealing the plane windows to the reaction vessel. Thus, iron was continuously leached from the seals during the rinsing process. This extraneous source of iron did not, however, affect the reactivity as the experiments performed in the absence of iron indicate. Many reactions were performed using pure carbon and the rate was always very slow. The introduction of a small quantity of ferrocene, however, immediately increased the rate of removal of carbon. This procedure was tested many times and in all cases, the same results were observed.

TABLE 8 Iron Content of Reaction Vessel after Reaction with H_2/H_2O Mixture

	Concentration of Iron (μg/mL)		Amount of Iron μg	
	Analysis Value	Net Value (Blank Subtracted)	Iron from each Rinse	Total Iron
Iron Introduced	-	-	-	3.38
Iron Recovered				
Blank	0.132	0	-	-
Rinse 1	0.447	0.315	9.64	9.64
Rinse 2	0.312	0.180	5.51	15.15
Rinse 3	0.237	0.105	3.21	18.36

5.4 Reactivity of Methane over the Iron-Carbon Film

5.4.1 Introduction

Following the results of the water vapour gasification experiments on the iron-carbon surface, the reactivity of methane was also tested. Some experimental modifications were made in order to avoid some of the problems experienced during the gasification experiments. The reaction vessel, which had previously been a quartz tube with plane windows, was replaced with a reaction vessel of the type used in the experiments in previous chapters and was constructed from a single quartz tube. This eliminated the procedure of sealing on the plane windows, thus reducing the possibility of contamination by iron from the glass-blowing torch.

5.4.2 Experimental

The ferrocene and propylene were introduced into the reaction vessel as described in Section 6.2.3. In these experiments, the reaction vessel was gradually heated to 977 K, allowing the two reactants to mix by convection, and then the vessel was maintained at 977 K for 30 minutes. The vessel was then evacuated to remove any unreacted material. The resultant film was similar to the other carbon films prepared. The conversion of methane on the surface of this iron/carbon film was tested using 20 Torr of methane at 977 K in a series of 15 minute reactions. After the reactions were completed, the carbon was oxidized and the carbon dioxide formed was analyzed, as described in Section 2.4.3.

After the completion of one set of consecutive experiments, the reaction vessel was cooled to room temperature. The vessel was removed from the furnace and the following treatment was applied to remove the iron deposited in the vessel. 10 mL of 1 M nitric acid was added to the vessel and it was placed in an ultrasonic bath maintained at 323 K for 20 minutes. The acid was removed and placed in container 1. This procedure was repeated three times, using 10 mL of 1 M nitric acid, and each time the acid was removed and placed in container 1 yielding a total volume of 30 mL. 20 mL of 1 M nitric acid was then placed in the vessel and it was placed in the ultrasonic bath for 20 minutes. The acid was removed and placed in container 2. This procedure was repeated with a 10 mL aliquot of 1 M nitric acid, and the removed acid was again placed in container 2, yielding a total volume of 30 mL. The vessel was then filled with distilled water and placed in the ultrasonic bath for 20 minutes. The distilled water was then discarded. 30 mL of 1 M nitric acid was placed in the vessel and it was placed in the ultrasonic bath for 20 minutes. The acid was removed and placed in container 3. The three containers were submitted for analysis by atomic emission spectroscopy (AES), as described in Section 6.2.6, along with a 30 mL sample of the acid.

5.4.3 Results

The pressure of propylene admitted along with the ferrocene ranged from 0.04 to 0.51 Torr. The amounts of carbon present in the resultant films ranged from 1.6×10^{-7} to 7.9×10^{-7} mol. The rates of formation of ethane and ethylene were close, and similar

to rates obtained for the conversion of 20 Torr of methane over a propylene carbon surface at the same temperature. In all cases, the rates dropped sharply after the first few experiments, but then approached a constant value. Initial rates were comparable to those obtained over the propylene carbon film with amounts of carbon in the neighbourhood of one monolayer. At lower amounts of carbon, the rates were higher, as shown in Figure 42. A carbon film was made using 0.008 Torr of ferrocene only (no propylene). The rate of product formation dropped only slightly during the consecutive reactions and eventually levelled. The amount of carbon deposited in this case was determined by complete oxidation of the carbon to carbon dioxide with subsequent measurement by gas chromatography. The amount of carbon recovered was more than the total amount of carbon present in the ferrocene admitted to the vessel.

Analysis of the AES results indicated that the majority of the iron was removed in the first container with the three initial rinses. By the third container, almost no iron was remaining. This result was obtained from two different sets of experiments, as shown in Table 9.

5.4.4 Discussion

The iron exhibited a catalytic effect with amounts of carbon less than 10^{-6} mol. In all cases where the amount of carbon was less than or close to a monolayer, the reactivity of the carbon-iron film was greater than the carbon film. The small amount of carbon present in these cases allowed the iron atoms to be exposed at the surface and

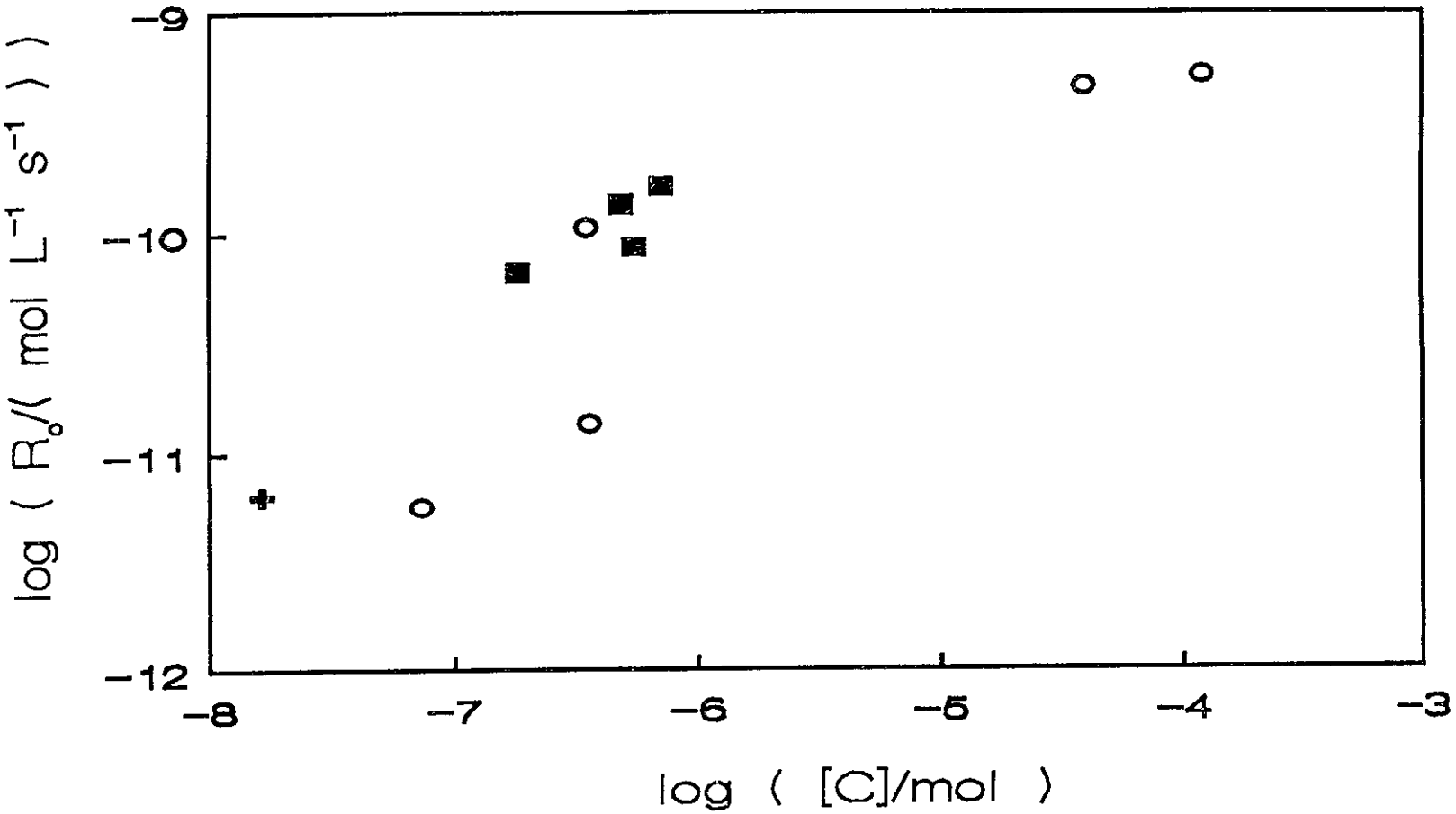

FIGURE 42 log R_o as a function of amount of carbon at 977 K in the presence and absence of iron.
+ 20Torr methane on quartz o 20Torr methane on C_p
■ 20Torr methane on Fe-C film

TABLE 9 Iron Recovered from Vessel after CH_4 Reactions

Batch	Sample	[Fe]	Sample Vol.	Total Fe	Total Fe	Fe Depos.
		µg/mL	mL	µg	mol	mol
1	Blank	0.000	30	0	0	-
	1	0.077	30	2.31	4.14×10^{-8}	5.15×10^{-8}
	2	0.000	30	0	0	-
	3	0.000	30	0	0	-
2	Blank	-0.010	30	0	0	-
	1	0.076	30	2.28	4.08×10^{-8}	5.05×10^{-8}
	2	0.000	30	0	0	-

their greater reactivity resulted in an increased rate. However, when the amount of carbon was greater than a monolayer, the reactivity approached that of the propylene carbon film. The deposition of greater carbon amounts may have covered the more active iron sites once a monolayer had been formed. If the iron atoms were covered by carbon, the surface of the film would then look similar to a propylene carbon film as the iron would be invisible under the carbon. The results of the experiment in which only ferrocene was pyrolyzed indicated that carbon must have been deposited by the dissociation of methane during the consecutive experiments. This would produce more carbon than could be accounted for by the pyrolysis of all the ferrocene.

In a series of consecutive experiments on the iron-carbon film, however, the reactivity dropped sharply after the first experiment and the subsequent decrease in rate was very small, as shown in Figure 43. This is consistent with the deposition of a small

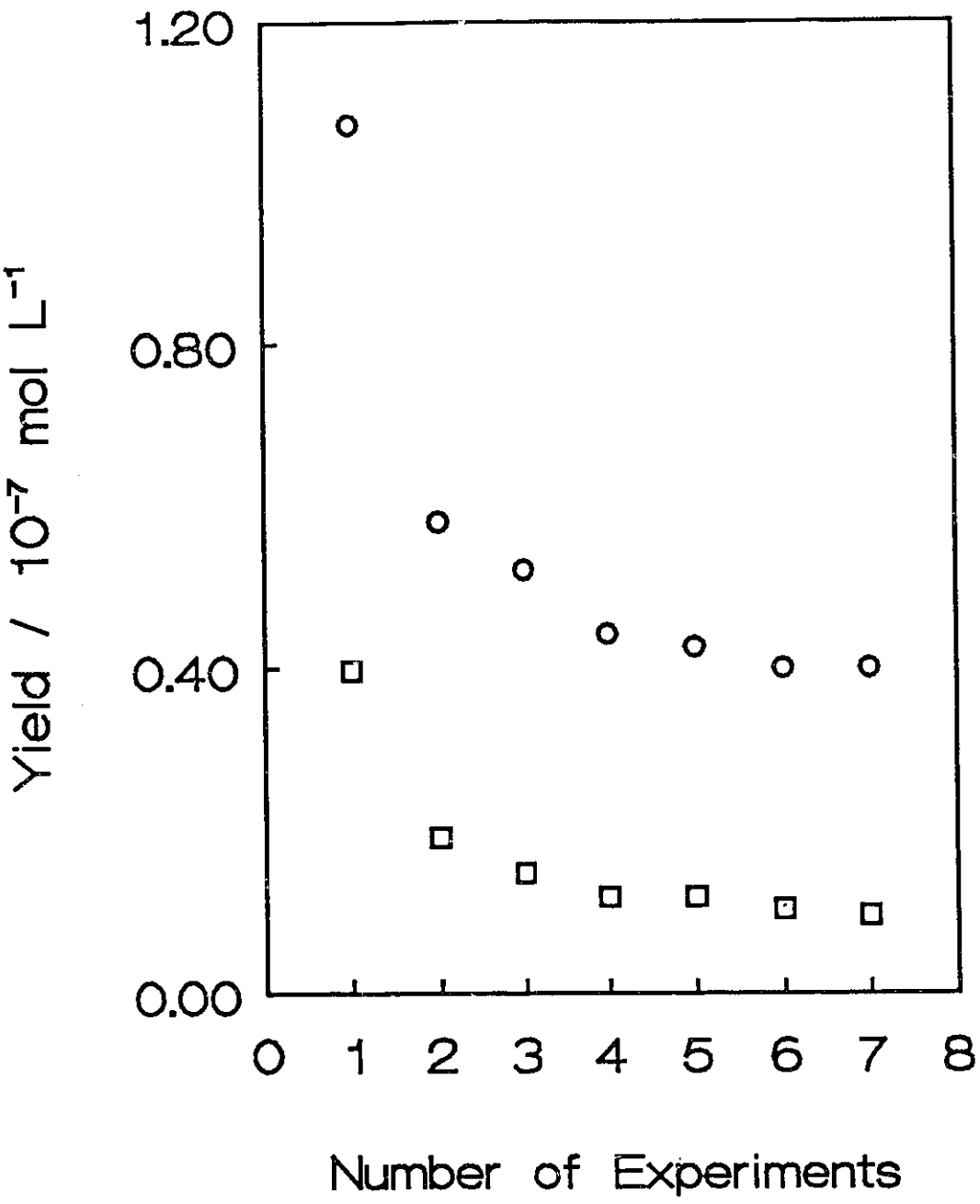

FIGURE 43 15 minute consecutive experiments using 20Torr methane at 977 K over a carbon-iron film formed by pyrolysis of 0.007Torr ferrocene and 0.041 Torr propylene from 298 K upto 977 K then held at 977 K for 30 minutes.
○ ethane □ ethylene

amount of carbon during the first reaction on the Fe-C film. The most active sites, which would most likely be the Fe atoms, were covered immediately with carbon, and this caused the reactivity of the Fe-C film to decrease significantly after the first reaction. Subsequent reactions only involved deposition of the carbon atoms on the carbon surface, as the iron atoms were covered, and the rate did not change much.

AES results indicated that the method of removal of iron from the vessel was quantitative. The maximum amount of iron expected to deposit from 0.007 Torr of ferrocene was 5.2×10^{-8} mol. The amount of iron recovered according to the AES results was in the range of 4.2×10^{-8} mol. Thus, the vessel used in these experiments contained no iron from extraneous sources. In the previous vessel, the recovery of excess iron must have been due to the glass-blowing procedure, as suggested.

CHAPTER 6

SUMMARY

5.1 Discussion

The experiments performed in the previous three chapters, and the results obtained from these experiments revealed a great deal of information as to the nature of the carbon surface and the effect of this surface on the dissociation of methane.

All the results indicated that carbon, when deposited in the form of thin films, acted as a catalyst. Irrespective of the conditions of deposition or the precursor to the formation of the carbon film, the rate of dissociation of methane was greatly increased in the presence of carbon compared to the rate over a quartz surface. Analysis of the oxidation products of the carbon film indicated that the films contained only carbon with small amounts of hydrogen. The hydrogen to carbon ratio was a factor which varied depending on the method of preparation of the carbon film. Deposition of the carbon film at high temperatures (around 1200 K) resulted in the formation of more ordered and dehydrogenated carbons, whereas deposition of carbon films at lower temperatures yielded films of greater disorder and higher hydrogen content. Studies on the carbon films formed by pyrolysis of three hydrocarbons at different temperatures indicated that the films with higher hydrogen content were more reactive. The results obtained from these studies suggests that the hydrogen content of the carbon is an important factor in its reactivity. Micrographs of the carbon surface confirmed that there were no filaments or irregularities in the surface which would have created additional carbon surface to account

for the reactivity of the carbon. The films were uniform, smooth and featureless and had essentially the same total surface area as the quartz reaction vessel surface, as shown in previous experiments[106]. Thus the reactivity of methane on the carbon films was due to the nature of the carbon itself.

During the course of the reactions, a small quantity of carbon was deposited on the carbon film. This carbon was formed even in the very early stages of reaction where none of the precursors to carbon formation through the "polyene" route, such as higher molecular weight hydrocarbons, were observed. This suggested that the carbon was formed by adsorption of methyl radicals, followed by successive dehydrogenation of these radicals to carbon atoms, which were then incorporated into the carbon film. Somorjai and coworkers[20-24] believed that in any reaction involving hydrocarbons in the presence of a metal, carbon was deposited almost instantaneously on the metal surface. They referred to this carbon as a "hydrocarbonaceous species" and they maintained that its presence was essential to the operation of the metal catalyst.

Due to the variety of different sites which were available on the surface of the carbon film, the deposited carbon influenced the subsequent reactivity of the carbon film in different ways. The different effects of the deposited carbon could be explained by the occurrence of two competing processes, the formation of building carbon and the formation of blocking carbon. The balance of these two processes determined the net reactivity. If mostly building carbon was deposited as more experiments were performed, the rate increased. If mostly blocking carbon was deposited, the rate decreased with consecutive experiments. When conditions were such that roughly the same amounts of

both building and blocking carbon were deposited, no distinct change was observed in the rate of methane decomposition after a number of experiments were performed. The predominance of one process or the other, that is, the formation of either building or blocking carbon, was determined by the reaction conditions. In fact, the effect of blocking carbon was also observed in the experimental results obtained in the presence of the iron-carbon films. When only small amounts of carbon were present in the films, the iron was exposed and the reactivity of the Fe-C films was higher, for the same amount of carbon, than the reactivity of the carbon films.

The reactivity of methane on the carbon films was not only dependent on the temperature of deposition of the film, but also depended on the amount of carbon present in the carbon film. Characterization of the change in reactivity after a number of experiments indicated that the reactivity depended on the temperature of reaction, the pressure of methane, and the amount of carbon present in the film.

The summary of the mechanism of formation of the products observed upon dissociation of methane on the carbon surface is shown in Figure 44. The relative importance of each step under particular temperature and pressure conditions, as identified by different colours in Figure 44, is presented below.

Effect of Pressure on the Mechanism

At pressures between 5 and 50 Torr of methane, the mechanism followed is that outlined in green. Methane is adsorbed onto the carbon surface, where it dissociates to

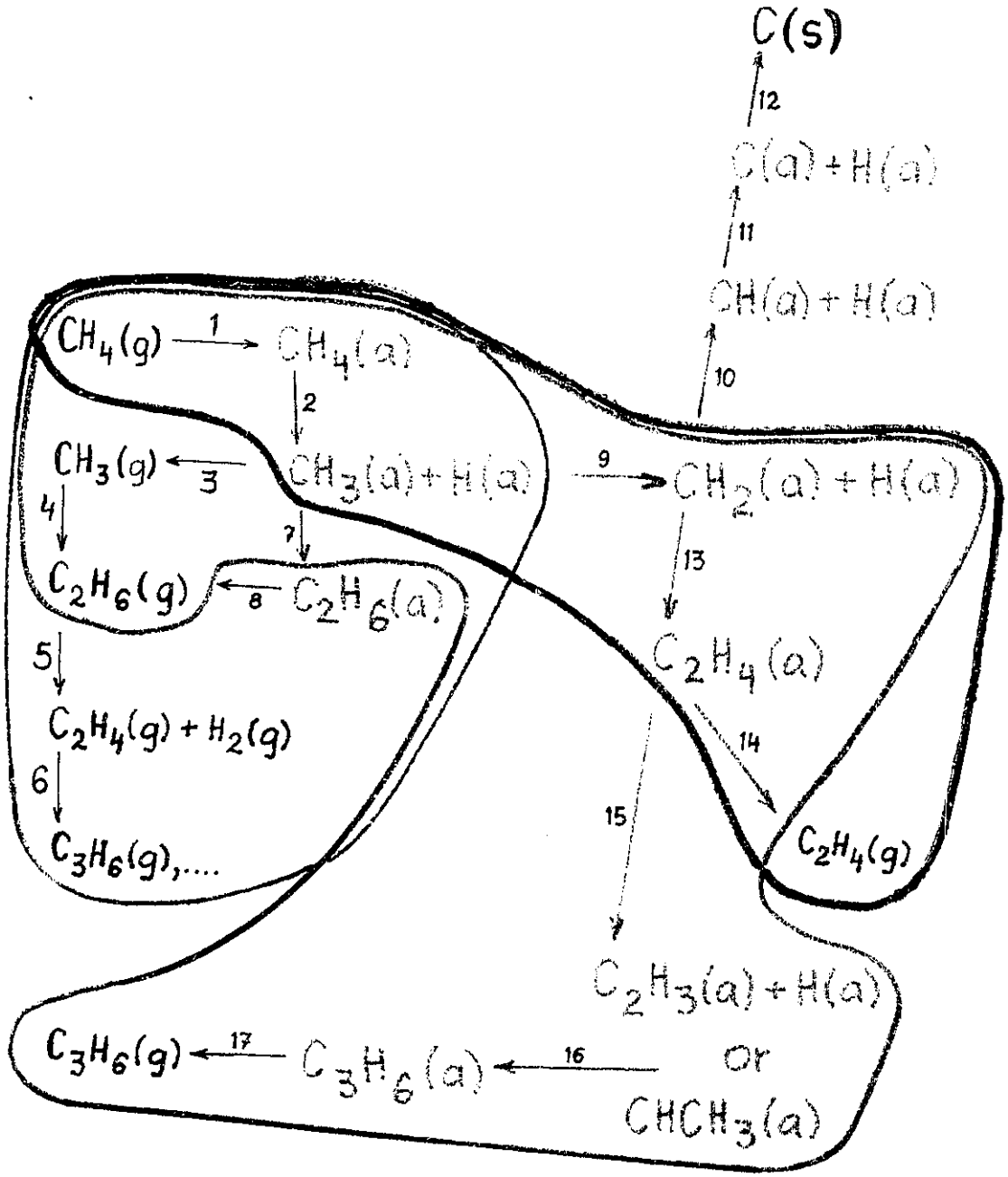

(g) = gas phase

(a) = surface species

C(s) = bulk carbon

FIGURE 44

form methyl and hydrogen radicals. The methyl radicals may remain on the surface to form ethane, by reaction [1], or they may desorb into the gas phase to form ethane by reactions [3] and [4]. Ethylene is formed mostly by reaction [5] although some may be formed by reactions [9], [13] and [14]. At lower methane pressures, there are fewer species formed which could adsorb onto the carbon surface and it is more likely that neighbouring sites are available, which could facilitate reaction [9]. Thus reaction [9] occurs before reaction [3] and the rate of formation of ethane decreases, and the rate of formation of ethylene may exceed that of ethane, as shown by the reactions enclosed in the blue ring. Ethylene is formed predominantly by reactions [13] and [14]. All other gas phase products are most likely formed by reactions [5] and [6]. As the methane pressure is increased, the mechanism described above still occurs but increasingly, reactions [9], [10], [11], and [12] become important.

Effect of Temperature on the Mechanism

At temperatures above 873 K, the reaction mechanism which occurs is the same as the reaction mechanism described for pressures above 5 Torr. As the temperature is increased, reactions [9] - [12] become increasingly important.

At temperatures below 873 K, the reaction mechanism may be described by the reactions enclosed in the pink ring in Figure 44. Ethane continues to be formed homogeneously by reactions [1] - [4]. Ethylene is formed by reactions [9] and [13], but at the lower temperatures, the rate of desorption will be slow and the adsorbed molecule

may rearrange on the surface to produce an intermediate species, as shown by reaction [15]. While the exact form of the intermediate species could not be determined in this study, it is possible that it could be ethylidene or ethylidyne. These rearranged forms of ethylene are highly reactive and may react with gas phase methane or with an adsorbed methyl radical to form propylene, as described by reactions [16] and [17].

Surface to Volume Ratio

The surface area of the reaction vessel was increased by a factor of 10, leading to a surface to volume ratio of about 20. Aside from an increase in rate, which could be explained by an increase in the number of active sites and a subsequent increase in the rate of reaction [2], the mechanism remained essentially unchanged. Due to the highly active nature of the surface, reactions [9] - [12] remained important. The dual nature of the deposited carbon, blocking or inhibitive and building or catalytic, could be seen more clearly in the packed vessel. In Figure 22, where the rate was plotted as a function of the amount of carbon in the packed and unpacked vessels, it could be seen that as the amount of carbon was increased, both the decrease and the increase in rate were more pronounced in the packed vessel. At higher pressures, higher temperatures, and at larger amounts of carbon the rate was not greater than the rate observed in the unpacked vessel, and in fact, in some cases was lower than the rate in the unpacked vessel. This apparent low rate was due to the loss of the products ethane and ethylene because they were unable to diffuse rapidly from the surface. Consequently, they were readsorbed onto the carbon film and

converted to carbon. The experimental results were thus not as clear as expected due to a limitation in the experimental system.

6.2 Direction of Further Study

Carbon, in greater than monolayer quantities, behaved as a catalyst. This catalytic effect should have increased significantly with the increase in surface to volume ratio. The diffusional constraint imposed by the experimental system in which the reaction was studied could be removed if the experiment was performed in a flow system. The higher pressure of methane would result in removal of the products before they could readsorb onto the carbon surface. A significantly higher rate of conversion of methane should be obtained. These reactions can be performed at temperatures similar to or lower than the temperatures used in oxidative coupling. No loss of methane to oxygenated products would occur and the methane reactant could be recycled after removal of the products.

Further studies should be performed to explore the mechanism involved in the formation of propylene at lower temperatures. Reaction was obtained in this study at temperatures as low as 573 K. The reaction at lower temperatures could be studied using different surface to volume ratios to determine the amount of surface required to obtain maximum gas phase product formation and minimum surface carbon formation.

The initial results obtained from experiments performed on the iron-carbon film indicated that this new method of formation of the iron-containing catalyst was successful. A significant increase in the gasification rate was obtained and promising results were

also obtained in the methane conversion reaction on the surface of the iron-carbon film. Further work in this area would involve testing different hydrogen/water vapour ratios in the gasification reaction. The highest reaction rates were obtained at the lowest temperature and the reaction could be tested at still lower temperatures to determine the efficiency of the catalyst. Studies of the methane conversion reaction were performed by admitting ferrocene at room temperature. Thus the amount of ferrocene admitted was limited by the vapour pressure. The one experiment performed in which the carbon film was formed by pyrolysis of only ferrocene indicated a high reactivity of the iron-carbon film formed from ferrocene. Further tests could be made in this area by heating the vacuum line and increasing the amount of ferrocene pyrolyzed. It is possible that still higher rates of reaction could be obtained.

CLAIMS TO ORIGINAL RESEARCH

1. The catalytic effect of thin films of carbon on the dissociation of methane was clearly demonstrated.
2. The inhibiting effect of small amounts of carbon, whether on quartz or on carbon, was clearly demonstrated.
3. The relation between the catalytic and inhibitive effects of carbon in terms of the total amount of carbon was clearly shown.
4. The increase or decrease in rate on the carbon surface with a series of consecutive experiments was explained in terms of the balance of two competing processes: the formation of building carbon and the formation of blocking carbon.
5. An overall mechanism for the formation of products was described in which homogeneous and surface processes were identified and the relation between these processes was discussed.
6. The mechanism was shown to be valid over a wide range of temperatures and pressures. In addition, the mechanism demonstrated that the reaction conditions could be altered to enhance the selectivity of the products.
7. A method was developed for measuring the hydrogen content of the thin carbon films. No method for this measurement has been previously reported.
8. The relationship between the reactivity of the carbon film, its hydrogen content and the conditions under which the carbon film was formed was determined.
9. A novel catalyst was prepared containing both carbon and iron. Its catalytic properties were demonstrated.

REFERENCES

1. J. P. Birk, Chemistry, Houghton Mifflin Company, Boston, U.S.A., 1994.

2. R. W. Coughlin, *Ind. Eng. Chem. Prod. Res. Dev.*, **8** (1969) 12.

3. V. S. Tripathi, P. K. Ramachandran, *Def. Sci. J.*, **35**(1) (1985) 115.

4. G. S. Szymański, G. Rychlicki, *Carbon*, **31**(2) (1993) 247.

5. G. F. Froment, *Rev. Chem. Eng.*, **6**(4) (1990) 293.

6. E. G. Derouane, Catalysis by Acids and Bases, Editors B. Imelik et al, Elsevier Science Publishers B.V., Amsterdam (1985) 221.

7. M. C. Demicheli, E. N. Ponzi, O. A. Ferretti, A. A. Yeramian, *Chem. Eng. J.*, **46** (1991) 129.

8. D. C. W. Blaikley, N. Jorgenson, *Catalysis Today*, **7** (1990) 277.

9. J. M. Parera, Catalyst Deactivation, Editors C. H. Bartholomew and J. B. Butt, Elsevier Science Publishers B.V., Amsterdam (1991) 103.

10. J. Van Doorn, J. A. Moulijn, *Catalysis Today*, **7** (1990) 257.

11. A. Sárkány, H. Lieske, T. Szilágyi, L. Tőth, *Proc. 8th Int. Congr. Catal.*, **2** (1984-Published 1988) II-613.

12. S. Purwono, P. L. Silveston, *Carbon*, **31**(4) (1993) 651.

13. K. Aika, H. Hari, A. Ozaki, *J. Catal.*, **27** (1972) 21.

14. P. H. Civen, L. W. Hill, *Carbon*, **6** (1968) 525.

15. P. H. Civen, L. W. Hill, *Carbon*, **7** (1969) 649.

16. W. P. Hoffman, F. J. Vastola, P. L. Walker Jr., *Carbon*, **23**(2) (1985) 151.

17. W. P. Hoffman, F. J. Vastola, P. L. Walker Jr., *Carbon*, **26**(4) (1988) 485.

18. B. Stöhr, H. P. Boehm, R. Schlögl, *Carbon*, **29**(6) (1991) 707.

19. K. I. Makarov, V. K. Pechik, *Carbon*, **7** (1969) 279.

20. G. A. Somorjai, D. W. Blakely, *Nature*, **258**(5536) (1975) 580.

21. S. M. Davis, F. Zaera, G. A. Somorjai, *J. Catal.*, **77** (1982) 439.

22. G. A. Somorjai, F. Zaera, *J. Am. Chem. Soc.*, **86**(16) (1982) 3070.

23. S. M. Davis, F. Zaera, B. E. Gordon, G. A. Somorjai, *J. Catal.* **92** (1985) 240.

24. G. A. Somorjai, S. T. Oyama, *Springer Series in Surface Sciences*, **14** (1988) 120.

25. S. E. Moore, J. H. Lunsford, *J. Catal.*, **77** (1982) 297.

26. G. Webb, *Catalysis Today*, **7** (1990) 139.

27. R. S. Hansen, N. C. Gardner, *J. Phys. Chem*, **74** (1970) 3646.

28. W. H. Weinberg, H. A. Deans, R. P. Merrill, *Surface Sci.*, **41** (1974) 312.

29. L. L. Kesmodel, P. C. Stair, R. C. Baetzold, G. A. Somorjai, *Phys. Rev. Letters*, **36** (1976) 1316.

30. R. Dus, *Surface Sci.*, **50** (1975) 241.

31. P. P. Lankhorst, G. C. De Jongste, V. Ponec, Catalyst Deactivation, Editors B. Delmon and G. F. Froment, Elsevier Publishers B.V., Amsterdam (1980) 43.

32. Z. Karpinski, T. Koscielski, *J. Catal.*, **63** (1980) 313.

33. E. G. Christoffel, Z. Paal, *J. Catal.*, **73** (1982) 30.

34. J. G. McCarty, P. Y. Hou, D. Sheridan, H. Wise, Coke Formation on Metal Surfaces, *ACS Symposium Series*, **202**, Washington, D. C. (1982) 253.

35. A. C. Frost, L. F. Elek, C.-L. Yang, A. P. Risch, J. A. Rabo, *Applied Catalysis*, **2** (1982) 347.

36. A. Maccoll, *J. Chem. Soc.* (1955) 965.

37. P. J. Agius, A. Maccoll, *J. Chem. Soc.* (1955) 973.

38. A. Maccoll, P. J. Thomal, *J. Chem. Soc.* (1955) 979.

39. G. A. Kapralova, N. N. Semenov, *Russ. J. Phys. Chem.*, **37**(1) (1963) 35.

40. G. A. Kapralova, N. N. Semenov, *Russ. J. Phys. Chem.*, **37**(2) (1963) 156.

41. C. F. Cullis, J. E. Manton, G. B. Thomas, H. Wilman, *Acta. Cryst.*, **12** (1959) 382.

42. D. H. R. Barton, P. F. Onyon, *Trans. Faraday Soc.*, **45** (1949) 725.

43. K. A. Holbrook, *Proc. Chem. Soc.* (1964) 418.

44. K. A. Holbrook, J. J. Rooney, *J. Chem. Soc.* (1965) 247.

45. K. A. Holbrook, R. W. Walker, W. R. Watson, *J. Chem. Soc. (B)* (1968) 1089.

46. B. W. Wojciechowski, K. J. Laidler, *Trans. Faraday Soc.*, **59** (1963) 369.

47. B. Notari, *Catal. Sci. Technol.*, 1 (1991) 55.

48. D. R. Stull, E. F. Westrum, Jr., G. C. Sinke, The Chemical Thermodynamics of Organic Compounds, R. E. Krieger Publishing Co., Malabar, Florida, U.S.A. (1987).

49. M. G. Poirier, A. R. Sanger, K. J. Smith, *Can. J. Chem. Eng.*, **69** (1991) 1027.

50. IGT World Reserves Survey, Institute of Gas Technology, Chicago, IL (1989).

51. R. Burch, N. Parkyns, *Chemistry in Britain* (November 1992) 1013.

52. C.-J. Chen, M. H. Back, R. A. Back, *Can. J. Chem.*, **53**(23) (1975) 3580.

53. M. S. Khan, B. L. Crynes, *Ind. Eng. Chem.*, **62**(10) (1970) 54.

54. V. Kevorkian, C. E. Heath, M. Boudart, *J. Phys. Chem.*, **64** (1960) 964.

55. P. S. Shantarovich, B. V. Pavlov, *Int. Chem. Eng.*, **2** (1962) 415.

56. H. B. Palmer, J. Layahe, K. C. Hou, *J. Phys. Chem.*, **72** (1968) 348.

57. A. R. Bossard, M. H. Back, *Can. J. Chem.*, **68** (1990) 1401.

58. R. Le Bec, P. M. Marquaire, G. M. Côme, *Ind. Eng Chem. Res.*, **29** (1990) 539.

59. J. R. Anderson, *Appl. Catal.*, **47** (1989) 177.

60. H. Mimoun, *New J. Chem.*, **11**(7) (1987) 513.

61. R. Pitchai, K. Klier, *Catal. Rev. - Sci. Eng.*, **28**(1) (1986) 13.

62. Y. Amenomiya, V. I. Birss, M. Goledzinowski, J. Galuszka, A. R. Sanger, *Catal. Rev. - Sci. Eng.*, **32**(3) (1990) 163.

63. E. J. Erekson, A. L. Lee, Symposium on Natural Gas Upgrading II, Division of Petroleum Chemistry, Inc., *ACS*, San Francisco (1992) 98.

64. R. R. Ferguson, R. H. Crabtree, *New J. Chem.*, **13** (1989) 647.

65. D. Michos, C. A. Sassano, P. Krajnik, R. H. Crabtree, *Angew. Chem. Int. Ed. Engl.*, **32**(10) (1993) 1491.

66. R. A. Periana, D. J. Taube, E. R. Evitt, D. G. Löffler, P. R. Wentrcek, G. Voss, T. Masuda, *Science*, **259** (1993) 340.

67a. C.-J. Chen, *Ph.D. Thesis*, University of Ottawa, 1977.

67b. D. B. Murphy, R. W. Carroll, *Carbon*, **30**(1) (1992) 47.

68. R. Venkateswaran, M. H. Back, G. Scacchi, *Carbon*, **32**(5) 911 (1994) .

69. C. J. Cobos, J. Troe, *Z. Phys. Chem. (Neue Folge)*, **167** (1990) 129.

70. D. Brennan, Comprehensive Chemical Kinetics, Editors C. H. Bamford, late C. F. H. Tipper, and R. G. Compton, **21**, Elsevier Science Publishers B.V., Amsterdam (1984) 151.

71. J. P. McCaffrey, *Microscopy Research and Technique*, 24, (1993) 180.

72. P. W. Atkins, Physical Chemistry, 4th Ed., W. H. Freeman and Company, New York, 1990.

73. G. H. Stout, L. H. Jensen, X-Ray Structure Determination, A Practical Guide, 2nd Ed., John Wiley and Sons, New York, 1989.

74. B. E. Warren, X-Ray Diffraction, Addison-Wesley Publishing Company, Reading, Massachusetts, 1969.

75. Hang Shi, *Disordered Carbons and Battery Applications*, Ph.D. Thesis, Simon Fraser University, 1993.

76. Hang Shi, J. N. Reimers, J. R. Dahn, *J. Appl. Crystallography*, (1993).

77. Philips PW1892 Total Access Diffraction Database, ©1991 Philips Export B.V., based upon PDF-2.

78a. P. Painter, M. Starsinic, M. Coleman, *Fourier Transform Infrared Spectroscopy: Applications to Chemical Systems*, **4**, Ed. J. R. Ferraro, L. J. Basile, Academic Press Inc., Orlando (1985) 169.

78b. M. J. D. Low, C. Morterra, *Carbon*, **21** (1983) 275.

79. R. Hahn, K. J. Hüttinger, P. Schleicher, *Proc. 5th London Intern. Carbon and Graph. Conf.*, **II** (1978) 151.

80. P. L. Walker, Jr., M. Shelef, R. A. Anderson, *Chem. Phys. Carbon*, **4** (1968) 287.

81. W. L. Holstein, M. Boudart, *J. Cat.*, **75** (1982) 337.

82. W.-Y. Wen, *Catal. Rev. - Sci. Eng.*, **22**(1) (1980) 1.

83. K. J. Hüttinger, *Fuel*, **62** (1983) 166.

84. K. J. Hüttinger, W. Krauss, *Fuel*, **61** (1982) 291.

85. Y. Nishiyama, T. Haga, O. Tamura, N. Sonehara, *Carbon*, **28**(1) (1990) 185.

86. K. Otto, L. Bartosiewicz, M. Shelef, *Fuel*, **58** (1979) 565.

87. M. Matsukata, T. Fujikawa, E. Kikuchi, Y. Morita, *Energy & Fuels*, **3** (1989) 336.

88. F. Delannay, W. T. Tysoe, H. Heinemann, G. A. Somorjai, *Carbon*, **22**(4/5) (1984) 401.

89. A. L. Cabrera, H. Heinemann, G. A. Somorjai, *Chem. Phys. Lett.*, **81**(3) (1981) 402.

90. K. Otto, L. Bartosiewicz, M. Shelef, *Carbon*, **17** (1979) 351.

91. D. W. McKee, *Carbon*, **12** (1974) 453.

92. R. Hahn, K. J. Hüttinger, *Chem.-Ing.-Tech.*, **50**(12) (1978) 954.

93. R. Hahn, K. J. Hüttinger, *13th Biennial Carbon Conf.*, Irvine, Calif. (1977) 44.

94. K. J. Hüttinger, J. Adler, G.Hermann, *NATO ASI Ser., Ser. E*, **105**(Carbon Coal Gasification) (1986) 213.

95. F. Rodriguez-Reinoso, C. Salinas-Martinez de Lecea, A. Sepulveda-Escribano, J. D. Lopez-Gonzalez, *Catalysis Today*, **7** (1990) 287.

96. T. Kotanigawa, K. Shimokawa, M. Yamamoto, *J. Chem Soc., Chem. Commun.* (1982) 29.

97. K. Otto, M. Shelef, *Carbon*, **15** (1977) 317.

98. L. M. Dyagileva, V. P. Mar'in, E. I. Tsyganova, G. A. Razuvaev, *J. Organomet. Chem.*, **175** (1979) 63.

99. L. M. Dyagileva, E. I. Tsyganova, Yu. A. Aleksandrov, *Zh. Obshch. Kh.*, **50**(10) (1980) 2257.

100. S.-I. Hirano, T. Yogo, H. Suzuki, S. Naka, *J. Mat. Sci.*, **18** (1983) 2811.

101. K. E. Lewis, G. P. Smith, *J. Am. Chem. Soc.*, **106** (1984) 4650.

102. E. Hedaya, *Flash Vacuum Pyrolysis*, **2** (1969) 367.

103. S. Ahmed, M. H. Back, *Carbon*, **23** (1985) 513.

104. C. F. Cullis, *ACS Symposium Series*, **21** (1976) 228.

105. S. Jasienko, J. Machnikowski, *Carbon*, **19** (1981) 199.

106. S. B. Tong, P. Pareja, M. H. Back, *Carbon*, **20**(3) (1982) 191.